Supplementary information

Total syntheses and antiproliferative activities of prenostodione and its analogues

Aldahir Ramos Orea,[a] Teresa Ramírez-Apan,[a] Rosa M. Chávez-Santos,[a] Rodrigo Aguayo-Ortiz,[b] Clara Espitia,[c] Mayra Silva Miranda,[c] Rubén O. Torres-Ochoa*[a] and Roberto Martínez*[a]

[a]Instituto de Química, Universidad Nacional Autónoma de México, Circuito Exterior, Ciudad Universitaria, Coyoacán, Ciudad de México, 04510, México. E-mail: romar.torres@iquimica.unam.mx; robmar@unam.mx www.iquimica.unam.mx

[b]Departamento de Farmacia, Facultad de Química, Universidad Nacional Autónoma de México, Circuito Escolar, Ciudad Universitaria, Coyoacán, Ciudad de México, 04510, México.

[c]Instituto de Investigaciones Biomédicas, Universidad Nacional Autónoma de México, Ciudad Universitaria, Coyoacán, Ciudad de México, 04510, México.

Table of contents

1. General remarks

Commercially available chemicals were purchased from Merck and Sigma Aldrich. ^{1}H NMR and ^{13}C NMR (300 and 75 MHz, respectively) spectra were acquired in $CDCl_3$ and DMSO-d_6 at 25 °C on a 300 MHz Jeol Eclipse and 300 MHz Fourier Brucker spectrometers. The chemical shifts are reported on the δ scale in parts per million (ppm) and calibrated to residual solvents (7.26 ppm in $CDCl_3$; 2.50 ppm in DMSO-d_6) for ^{1}H NMR and (77.16 ppm in $CDCl_3$; 39.50 ppm in DMSO-d_6) ^{13}C NMR. The peak shapes are indicated as follows: s, singlet; br s, broad singlet; d, doublet; t, triplet; q, quartet; m, multiplet. The coupling constant values (*J*) are reported in Hertz (Hz). Melting points were measured in open capillaries using a Mel-Temp apparatus. IR spectra were obtained using an FTIR Tensor 27 Bruker spectrometer. Mass spectra were recorded with JEOL SX 102 A spectrometers by electronic impact (EI). Reactions were monitored by TLC and visualized by using a dual short-wavelength/long-wavelength UV lamp. Flash column chromatography was carried out on silica gel 60 (230-400 mesh ASTM) from Macherey-Nagel GmbH & Co. All solvents were distilled under a nitrogen atmosphere. Dichloromethane and acetonitrile were distilled from calcium hydride, toluene was distilled from sodium benzophenone ketyl. X-ray diffraction data were obtained from Bruker Smart APEX II CCD diffractometer equipped with graphite monochromatic MoKα radiation. HPLC was performed in Agilent 1200 Liquid Chromatograph with Waters 2996 diode array: Luna® 3 μm C18(2) 100 Å 100 x 2 mm; acetonitrile:water-0.1% HOAc (30:70) initial eluent and acetonitrile after 30 minutes; flow = 0.2 mL/min; wavelength 254 nm; sample solvent: dichloromethane.

2. Procedures for the synthesis of starting materials

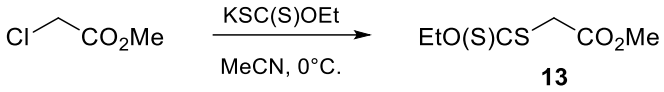

13

Methyl 2-((ethoxycarbonothioyl)thio)acetate (13).[1] This compound was synthesized from methyl chloroacetate (2.85 g, 26.26 mmol) following Gutierrez's method.

Yellow oil (5.02 g, 98%). ^{1}H NMR (300 MHz, $CDCl_3$): δ 4.63 (q, *J* = 7.2 Hz, 2H), 3.92 (s, 2H), 3.75 (s, 3H), 1.41 (t, *J* = 7.2 Hz, 3H).

Supplementary Table 1. Optimization of the synthesis of ester **12**.

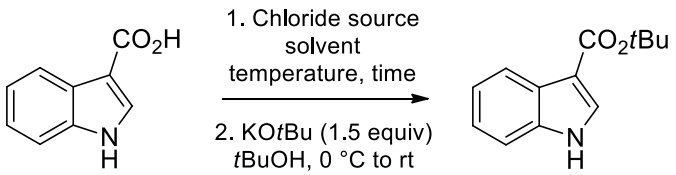

11 **12**

[1] P. E. Reyes-Gutiérrez, R. O. Torres-Ochoa, R. Martínez and L. D. Miranda, *Org. Biomol. Chem.*, 2009, **7**, 1388.

Entry	Chloride source	Solvent	Temperature (°C)	Time (h)	%Yield (12)
1	$(COCl)_2$	CH_2Cl_2	25	6	25
2	Undistilled $SOCl_2$	Toluene	110	6	42
3	Distilled $SOCl_2$	Toluene	110	6	76
4	Distilled $SOCl_2$	Toluene	110	4	85

***tert*-Butyl 1*H*-indole-3-carboxylate (12).**[2] A solution of 1*H*-indole-3-carboxilic acid (2.33 g, 14.4 mmol, 1 equiv) in anhydrous toluene (25 mL) was added $SOCl_2$ (26 mL, 361.2 mmol, 25 equiv) dropwise. The mixture was stirred at reflux for 4 h. The reaction mixture was cooled down to room temperature and subsequently a distillation equipment was connected to remove the excess of thionyl chloride and toluene. The complete elimination of both was achieved under reduced pressure. The crude mixture was dissolved in *t*BuOH (25 mL), then KO*t*Bu (4.50 g, 36.2 mmol, 2.5 equiv) was added at 0 °C in three portions. The resulting mixture was stirred at 0 °C for 10 min and 1 h at room temperature. The solvent was removed under reduced pressure and the residue was diluted in CH_2Cl_2 (30 mL) and water (30 mL). The reaction crude was extracted was extracted with CH_2Cl_2. The organic phases were combined, dried over Na_2SO_4, and concentrated in vacuo. The residue was purified by column chromatography on silica gel eluting with hexane:EtOAc (4:1) to give *tert*-butyl 1*H*-indole-3-carboxylate (**12**).

Yellow oil (2.06 g, 85%). ^{1}H NMR (300 MHz, $CDCl_3$): δ 9.03 (br s, 1H), 8.18 (m, 1H), 7.84 (d, *J* = 3.0 Hz, 1H), 7.39 (m, 1H), 7.27 (m, 1H), 7.24 (m, 1H), 1.66 (s, 9H); ^{13}C NMR (75 MHz, $CDCl_3$): δ 165.3, 136.3, 131.2, 125.8, 123.0, 121.9, 121.5, 111.7, 110.5, 80.3, 28.7.

Supplementary Table 2. Optimization of the synthesis of diester **10**.

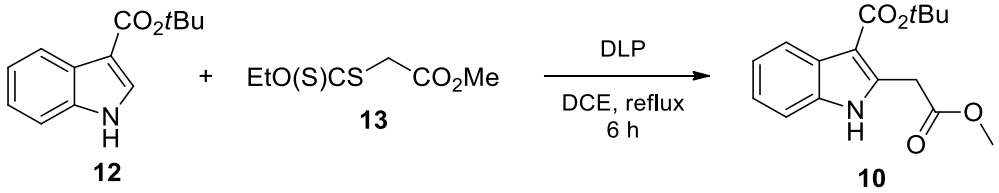

Entry	DLP (equiv)	%Yield (10)
1	1.2	64
2	1.5	67
3	1.8	72

***tert*-Butyl 2-(2-methoxy-2-oxoethyl)-1*H*-indole-3-carboxylate (10).** To a refluxing solution of xanthate **13** (0.804 g, 4.1 mmol, 1.2 equiv) and indole **12** (0.75 g, 3.4 mmol, 1 equiv) in degassed 1,2-dichoroethane (10 mL), dilauroyl peroxide (2.48 g, 6.21 mmol, 1.8 equiv) was added portionwise (0.3 equiv/h). The solvent was removed under reduced pressure and the crude was dissolved in CH_3CN and washed with hexane until the oily layer formed is removed. The polar

[2] J. Ludwig and M. Lehr, *Synth. Commun.*, 2004, **34**, 3691.

phase was concentrated in and purified by column chromatography on silica gel eluting with hexane:EtOAc (9:1) to give the alkylated indole **10**.

Yellow solid (0.718 g, 72%), m. p. 98-100 °C. ^{1}H NMR (300 MHz, $CDCl_3$): δ 9.66 (br s, 1H), 8.10 (dd, *J* = 6.0, 3.0 Hz, 1H), 7.37 (dd, *J* = 6.0, 3.0 Hz, 1H), 7.25-7.20 (m, 2H), 4.38 (s, 2H), 3.79 (s, 3H), 1.66 (s, 9H); ^{13}C NMR (75 MHz, $CDCl_3$): δ 171.6, 165.2, 138.1, 134.9, 126.6, 122.8, 121.8, 121.6, 111.2, 106.8, 80.4, 52.5, 32.3, 28.8. IR (KBr): ν (cm^{-1}) 3270, 1737, 1654. HR-MS (EI) *m/z* calcd for $C_{16}H_{19}NO_4$ [M + H^+]: 290.1392; found: 290.1394.

3. Antiproliferative activity of compounds 3 and 14

Cell lines and culture medium

The compounds **3** and **14** were screened *in vitro* against six human cancer cell lines: HCT-15 (human colorectal adenocarcinoma), MCF- 7 (human mammary adenocarcinoma), K-562 (human chronic myelogenous leukemia), U-251 (human glioblastoma), PC-3 (human prostatic adenocarcinoma), and SKLU-1 (human lung adenocarcinoma) cell lines, supplied by the National Cancer Institute (NCI, USA). The human tumor cytotoxicities were determined following protocols established by the NCI.[3] Compound **14** was also evaluated against COS-7 (noncancerous monkey kidney fibroblast-like-cell-line) supplied by the Hospital General Siglo XXI-IMSS (México). The cell lines were cultured in RPMI-1640 medium supplemented with 10% fetal bovine serum, 2 mM L-glutamine, 10000 units/mL penicillin G sodium, 10000 μg mL^{-1} streptomycin sulfate, 25 μg mL^{-1} amphotericin B (Gibco), and 1% non-essential amino acids (Gibco). Cells were maintained at 37 °C in a humidified atmosphere with 5% CO_2. The viability of the cells used in the experiments exceeded 95%, as determined using a trypan blue assay.

Cytotoxicity assay

After treating the tumor cells with the test compounds, the cytotoxicity was determined using a protein binding dye, sulforhodamine B (SRB), in a microculture assay to measure cell growth. The cells were removed from the tissue culture flasks by treatment with trypsin and diluted with fresh media. One-hundred microliters of the cell suspension were pipetted into 96 well microtiter plates (Costar), yielding 5000 or 7500 cells per well, and the material was incubated at 37 °C for 24 h in

[3] A. Monks, D. Scudiero, P. Skehan, R. Shoemaker, K. Paull, D. Vistica, C. Hose, J. Langley, P. Cronise, A. Vaigro-Wolff, M. Gray-Goodrich, H. Campbell, J. Mayo and M. Boyd, *J. Natl. Cancer Inst.*, 1991, **83**, 757.

a 5% CO_2 atmosphere. Subsequently, a 100 µL aliquot of the test compounds in solution, obtained by dilution of the stock solutions, was added to each well. The cultures were exposed for 48 h to the drug at concentrations ranging from 1-50µm After the incubation period, cells were fixed to the plastic substratum by the addition of 50 µL cold 50% aqueous trichloroacetic acid. The plates were incubated at 4 °C for 1 h, washed with tap H_2O, and air-dried. The trichloroacetic acid-fixed cells were stained by the addition of 0.4% SRB. The free SRB solution was then removed by washing with 1% aqueous acetic acid. The plates were air-dried, and the bound dye was solubilized by the addition of 10 mM unbuffered Tris base (100 µL). The plates were placed on a shaker for 5 min, and the absorption was determined at 515 nm using an ELISA plate reader (Bio-Tex Instruments).

Supplementary Table 3. % Inhibition of compounds **3a-k** to the six cancer cell lines (25 µM).

Comp.	R	U251 SNC	PC-3 prostate	K562 leukemia	HCT15 colon	MCF7 breast	SKLU lung
3a	-OH	NA	23.8	10.5	5.27	7.5	10.8
3b	-H	NA	NA	NA	NA	NA	NA
3c	-Me	NA	NA	NA	NA	NA	NA
3d	-OMe	7.1	NA	NA	NA	NA	3.0
3e	$-N(CH_3)_2$	7.3	21.9	32.5	NA	10.6	9.2
3f	$-NO_2$	24.0	0.4	7.6	NA	18.5	32.3
3g	-CN	10.9	2.5	29.7	NA	17.2	19.5
3h	$-CF_3$	NA	NA	59.1	38.4	37.0	32.0
3i	-Br	NA	NA	19.5	32.5	33.0	26.0
3j	-Cl	NA	NA	38.6	28.9	46.0	25.9
3k	-F	NA	NA	NA	5.1	NA	22.5

NA = Not active

Active compounds: % Inhibition ≥ 50

Supplementary Table 4. % Inhibition of compounds **14a-k** to the six cancer cell lines (25 μM).

Compound	R	U251 CNS	PC-3 prostate	K562 leukemia	HCT15 colon	MCF7 breast	SKLU lung	COS-7*
14a	-OH	18.9	6.5	18.6	7.0	NA	NA	41.3
14b	-H	57.3	46.1	73.0	60.0	54.1	63.9	65.9
14c	-Me	50.6	36.7	67.1	69.3	61.6	66.5	68.1
14d	-OMe	62.5	79.0	51.7	15.6	100	93.6	NA
14e	$-N(CH_3)_2$	42.0	42.0	47.9	23.6	34.0	71.7	69.5
14f	$-NO_2$	57.7	16.3	50.2	24.7	52.2	63.5	30.2
14g	-CN	72.0	65.1	NA	52.1	2.6	NA	3.0
14h	$-CF_3$	21.8	25.3	43.6	68.4	47.0	54.7	61.9
14i	-Br	63.8	83.1	58.5	7.1	70.3	59.7	NA
14j	-Cl	55.9	71.0	67.4	48.9	53.2	68.8	49.0
14k	-F	26.3	1.1	26.9	82.6	16.6	41.5	40.4

NA = Not active

Active compounds: % Inhibition ≥ 50

*COS-7 = Noncancerous kidney monkey fibroblast-like-cell-line.

4. Antitubercular activity of compounds 3 and 14

In vitro antimycobacterial assay

Stock solutions of all compounds were prepared in 100% DMSO at a concentration of 10 mg/mL. For the resazurin microtiter assay (REMA), the compounds were each diluted in Middlebrook 7H9 broth medium (TH9) without tyloxapol. For reference drugs, stock solutions with a concentration of 64 μg/mL were prepared and filtered using a membrane with a pore diameter of 0.22 μm (Millipore; Darmstadt, Germany). All working solutions were kept refrigerated at −20°C until they were evaluated.

Cell culture

The cytotoxicity assays were carried out using on Vero cell line (from the kidney of an African green monkey) from ATCC. These cells were cultured in RPMI 1640 medium supplemented with 10% fetal bovine serum (FBS) and nonessential amino acids.

Cytotoxicity assay

To assess the cytotoxicity of each tested compound, 10,000 Vero cells were placed in a 96 well plate and incubated for 24 h in 100 μL of RPMI medium. After incubation, the plate was washed, and fresh medium containing the compounds in different concentrations was added. Each tested compound was incubated for 48 h at 37 °C under a 5% CO_2 atmosphere. A 10 μL MTT solution (5 mg/mL in sterile PBS) was added to each well, and the resulting mixtures were incubated for another 4 h. The medium was then removed, and a volume of 100 μL of DMSO was used to solubilize the formazan. The formazan absorbance at 570 nm was measured, and cytotoxicity was calculated as %Toxicity = (1 − (ABS problem/ABS control)) × 100. Controls were cells without treatment but following the same procedures above described.[4]

***M. tuberculosis* inocula preparation**

M. tuberculosis H37Rv, H37Ra, and 209 strains were cultivated in 7H9–glycerol–10% ADC–0.01% tyloxapol medium at 37 °C until an O.D. of 0.4 at a wavelength of 600 nm was reached. In each case, bacteria working samples were prepared as a 1:25 dilution in 7H9–ADC 10%.

Antimicrobial susceptibility test using the REMA

The assay used here was described previously.[5] In brief, the outer wells of a 96-well plate were each filled with 200 μL of sterile PBS to prevent dehydration from occurring during the long (8-day) incubation period. RIF was used as a reference drug (16 -0.001 μg/mL serial two-fold dilutions) in each plate, and controls of DMSO, DMSO+Mtb, medium, media+Mtb, and compound alone were included to validate the plate. Compounds were evaluated at various concentrations from 0.98 μg/mL to 250 μg/mL and in triplicate in independent assays. Plates were incubated for 6 days; then, a volume of 30 μL of 0.01% resazurin (weight/volume) (Sigma–Aldrich) was added to each well, and the plates were incubated for an additional 2 days. Visual inspection was used to determine the color of each well: blue was interpreted as no growth, pink

[4] T. Mossman, *J. Immunol. Methods*, 1983, **65**, 55.
[5] L. A. Collins and S. G. Franzblau, *Antimicrob. Agents Chemother.*, 1997, **41**, 1004.

as growth. The MIC value for each experiment was defined as the lowest concentration at which the blue color was observed.

Selectivity index (SI)

SI was obtained using the formula SI = IC_{50} in Vero cells / MIC100 determined using REMA.

Minimal bactericidal concentration (MBC)

MBC was assessed for some of the compounds as described previously.[6] Briefly, volumes of 5 μL of the undeveloped duplicate bacteria suspensions from REMA were transferred to a new microplate containing 195 μL of fresh culture medium per well. Then, microplates were incubated as described for REMA. The MBC values corresponded to the minimum compound concentration that did not cause a color shift in the cultures re-incubated in fresh medium.

Supplementary Table 5. Anti-*M. tuberculosis* effects and cytotoxicity of compounds **3a**-**k**.

Compound	R	MIC (μg/mL)	IC_{50} (μg/mL)	SI
3a	OH	125	33.3	0.2664
3b	H	250	643	2.572
3c	Me	500	245	0.49
3d	OMe	500	379	0.758
3e	$N(CH_3)_2$	>500	307	ND
3f	NO_2	500	363	0.726
3g	CN	250	379	1.516
3h	CF_3	250	136	0.544
3i	Br	250	211	0.844
3j	Cl	500	237	0.474
3k	F	500	315	0.63
Rifampicin		0.06	>1000	>16,666

ND = Not determined

[6] G. M. Molina-Salinas, M. C. Ramos-Guerra, J. Vargas-Villarreal, D. B. Mata-Cárdenas, P. Becerril-Montes and S. Said-Fernández, *Arch. Med. Res.*, 2006, **37**, 45.

Supplementary Table 6. Anti-*M. tuberculosis* effects and cytotoxicity of compounds **14a-k**.

Compound	R	MIC (μg/mL)	IC_{50} (μg/mL)	SI
14a	OH	250	373	1.492
14b	H	>500	50.7	ND
14c	Me	>500	280	ND
14d	OMe	>500	356	ND
14e	$N(CH_3)_2$	>500	330	ND
14f	NO_2	500	144	0.288
14g	CN	125	107	0.856
14h	CF_3	500	<50	ND
14i	Br	>500	20.8	ND
14j	Cl	500	<50	ND
14k	F	500	40	0.08
Rifampicin		0.06	>1000	>16,666

ND = Not determined

5. Physicochemical properties and ADMET prediction of compounds 14

The physicochemical properties of **14a-k** were computed with the free ADME-Tox filtering tool FAF-Drugs4.[7] Absorption, metabolism and toxicity were predicted using the consensus result of three different web servers: vNN-ADMET,[8] admetSAR 2.0[9] (unrestricted applicability domain), and pkCSM (Supplementary Table 7).[10] ADMET consensus analysis indicated that these molecules, except for **14h**, are not pumped out of the cell through the P-glycoprotein, but that they could inhibit the activity of this multidrug-resistant protein. Regarding their metabolism (Supplementary Table 8), the molecules could inhibit cytochrome P450 (CYP) isoforms CYP2C9, CYP2C19, and CYP3A4, being also a possible substrate of the latter. Interestingly, they are

[7] D. Lagorce, L. Bouslama, J. Becot, M. A. Miteva and B. O. Villoutreix, *Bioinformatics*, 2017, **33**, 3658.
[8] P. Schyman, R. Liu, V. Desai and A. Wallqvist, *Front. Pharmacol.*, 2017, **8**, 889.
[9] H. Yang, C. Lou, L. Sun, J. Li, Y. Cai, Z. Wang, W. Li, G. Liu and Y. Tang, *Bioinformatics*, 2019, **35**, 1067.
[10] D. E. V. Pires, T. L. Blundell and D. B. Ascher, *J. Med. Chem.*, 2015, **58**, 4066.

unlikely to exhibit mutagenicity, cardiotoxicity, mitochondrial toxicity, cytotoxicity, and skin sensitization, but do have a high risk of damaging the liver (Supplementary Table 9).

Supplementary Table 7. Calculated physicochemical properties of the **14a-k** compounds.

Cmpd	MW	logP	logD	logSw	tPSA	RB	HBD	HBA	HA	PAINS
14a	393.43	4.48	4.95	-4.85	88.62	7	2	6	29	No
14b	377.43	4.84	5.26	-4.98	68.39	7	1	5	28	No
14c	391.46	5.20	5.77	-5.29	68.39	7	1	5	29	No
14d	407.46	4.81	5.10	-5.07	77.62	8	1	6	30	No
14e	420.50	4.96	5.37	-5.23	71.63	8	1	6	31	No
14f	422.43	4.66	5.20	-5.08	114.21	8	1	8	31	No
14g	402.44	4.55	5.12	-4.95	92.18	7	1	6	30	No
14h	445.43	5.72	6.14	-5.88	68.39	8	1	5	32	No
14i	456.33	5.53	6.03	-5.91	68.39	7	1	5	29	No
14j	411.88	5.46	5.86	-5.59	68.39	7	1	5	29	No
14k	395.42	4.94	5.40	-5.16	68.39	7	1	5	29	No

Compound (Cmpd); molecular weight (MW); logarithm of the partition coefficient between *n*-octanol and water (logP); logP of compounds at physiological pH (logD); logarithm of compounds water solubility (logSw); rotable bonds (RB); hydrogen bond donors (HBD); hydrogen bond acceptors (HBA); heavy atoms (HA); pan-assay interference compounds (PAINS).

Supplementary Table 8. Absorption and metabolism predictions of the **14a-k** compounds.

Cmpd	Absorption					Metabolism				
	Lipinski Ro5	Veber's rule	Egan's rule	P-gp inh	P-gp sub	CYP1A2 inh	CYP2C9 inh / sub	CYP2C19 inh	CYP2D6 inh / sub	CYP3A4 inh / sub
14a	0	Good	Good	+	-	-	+ / -	+	- / -	+ / +
14b	0	Good	Good	+	-	+	+ / -	+	- / -	+ / +
14c	1	Good	Good	+	-	-	+ / -	+	- / -	+ / +
14d	0	Good	Good	+	-	+	+ / +	+	- / -	+ / +
14e	0	Good	Good	+	-	-	+ / -	+	- / -	+ / +
14f	0	Good	Good	+	-	-	+ / -	+	- / -	+ / +
14g	0	Good	Good	+	-	-	+ / -	+	- / -	+ / +
14h	1	Good	Good	+	+	-	+ / -	+	- / -	+ / +
14i	1	Good	Good	+	-	-	+ / -	+	- / -	+ / +
14j	1	Good	Good	+	-	-	+ / -	+	- / -	+ / +
14k	0	Good	Good	+	-	-	+ / -	+	- / -	+ / +

Compound (Cmpd); Lipinski rule-of-5 (Ro5); P-glycoprotein (P-gp); Cytochromes P450 (CYP); inhibitor (inh); substrate (sub); no inhibitor/substrate (-); inhibitor/substrate (+).

Supplementary Table 9. Toxicity prediction of the **14a-k** compounds.

Compound	Mutagenicity (AMES test)	Cardiotoxicity (hERG blocker)	Mitochondrial toxicity (MMP)	Hepatotoxicity	DILI	Cytotoxicity	Skin sensitization	AO
14a	+	-	-	+	+	-	-	III
14b	-	-	-	+	+	-	-	III
14c	-	-	-	+	+	-	-	III
14d	-	-	-	+	+	-	-	III
14e	+	-	-	+	+	-	-	III
14f	+	-	-	+	+	-	-	III
14g	-	-	-	+	+	-	-	III
14h	-	-	-	+	+	-	-	III
14i	-	-	-	+	+	-	-	III
14j	-	-	-	+	+	-	-	III
14k	-	-	-	+	+	-	-	III

Human ether-à-go-go-related gene (hERG); mitochondrial membrane potential (MMP); drug-induced liver injury (DILI); acute oral toxicity category (AO); no risk (-); high risk (+).

6. Permeability prediction

The compounds, including their carboxylic acids **3a-k** and *tert*-butyl esters **14a-k**, were generated with Avogadro v1.1.1[11,12] using the prenostodione crystal structure as template (CCDC 1999796). The optimized molecules were energy minimized employing the universal force field (UFF)[13] implemented in Open Babel v2.3.2.[14] Chemicalize tool[15] (https://chemicalize.com/, RA-O Academic License) of ChemAxon[16] (http://www.chemaxon.com) was used to compute the pK_a values of the carboxylic acid substituents. The coordinate files with the pK_a values assigned to the

[11] Avogadro: An Open-Source Molecular Builder and Visualization Tool. http://avogadro.cc/.
[12] M. D. Hanwell, D. E. Curtis, D. C. Lonie, T. Vandermeersch, E. Zurek and G. R. Hutchison, *J. Cheminform.*, 2012, **4**, 17.
[13] A. K. Rappe, C. J. Casewit, K. S. Colwell, W. A. Goddard and W. M. Skiff, *J. Am. Chem. Soc.*, 1992, **114**, 10024.
[14] N. M. O'Boyle, M. Banck, C. A. James, C. Morley, T. Vandermeersch and G. R. Hutchison, *J. Cheminform.*, 2011, **3**, 1.
[15] M. Swain, *J. Chem. Inf. Model.*, 2012, **52**, 613.
[16] H. E. Pence and A. Williams, *J. Chem. Educ.* 2010, **87**, 1123.

carboxylate group oxygens were submitted to PerMM web server[17,18] (*T* = 298 K, *pH* = 7.0) to predict the passive permeability of each molecule using an implicit solvent model of the DOPC bilayer and the "drag" optimization method.[19] Figures and plots were generated with PyMOL v1.7[20] and Gnuplot v5.2,[21] respectively.

7. Crystallographic data of compound 3i

The single crystal was prepared by diffusing of hexanes into an acetone solution of **3i**.

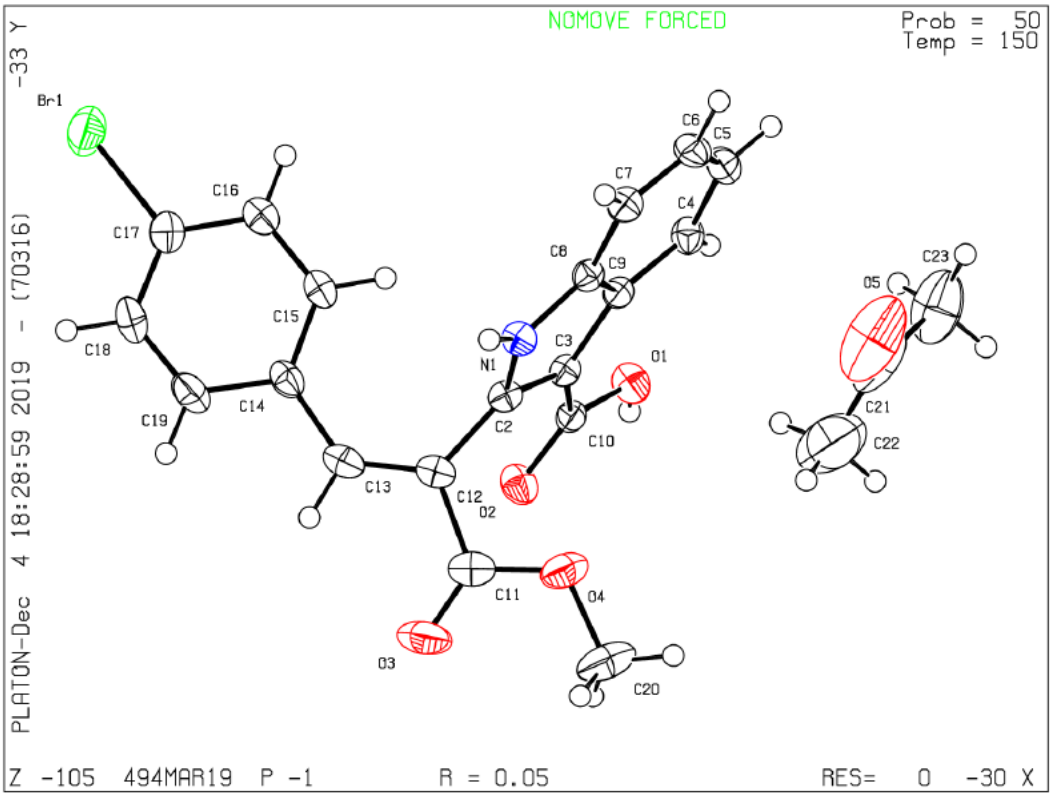

Supplementary Figure 1 ORTEP drawing of **3i** showing thermal ellipsoids at the 50% probability level. CCDC deposition number 1999796 contains the supplementary crystallographic data for this paper which can be obtained free of charge at https://www.ccdc.cam.ac.uk/structures/

[17] A. L. Lomize, J. M. Hage, K. Schnitzer, K. Golobokov, M. B. LaFaive, A. C. Forsyth and I. D. Pogozheva, *J. Chem. Inf. Model.*, 2019, **59**, 3094.
[18] A. L. Lomize and I. D. Pogozheva, *J. Chem. Inf. Model.*, 2019, **59**, 3198.
[19] G. Henkelman, G. Jóhannesson and H. Jónsson, Methods for Finding Saddle Points and Minimum Energy Paths. In *Theoretical Methods in Condensed Phase Chemistry*; Kluwer Academic Publishers: Dordrecht, 2002; pp 269.
[20] L. Schrödinger, *The PyMOL Molecular Graphics System, Version 1.7 Schrödinger, LLC.*; 2015.
[21] T. Williams and C. Kelley, Gnuplot: An Interactive Plotting Program. 2016.

Bond precision: C-C = 0.0034 A Wavelength=0.71073

Cell: a=7.7741(4) b=11.2133(6) c=13.2379(7)
alpha=71.466(1) beta=74.538(1) gamma=81.457(1)
Temperature: 150 K

	Calculated	Reported
Volume	1051.97(10)	1051.97(10)
Space group	P -1	P -1
Hall group	-P 1	-P 1
Moiety formula	C19 H14 Br N O4, C3 H6 O	C19 H14 Br N O4, C3 H6 O
Sum formula	C22 H20 Br N O5	C22 H20 Br N O5
Mr	458.29	458.30
Dx,g cm-3	1.447	1.447
Z	2	2
Mu (mm-1)	1.986	1.986
F000	468.0	468.0
F000'	467.64	
h,k,lmax	10,15,18	10,15,18
Nref	6170	6160
Tmin,Tmax	0.448,0.556	0.570,0.746
Tmin'	0.439	

Correction method= # Reported T Limits: Tmin=0.570 Tmax=0.746
AbsCorr = MULTI-SCAN

Data completeness= 0.998 Theta(max)= 30.098

R(reflections)= 0.0478(3767) wR2(reflections)= 0.1067(6160)

S = 1.011 Npar= 272

8. Copies of ^{1}H NMR and ^{13}C NMR spectra

^{1}H and ^{13}C NMR Spectra of 10

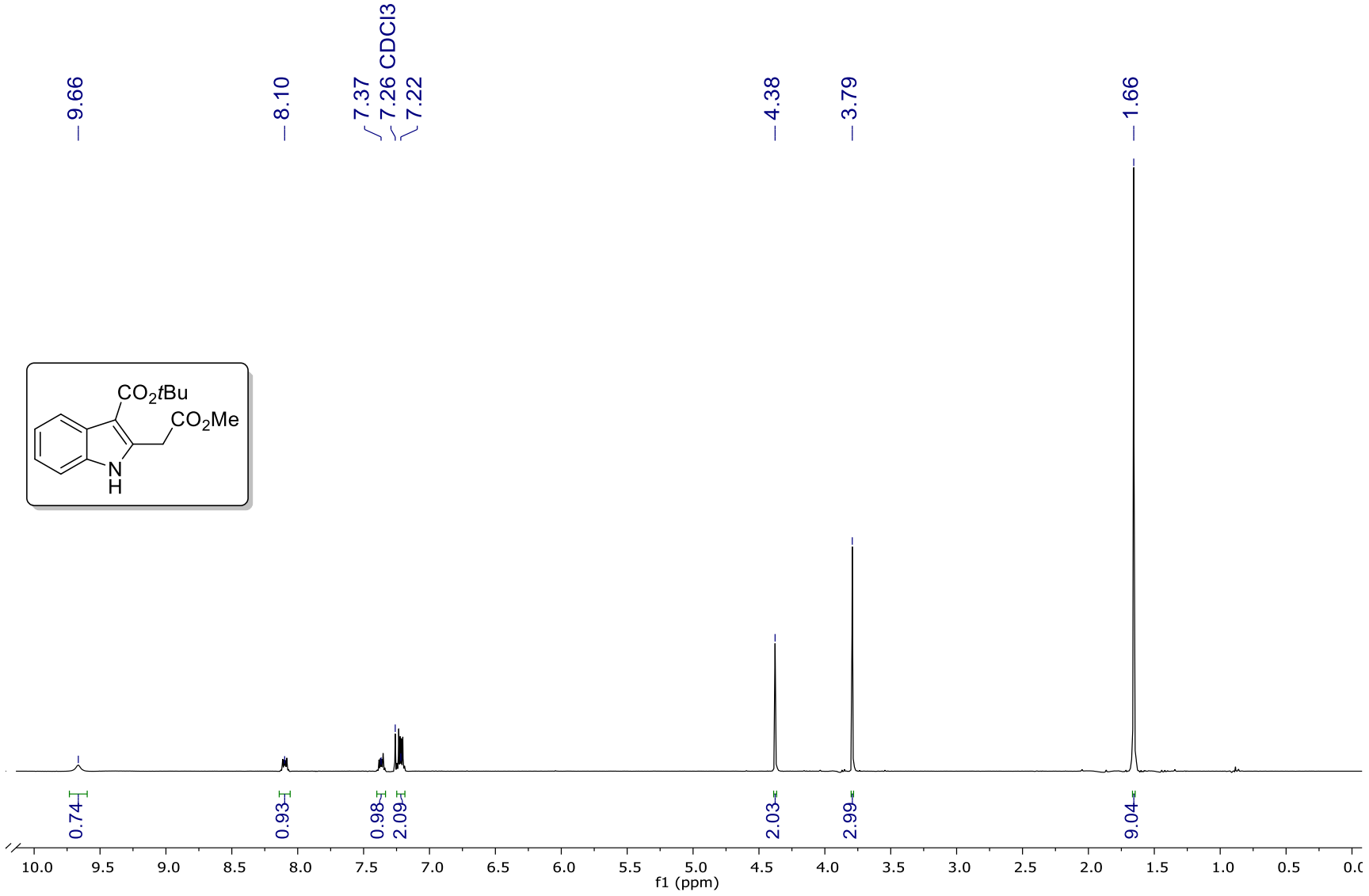

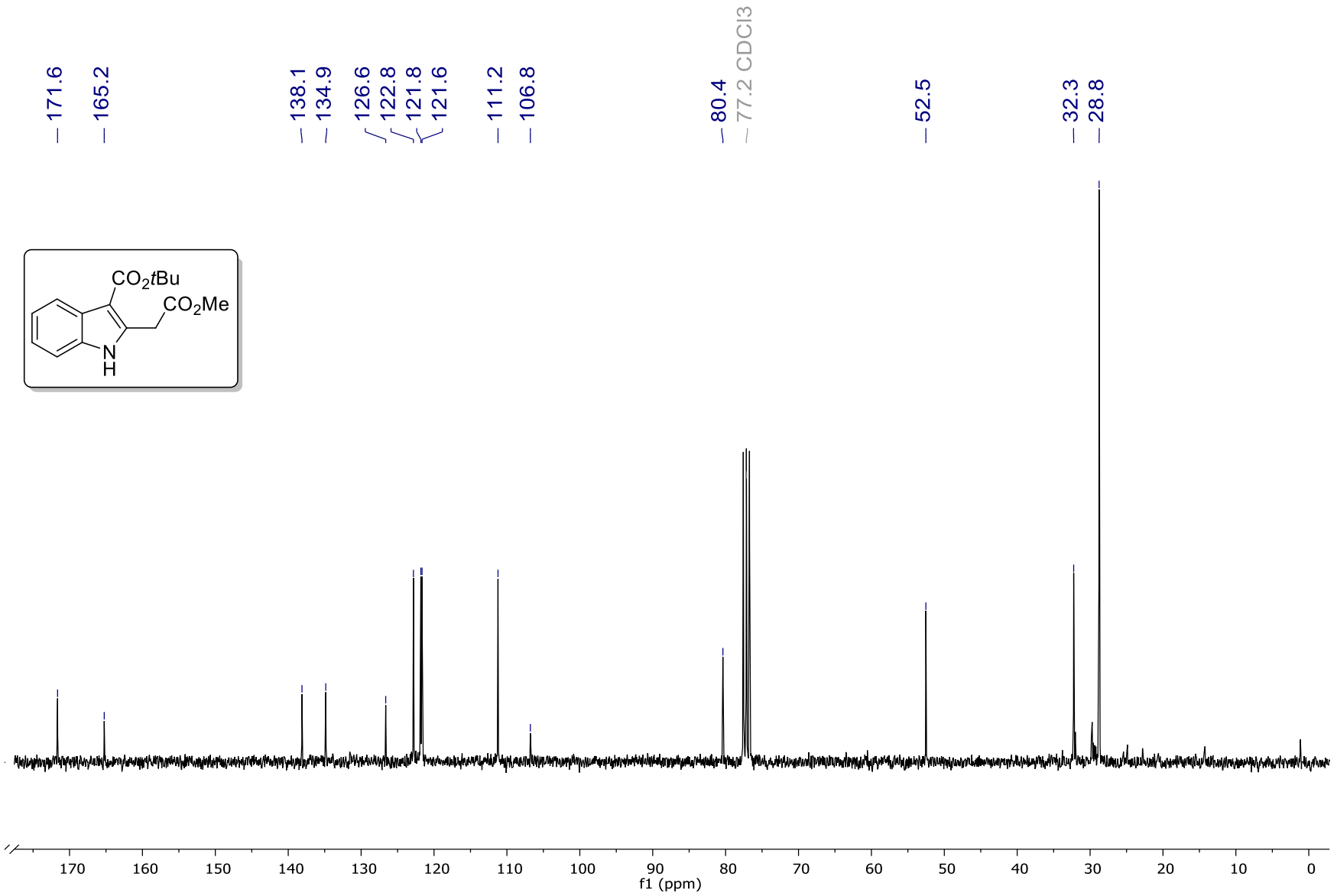
171.6
165.2
138.1
134.9
126.6
122.8
121.8
121.6
111.2
106.8
80.4
77.2 CDCl3
52.5
32.3
28.8
CO2tBu
CO2Me
N
H
170
160
150
140
130
120
110
100
90
80
70
60
50
40
30
20
10
0
f1 (ppm)

^{1}H and ^{13}C NMR Spectra of 14a

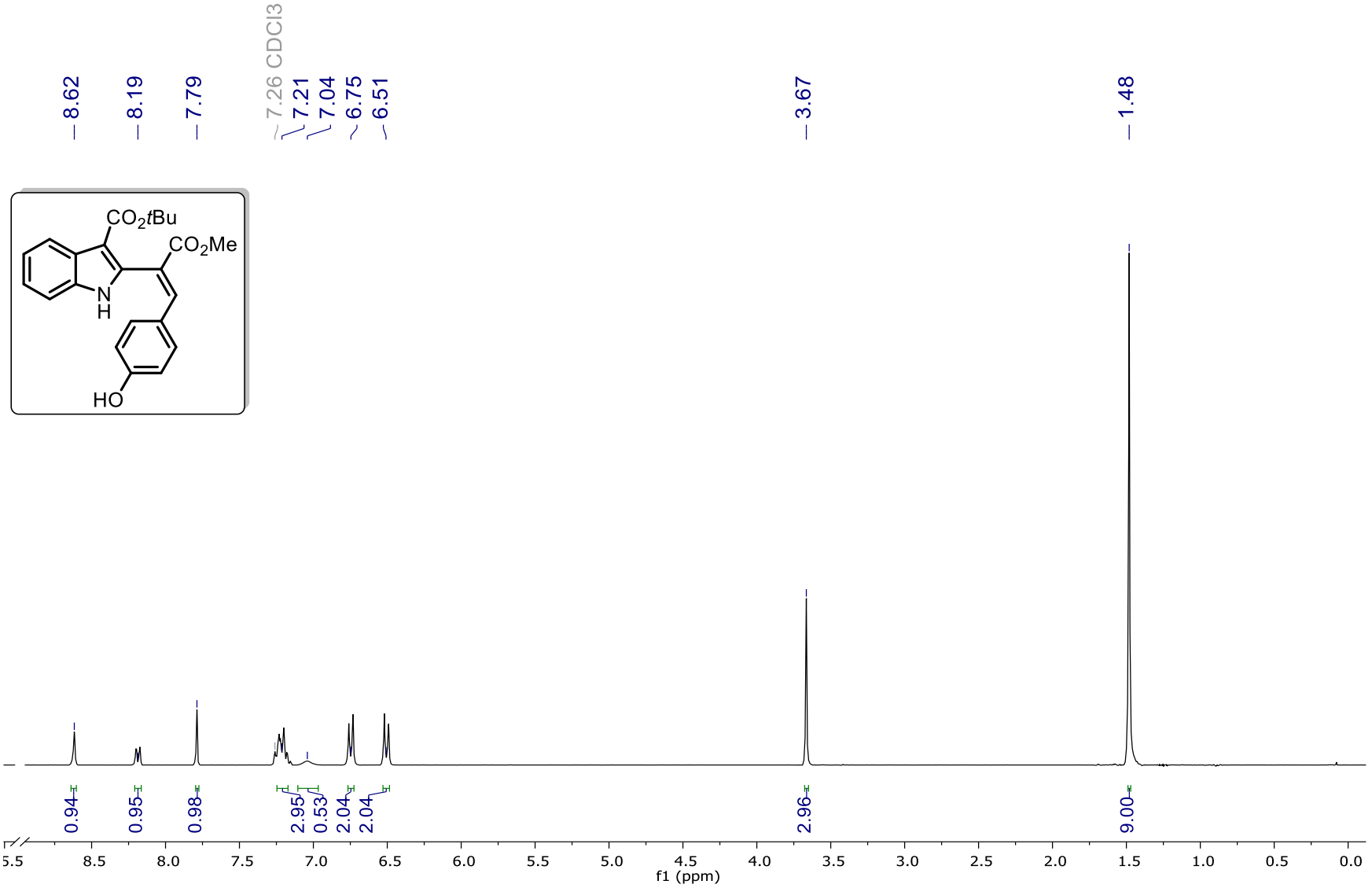

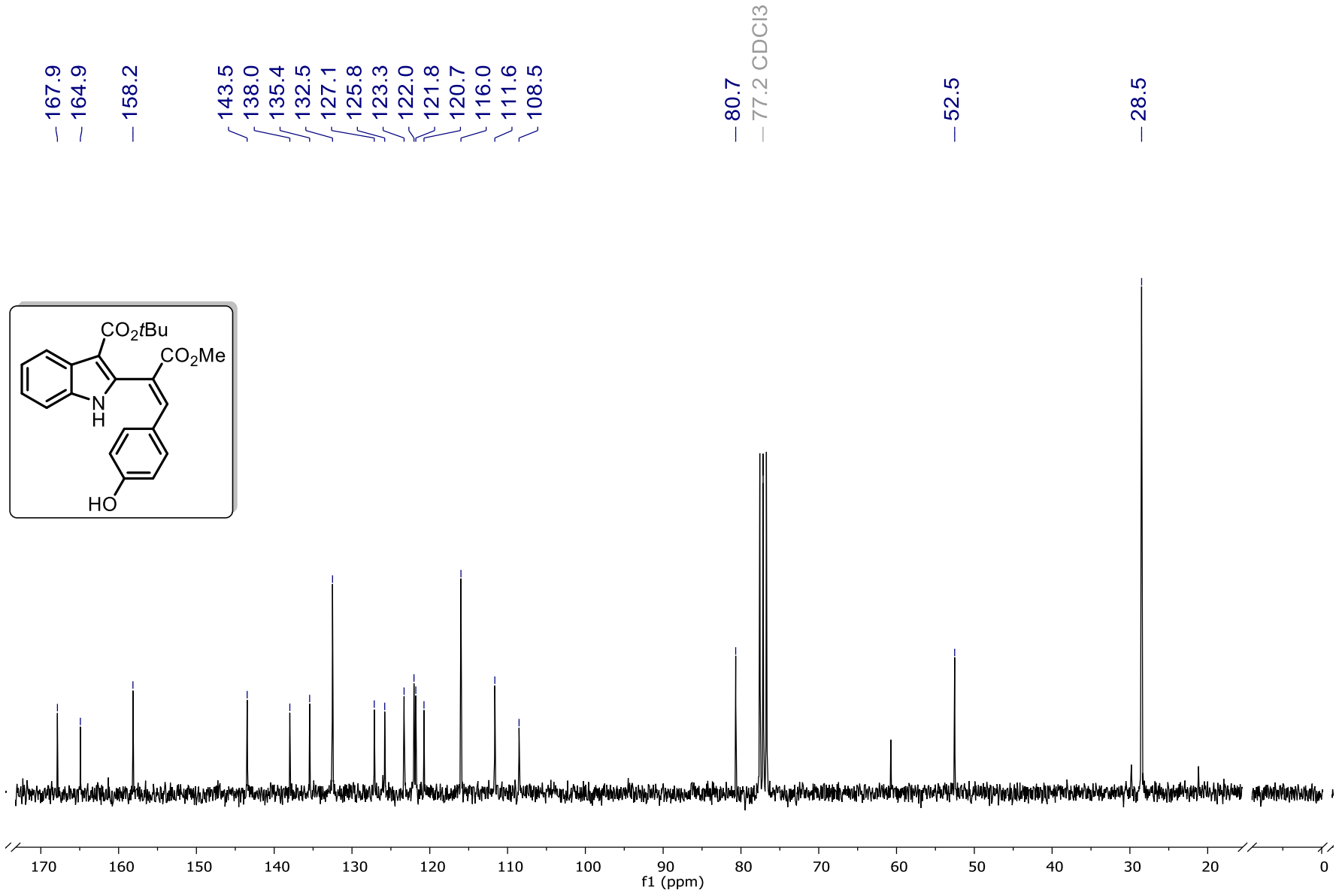
167.9
164.9
158.2
143.5
138.0
135.4
132.5
127.1
125.8
123.3
122.0
121.8
120.7
116.0
111.6
108.5
80.7
77.2 CDCl3
52.5
28.5
CO2tBu
CO2Me
N
H
HO
170
160
150
140
130
120
110
100
90
80
70
60
50
40
30
20
0
f1 (ppm)

^{1}H and ^{13}C NMR Spectra of 14b

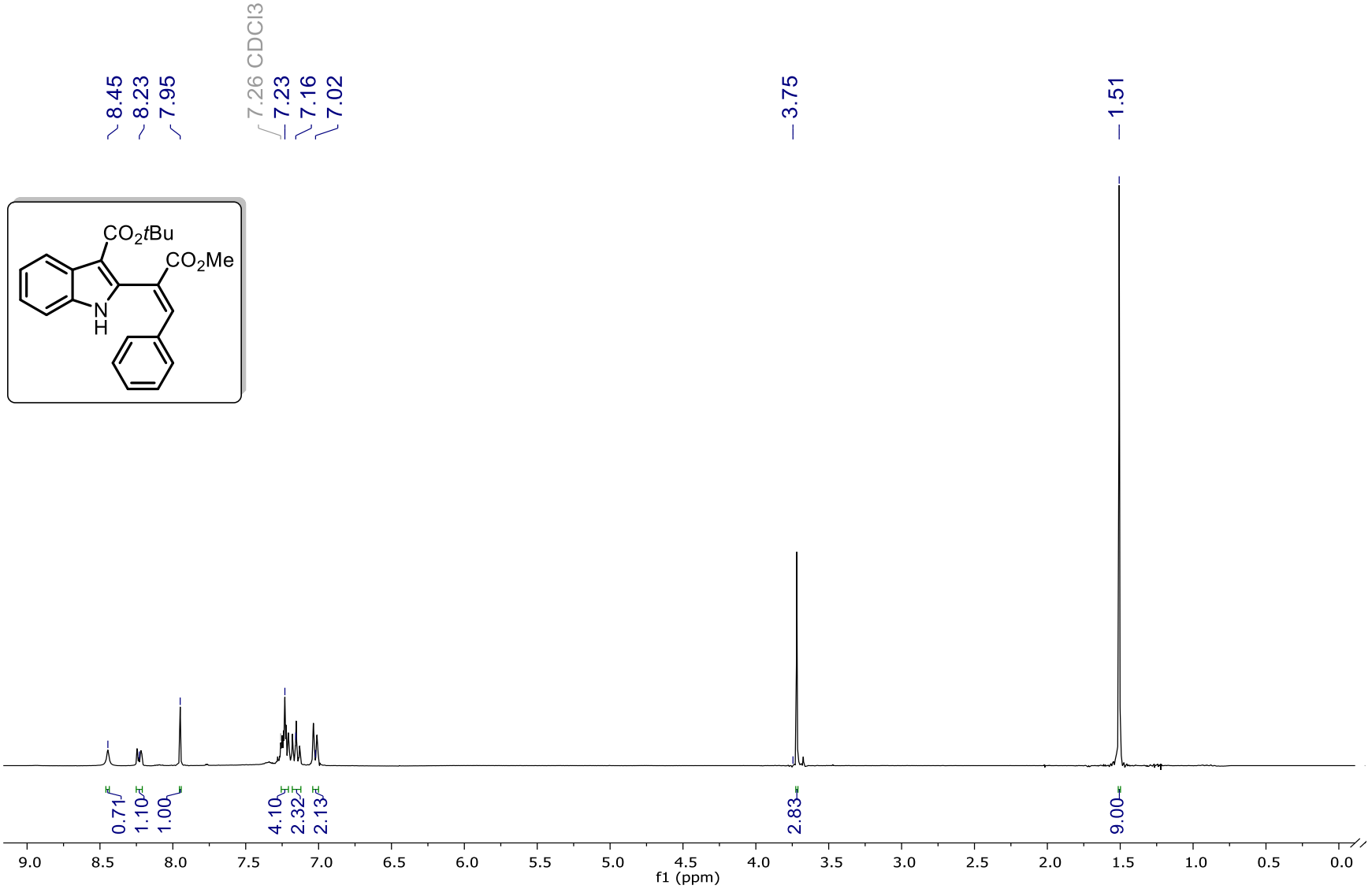

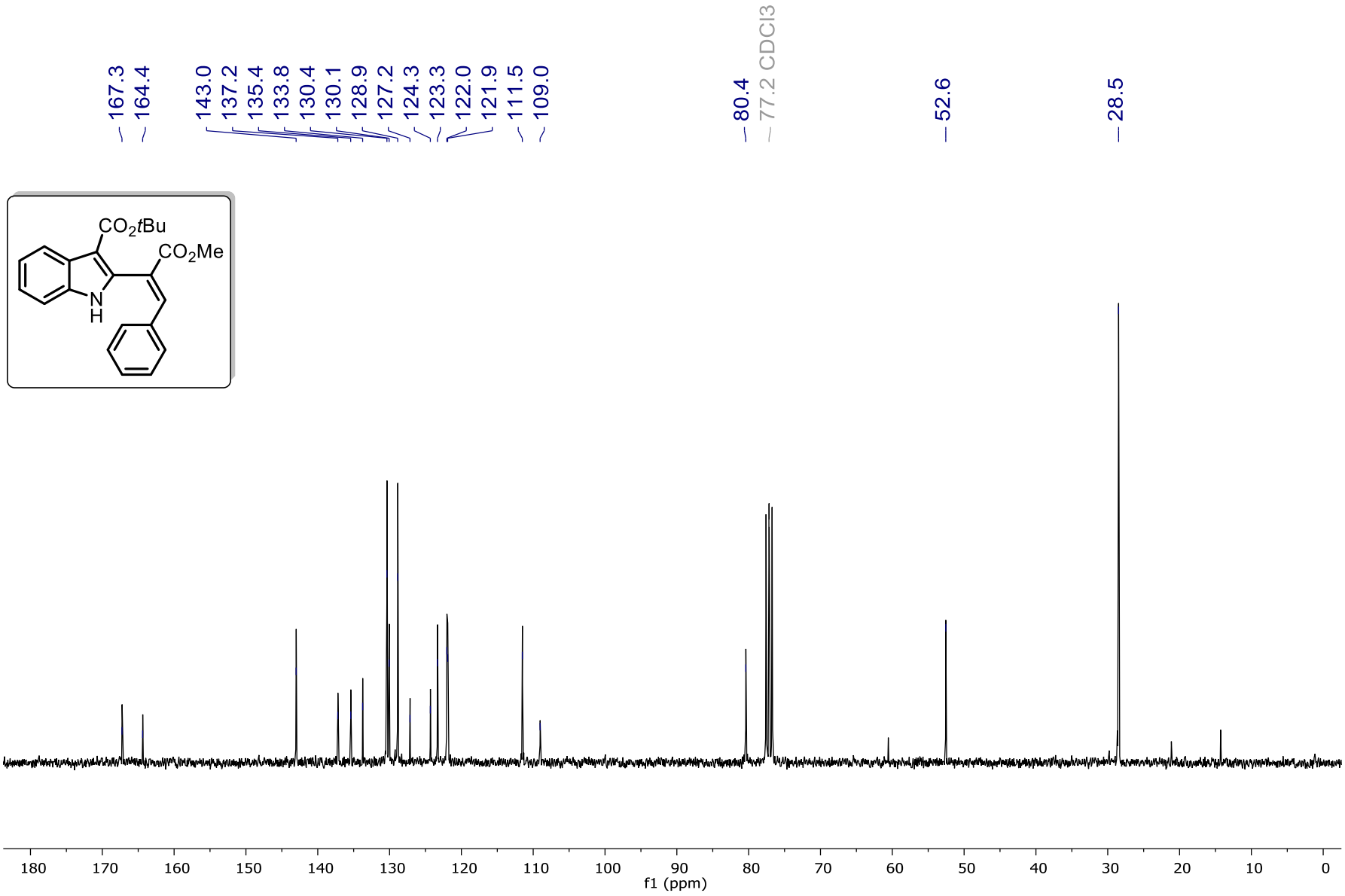
167.3
164.4
143.0
137.2
135.4
133.8
130.4
130.1
128.9
127.2
124.3
123.3
122.0
121.9
111.5
109.0
80.4
77.2 CDCl3
52.6
28.5
CO2tBu
CO2Me
N
H
180
170
160
150
140
130
120
110
100
90
80
70
60
50
40
30
20
10
0
f1 (ppm)

^{1}H and ^{13}C NMR Spectra of 14c

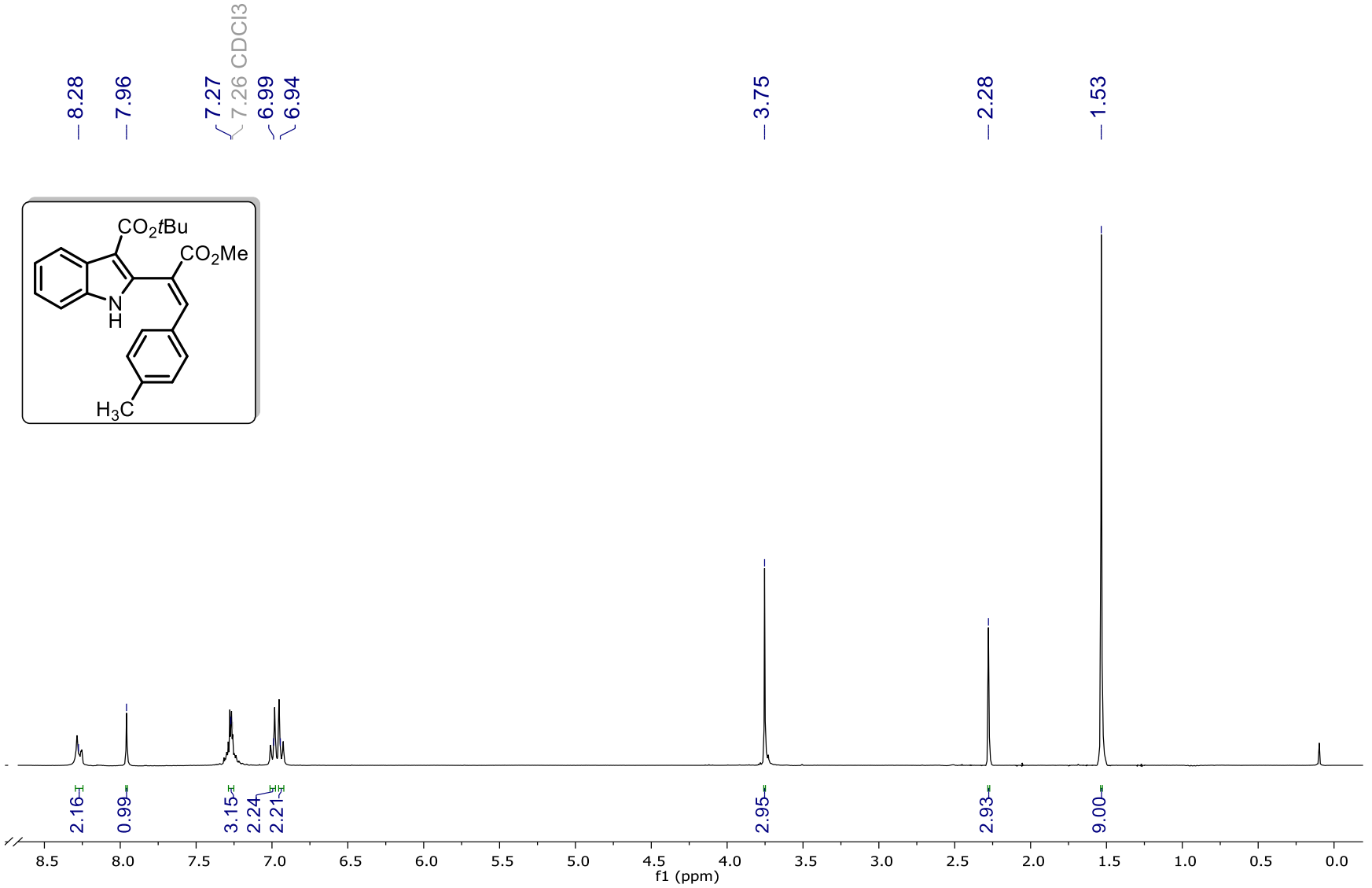

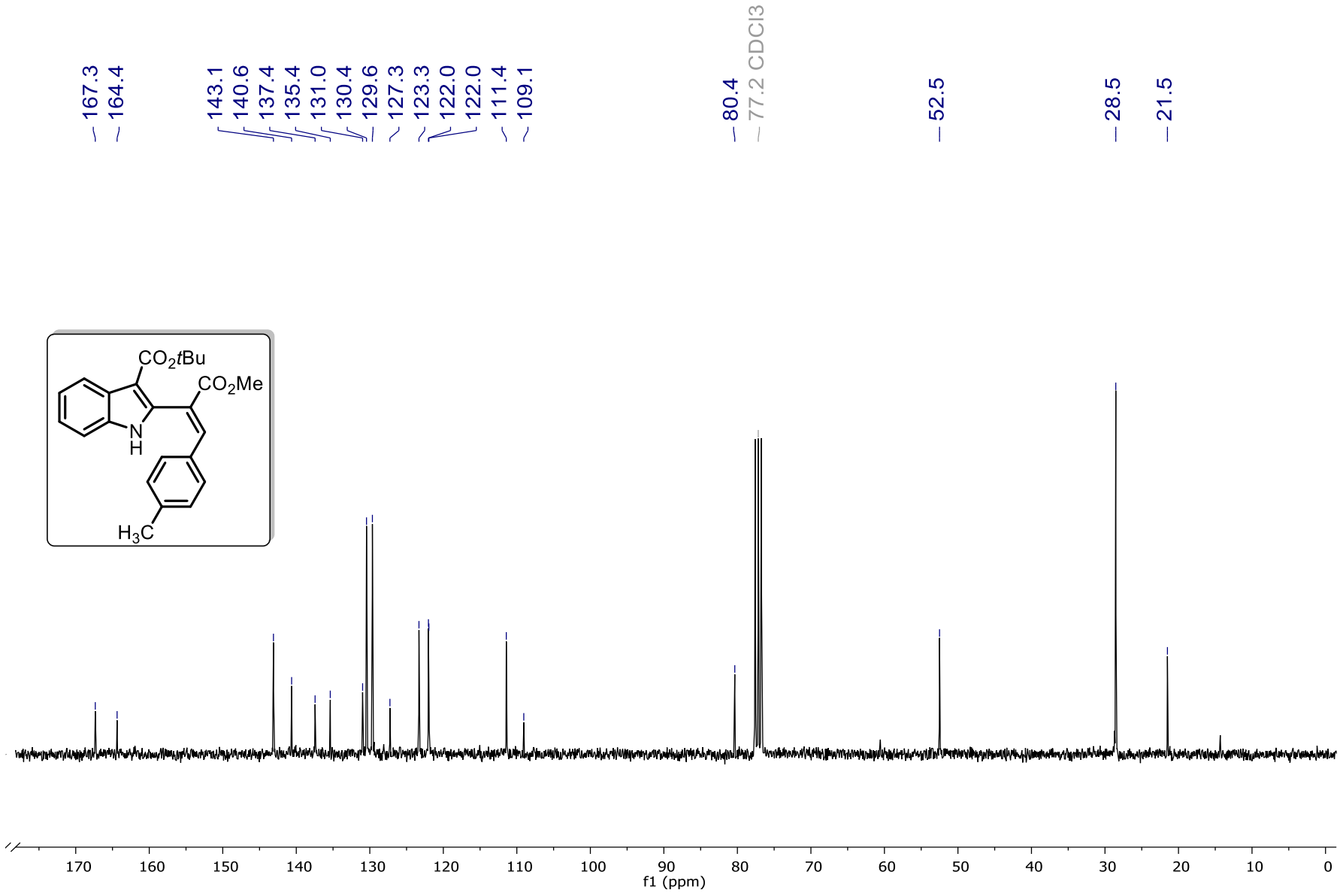
167.3
164.4
143.1
140.6
137.4
135.4
131.0
130.4
129.6
127.3
123.3
122.0
122.0
111.4
109.1
80.4
77.2 CDCl3
52.5
28.5
21.5
CO2tBu
CO2Me
N
H
H3C
170
160
150
140
130
120
110
100
90
80
70
60
50
40
30
20
10
0
f1 (ppm)

^{1}H and ^{13}C NMR Spectra of 14d

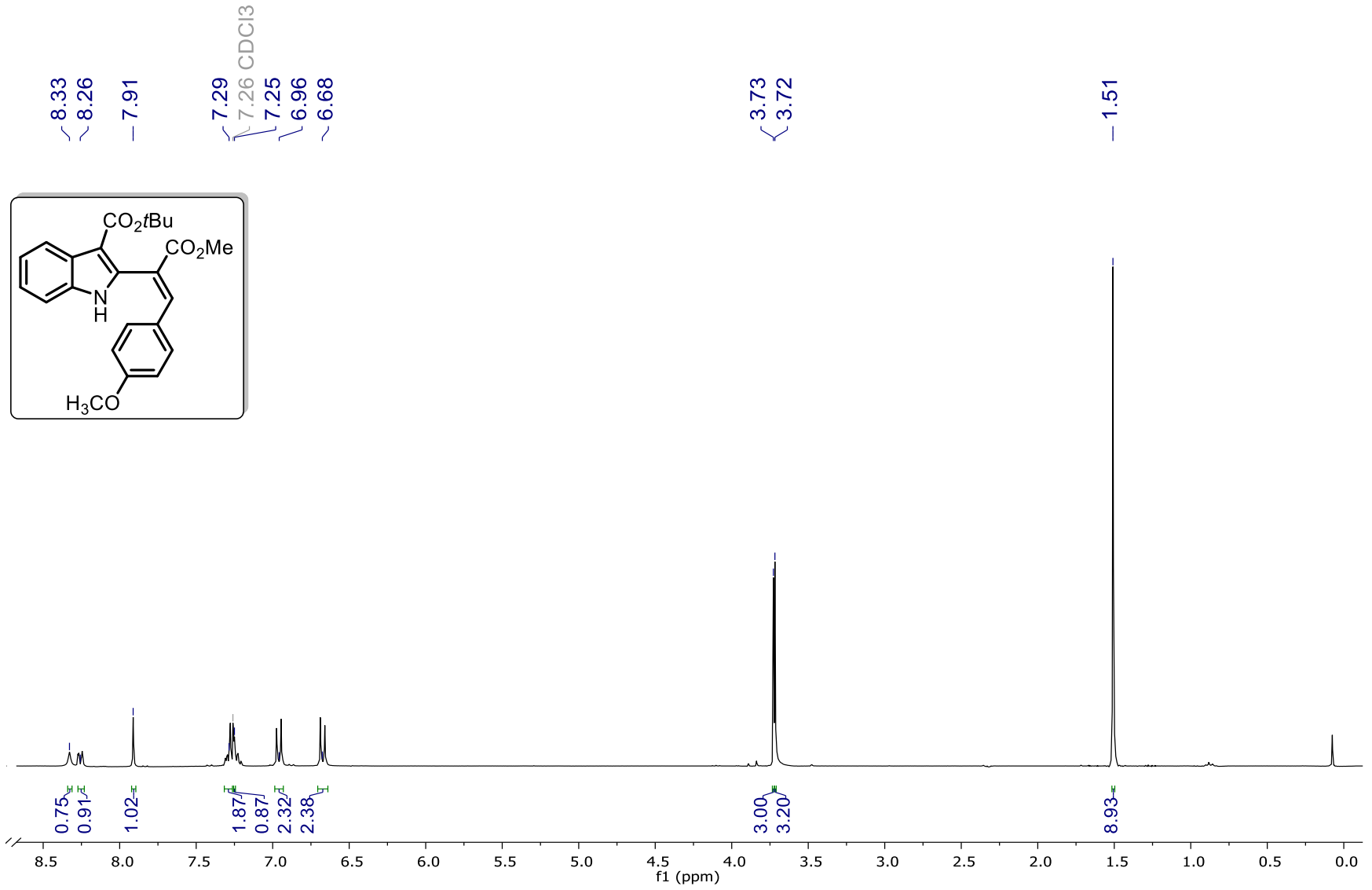

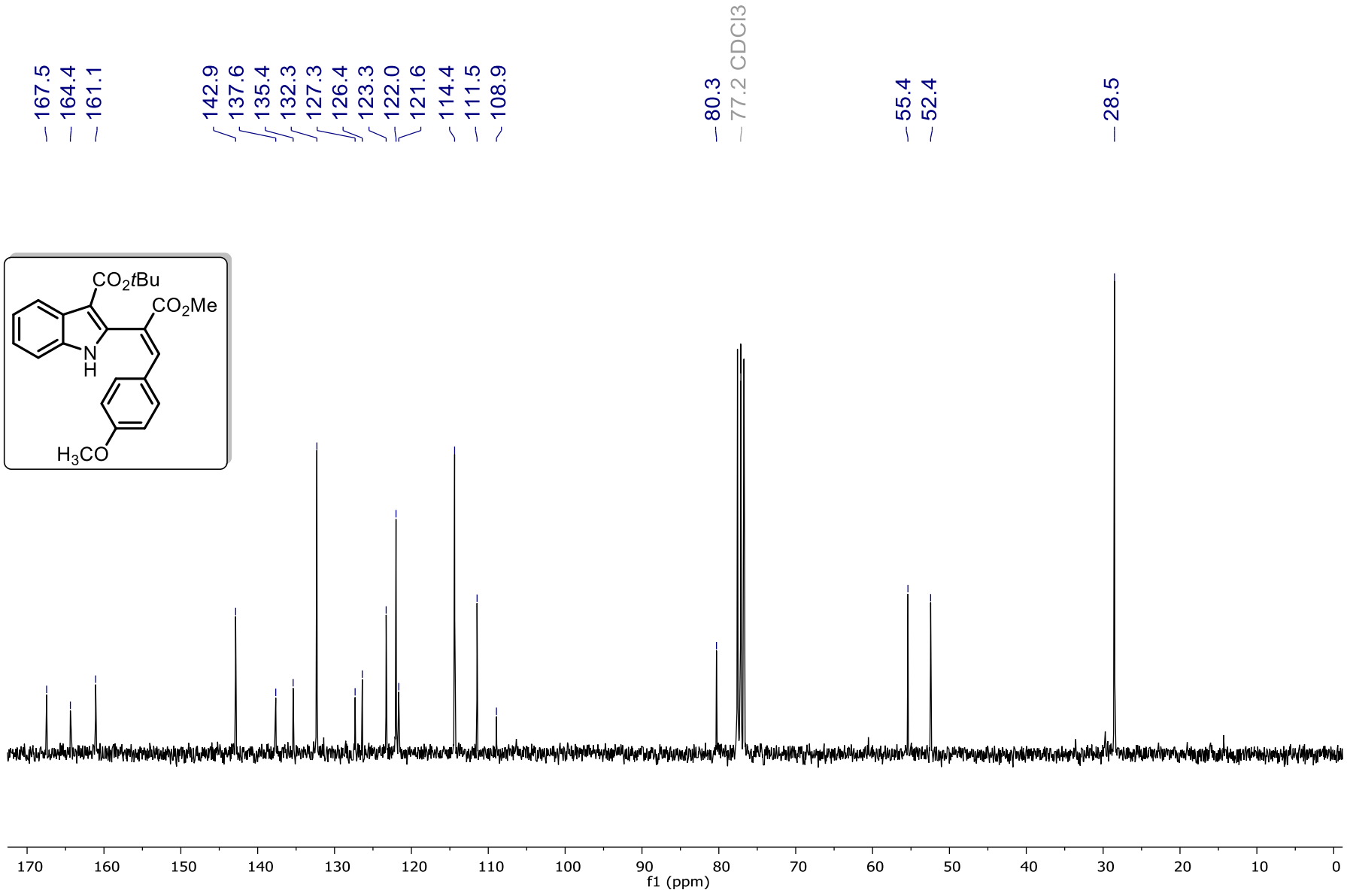
167.5
164.4
161.1
142.9
137.6
135.4
132.3
127.3
126.4
123.3
122.0
121.6
114.4
111.5
108.9
80.3
77.2 CDCl3
55.4
52.4
28.5
CO2tBu
CO2Me
N
H
H3CO
170
160
150
140
130
120
110
100
90
80
70
60
50
40
30
20
10
0
f1 (ppm)

^{1}H and ^{13}C NMR Spectra of 14e

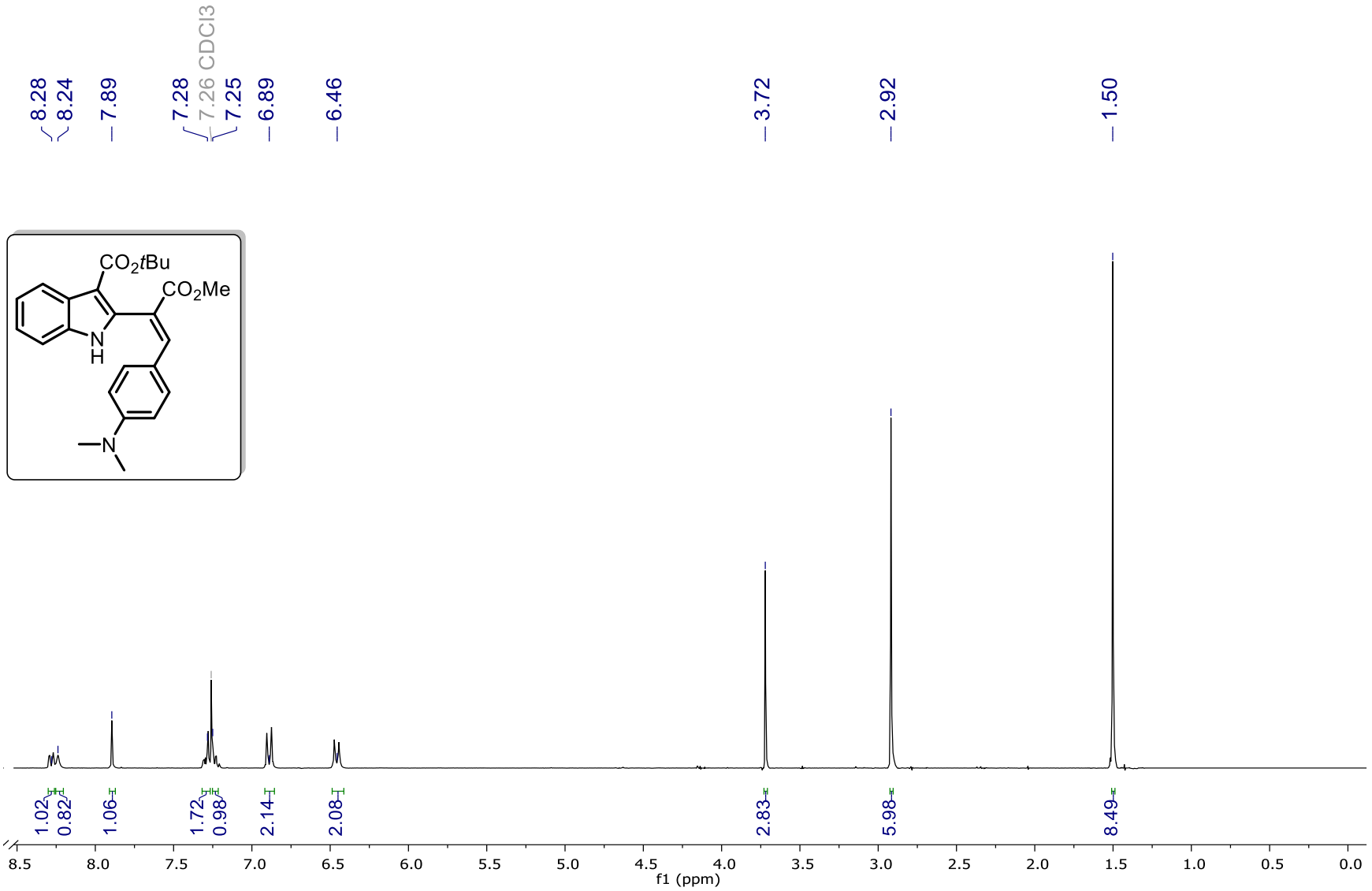

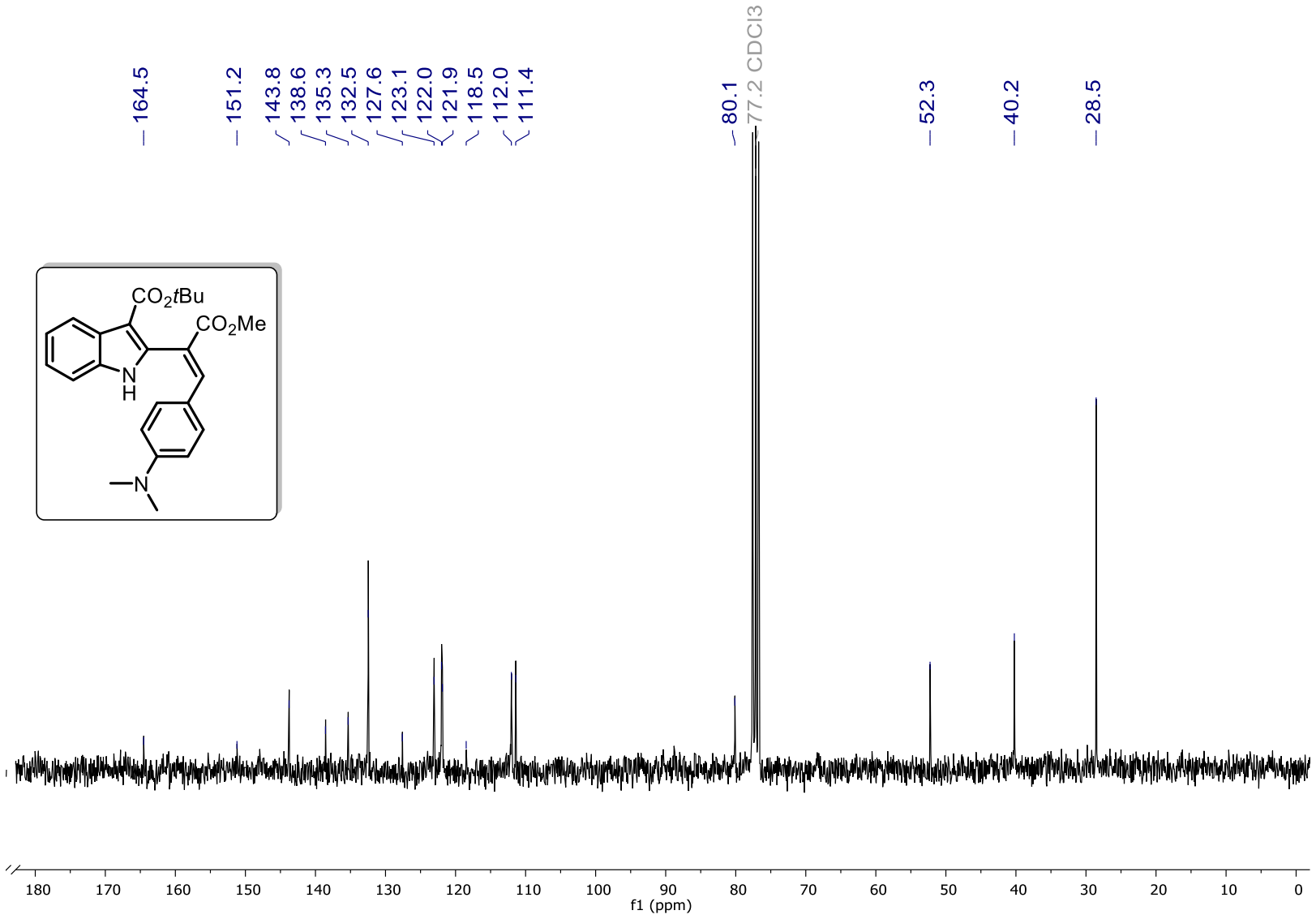
164.5
151.2
143.8
138.6
135.3
132.5
127.6
123.1
122.0
121.9
118.5
112.0
111.4
80.1
77.2 CDCl3
52.3
40.2
28.5
CO2tBu
CO2Me
N
H
N
180
170
160
150
140
130
120
110
100
90
80
70
60
50
40
30
20
10
0
f1 (ppm)

^{1}H and ^{13}C NMR Spectra of 14f

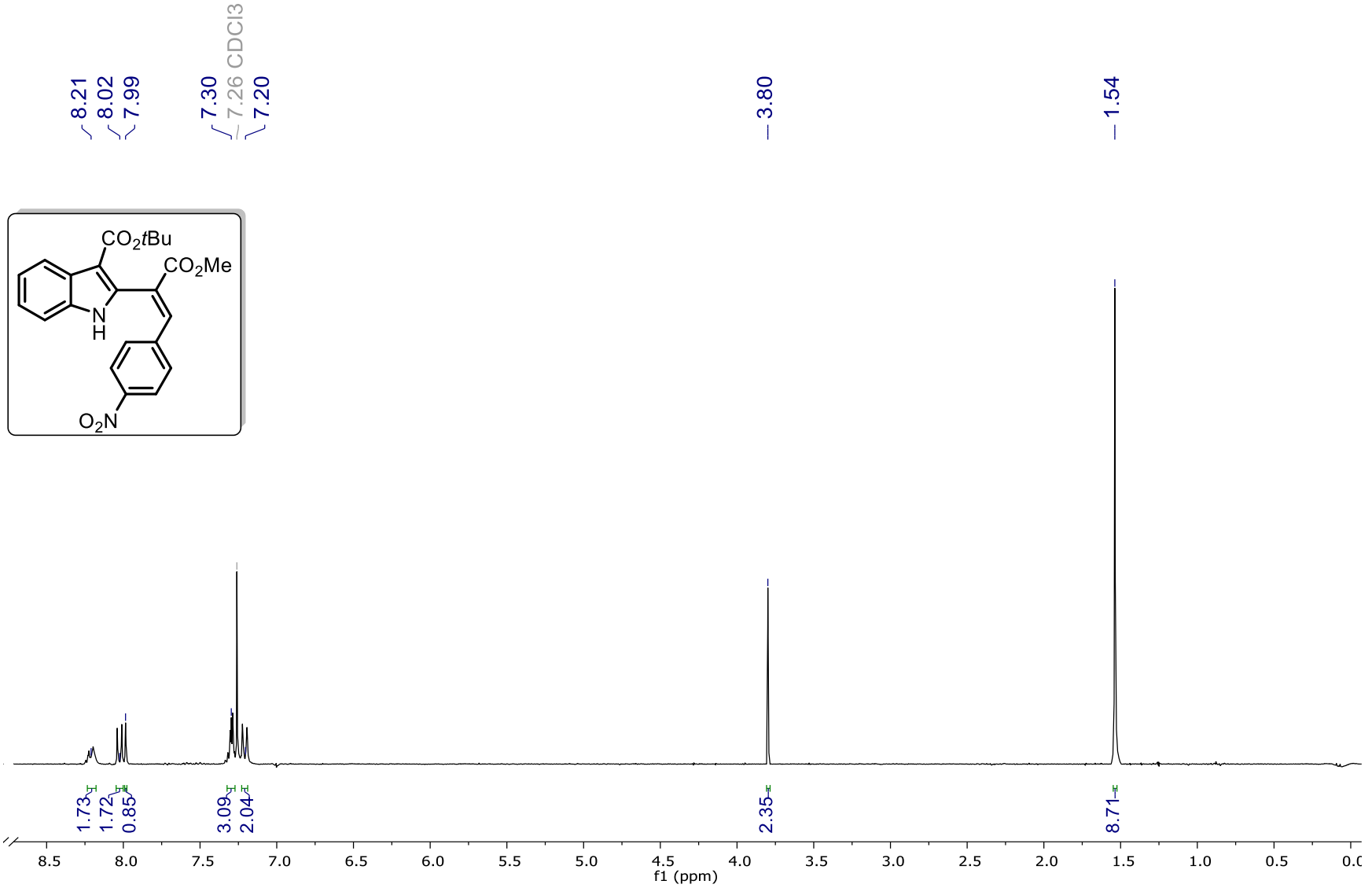

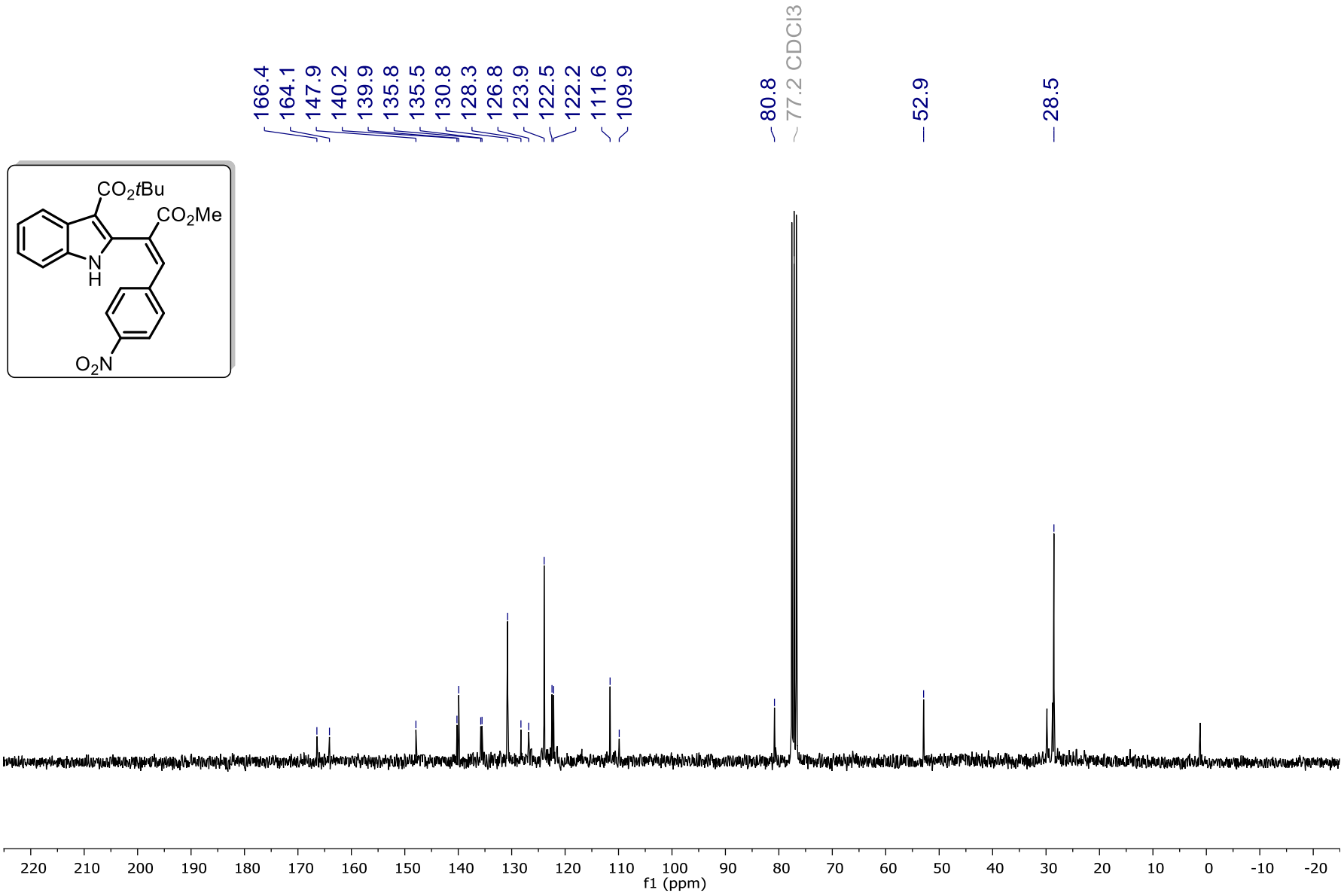
166.4
164.1
147.9
140.2
139.9
135.8
135.5
130.8
128.3
126.8
123.9
122.5
122.2
111.6
109.9
80.8
77.2 CDCl3
52.9
28.5
CO2tBu
CO2Me
N
H
O2N
220 210 200 190 180 170 160 150 140 130 120 110 100 90 80 70 60 50 40 30 20 10 0 -10 -20
f1 (ppm)

^{1}H and ^{13}C NMR Spectra of 14g

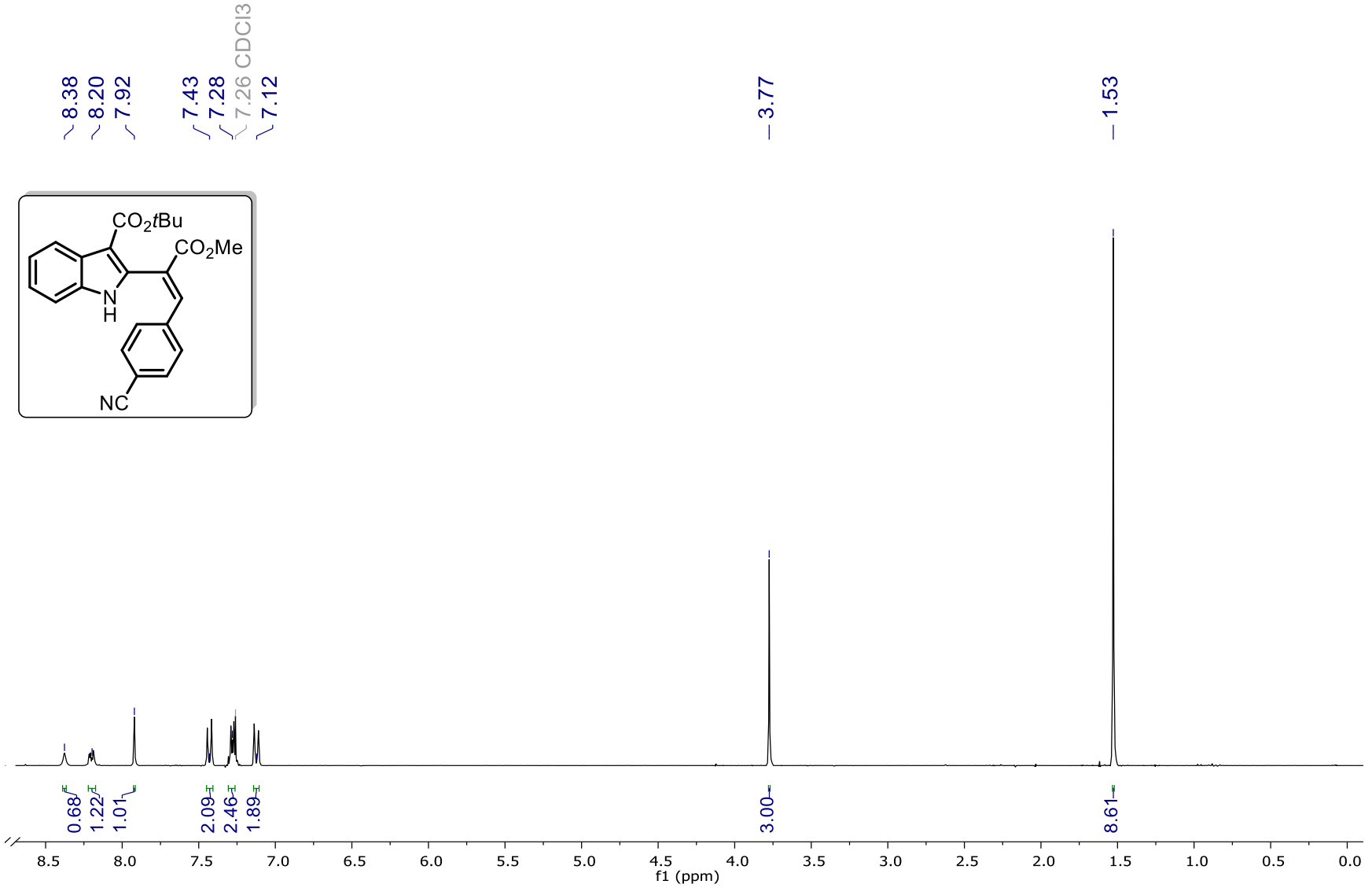

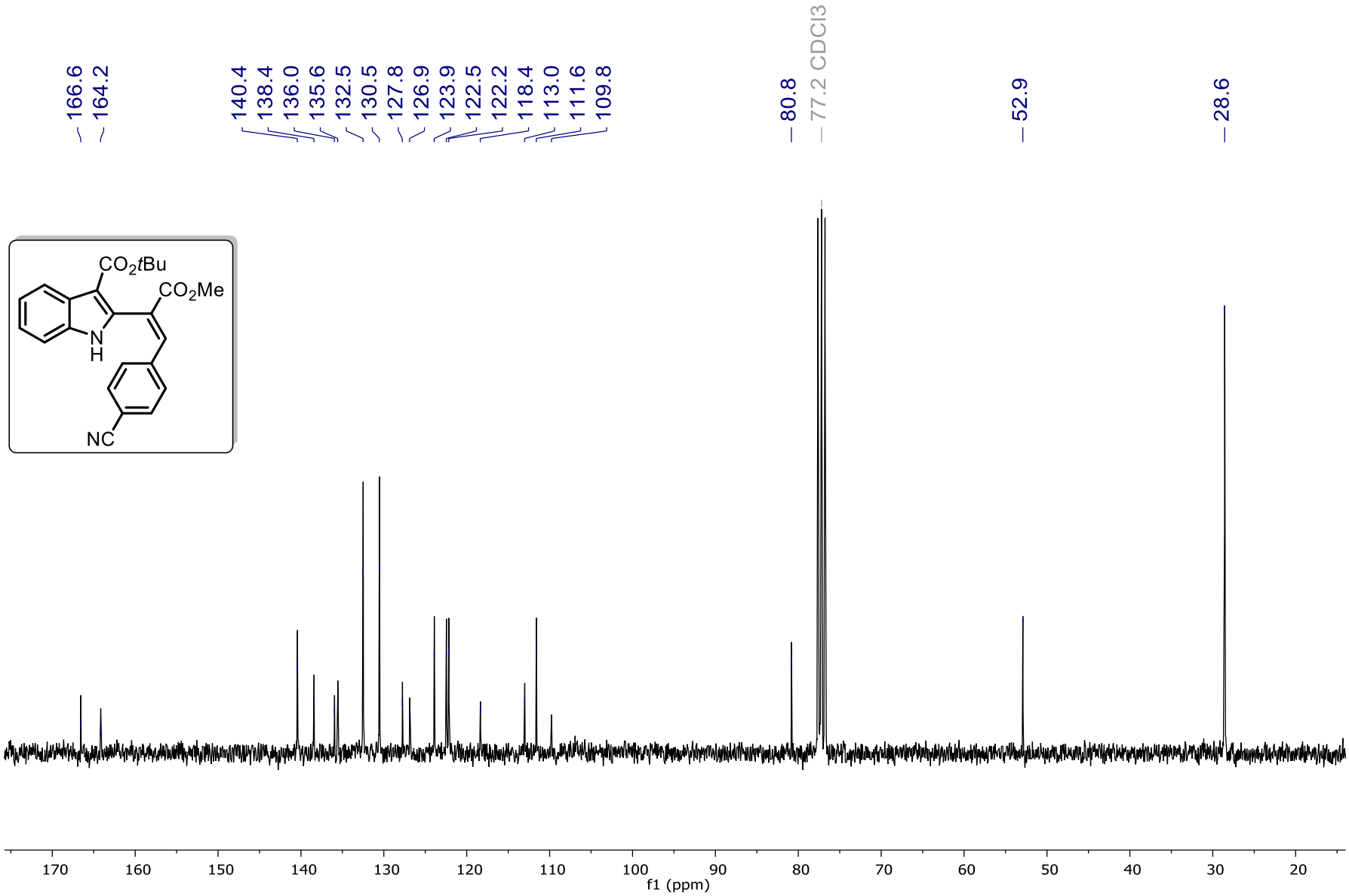
166.6
164.2
140.4
138.4
136.0
135.6
132.5
130.5
127.8
126.9
123.9
122.5
122.2
118.4
113.0
111.6
109.8
80.8
77.2 CDCl3
52.9
28.6
CO2tBu
CO2Me
N
H
NC
170
160
150
140
130
120
110
100
90
80
70
60
50
40
30
20
f1 (ppm)

^{1}H and ^{13}C NMR Spectra of 14h

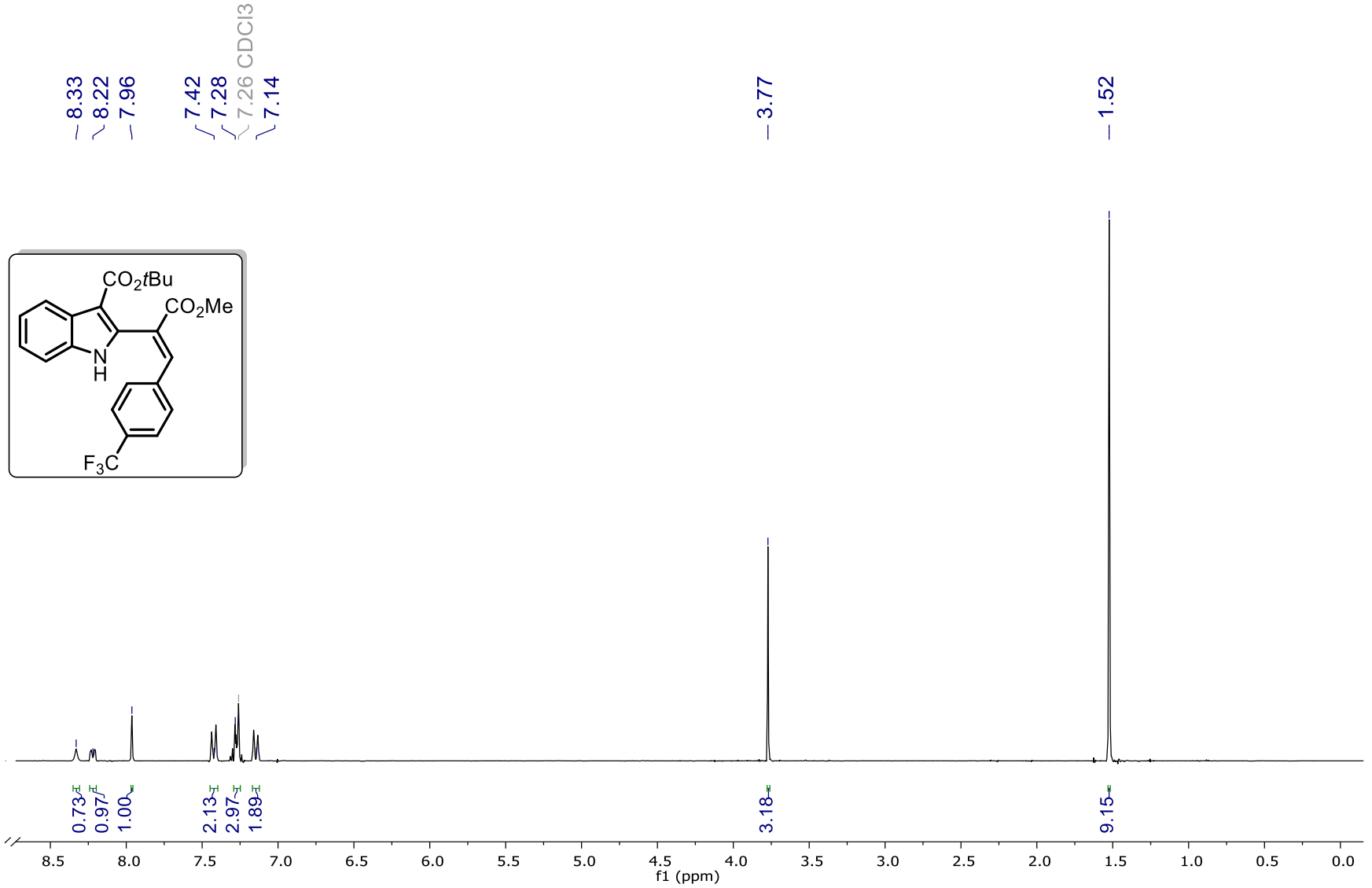

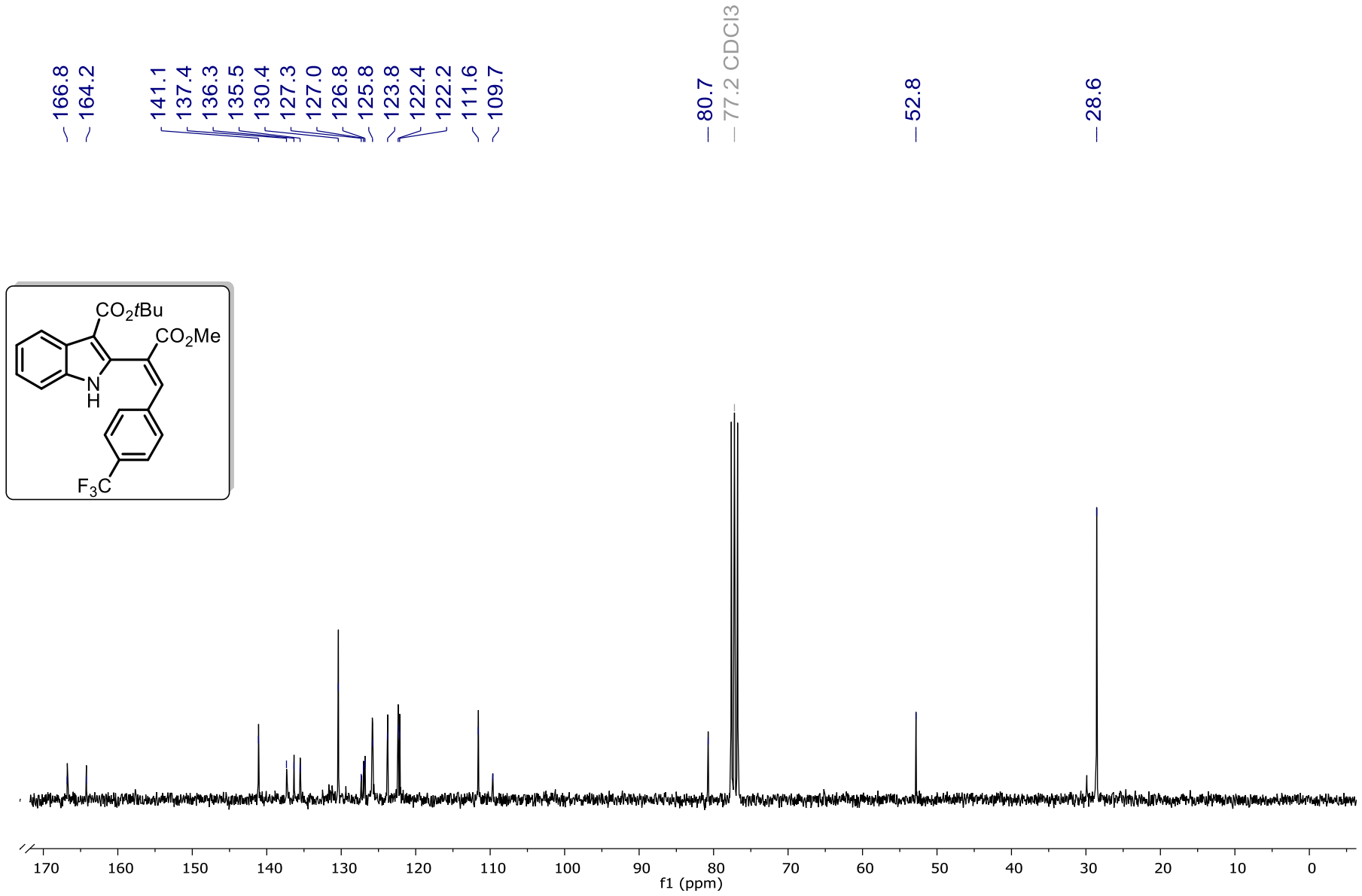
166.8
164.2
141.1
137.4
136.3
135.5
130.4
127.3
127.0
126.8
125.8
123.8
122.4
122.2
111.6
109.7
80.7
77.2 CDCl3
52.8
28.6
CO2tBu
CO2Me
N
H
F3C
170
160
150
140
130
120
110
100
90
80
70
60
50
40
30
20
10
0
f1 (ppm)

^{1}H and ^{13}C NMR Spectra of 14i

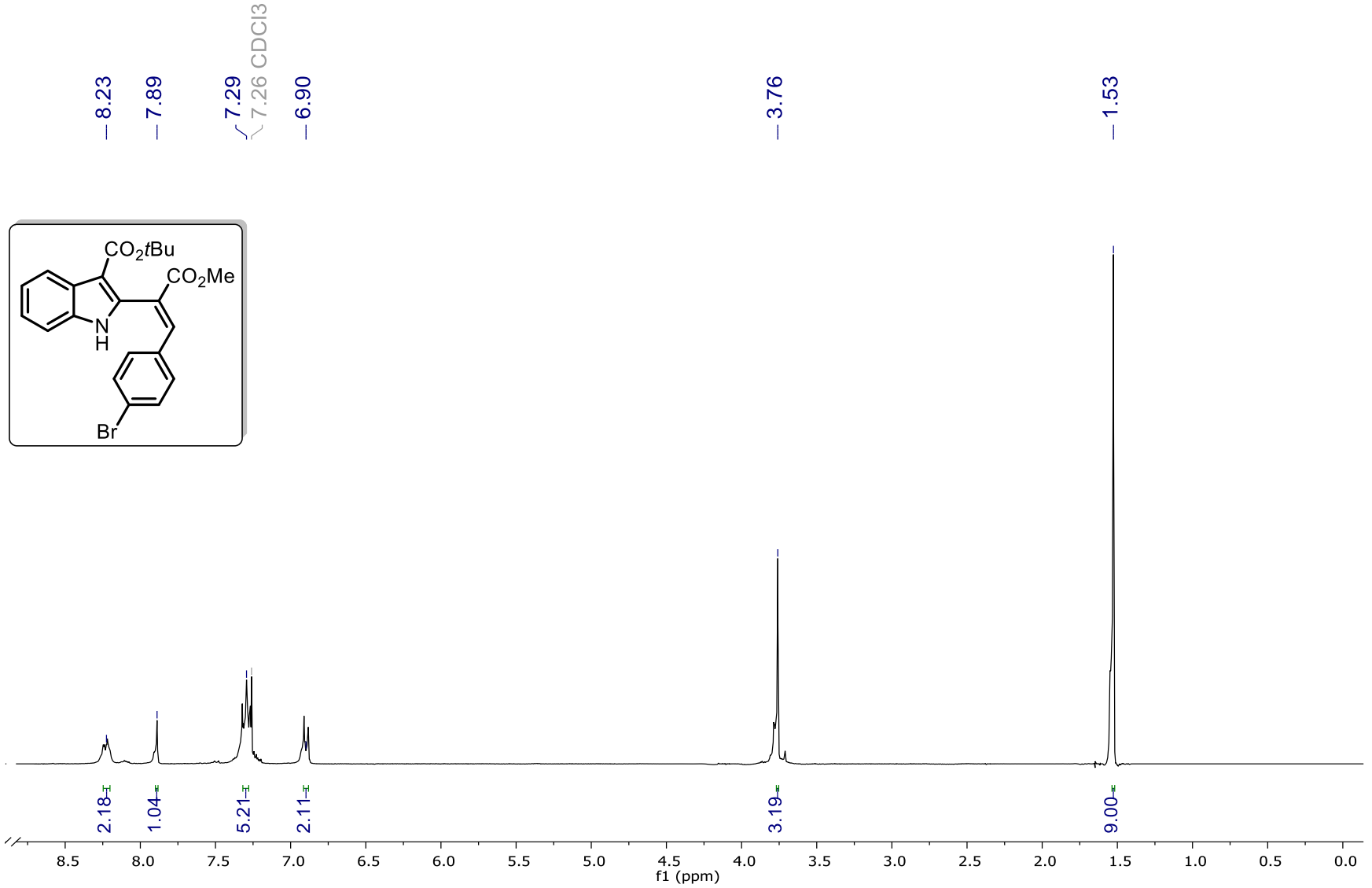

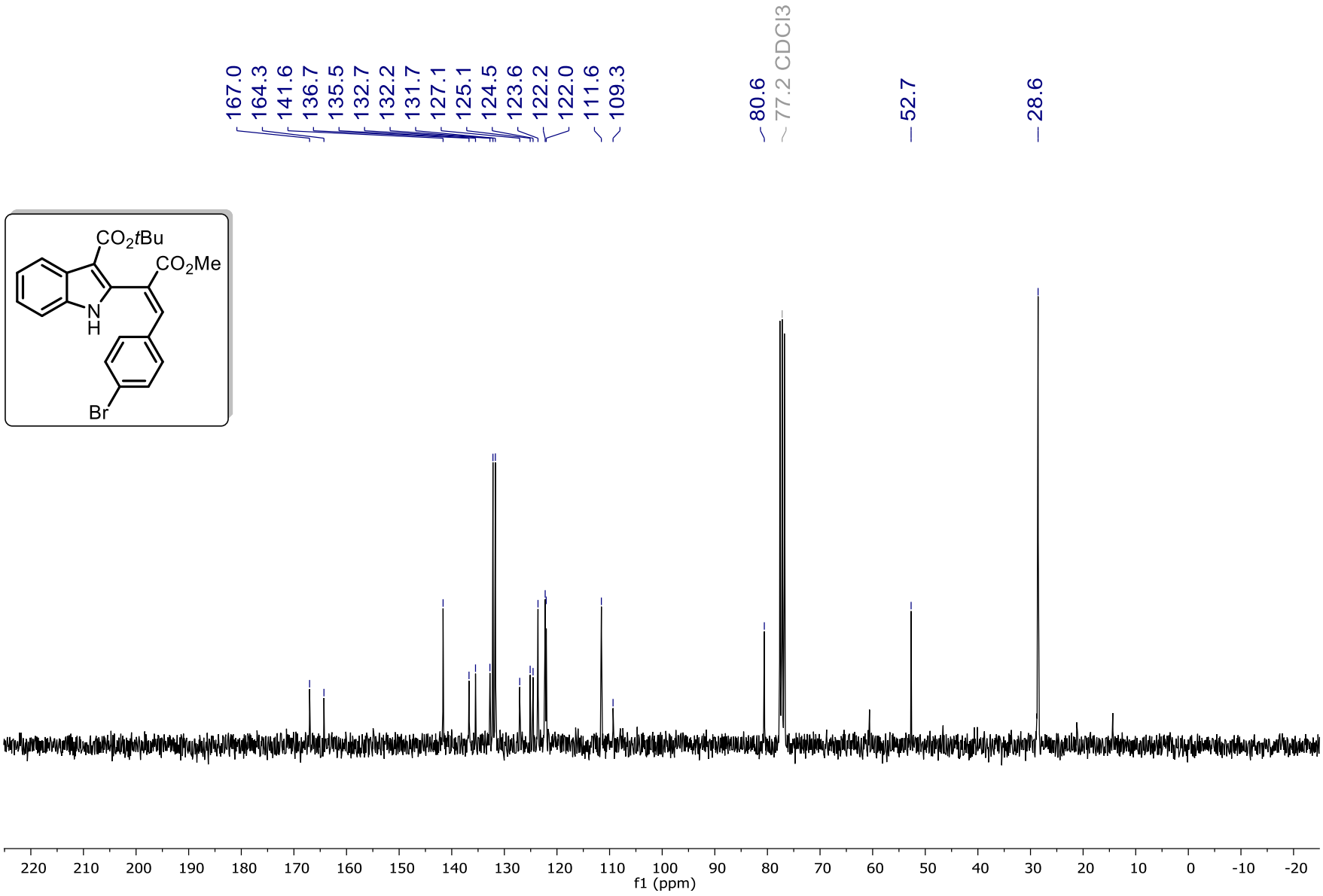
167.0
164.3
141.6
136.7
135.5
132.7
132.2
131.7
127.1
125.1
124.5
123.6
122.2
122.0
111.6
109.3
80.6
77.2 CDCl3
52.7
28.6
CO2tBu
CO2Me
N
H
Br
220 210 200 190 180 170 160 150 140 130 120 110 100 90 80 70 60 50 40 30 20 10 0 -10 -20
f1 (ppm)

^{1}H and ^{13}C NMR Spectra of 14j

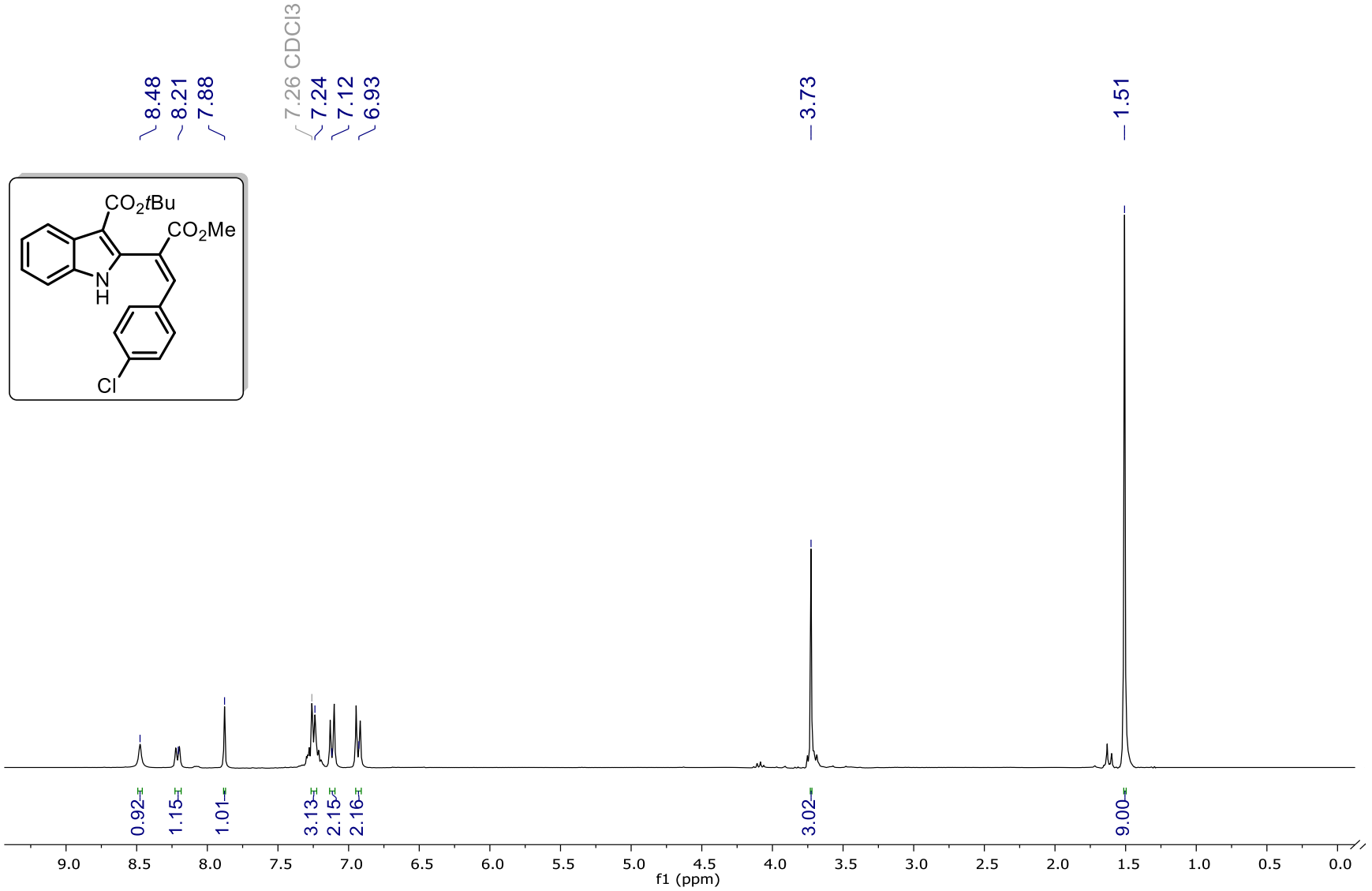

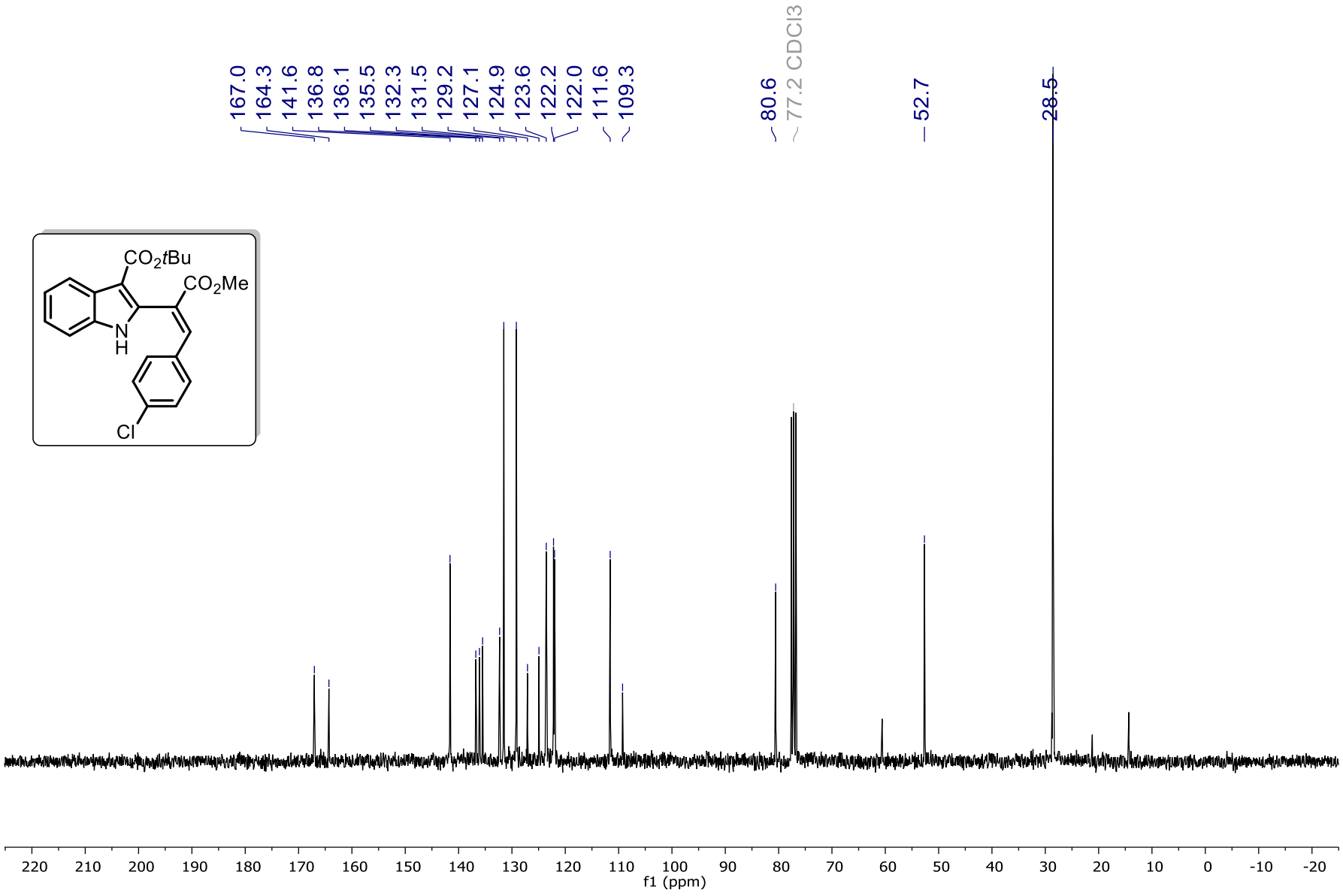
167.0
164.3
141.6
136.8
136.1
135.5
132.3
131.5
129.2
127.1
124.9
123.6
122.2
122.0
111.6
109.3
80.6
77.2 CDCl3
52.7
28.5
CO2tBu
CO2Me
N
H
Cl
220 210 200 190 180 170 160 150 140 130 120 110 100 90 80 70 60 50 40 30 20 10 0 -10 -20
f1 (ppm)

^{1}H and ^{13}C NMR Spectra of 14k

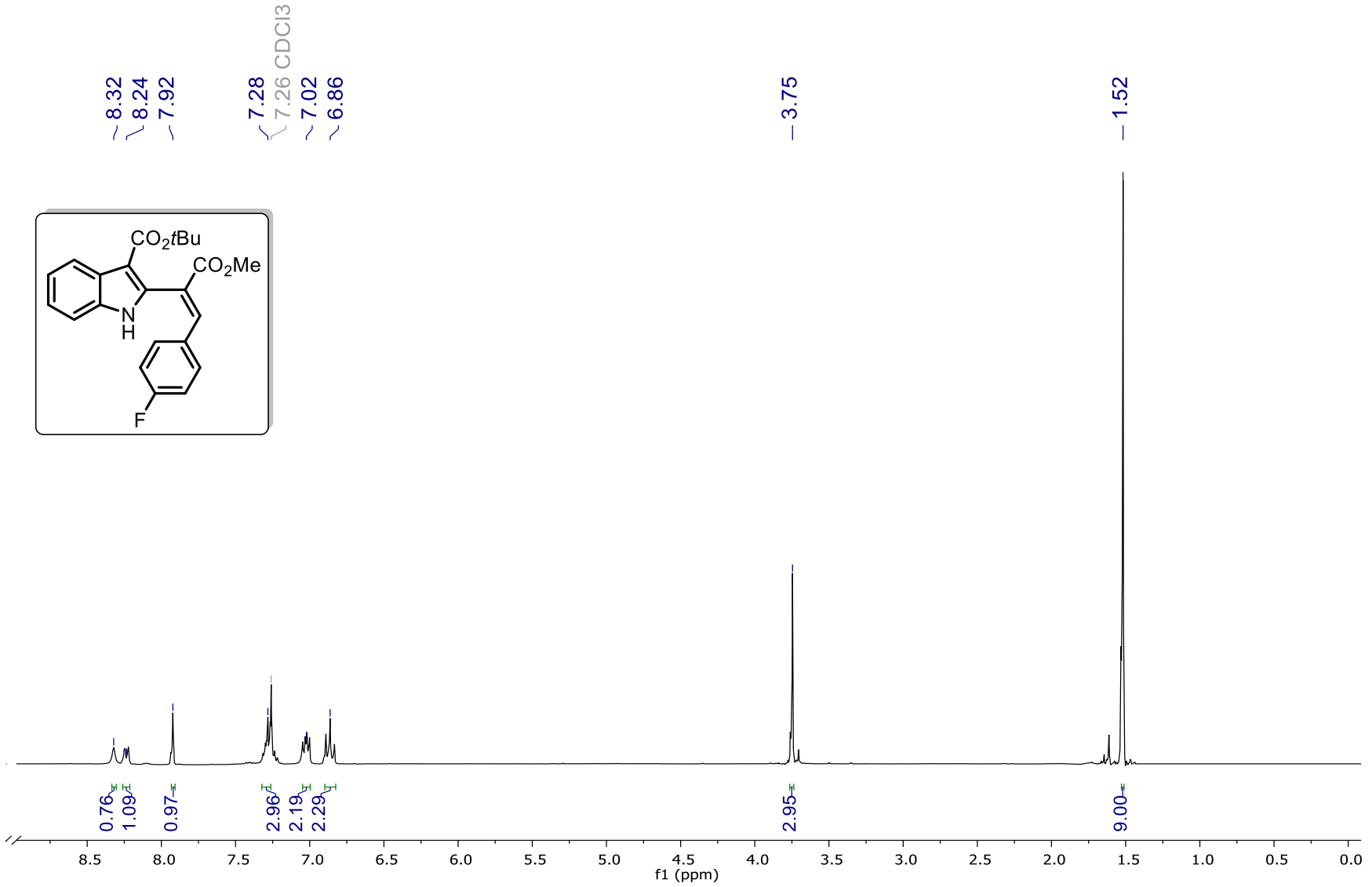

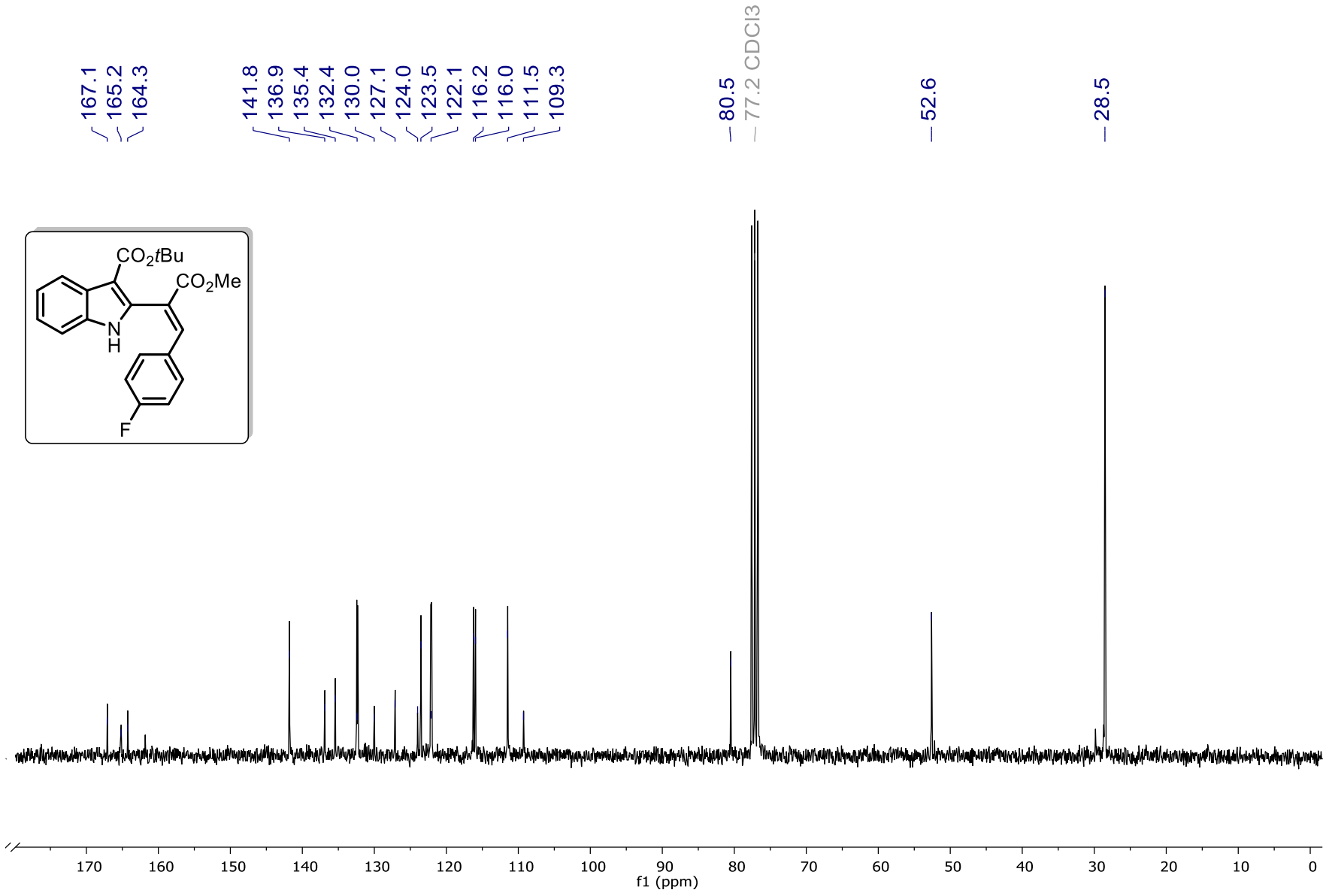
167.1
165.2
164.3
141.8
136.9
135.4
132.4
130.0
127.1
124.0
123.5
122.1
116.2
116.0
111.5
109.3
80.5
77.2 CDCl3
52.6
28.5
CO2tBu
CO2Me
N
H
F
170
160
150
140
130
120
110
100
90
80
70
60
50
40
30
20
10
0
f1 (ppm)

^{1}H, ^{13}C NMR and NOESY Spectra of prenostodione (3a)

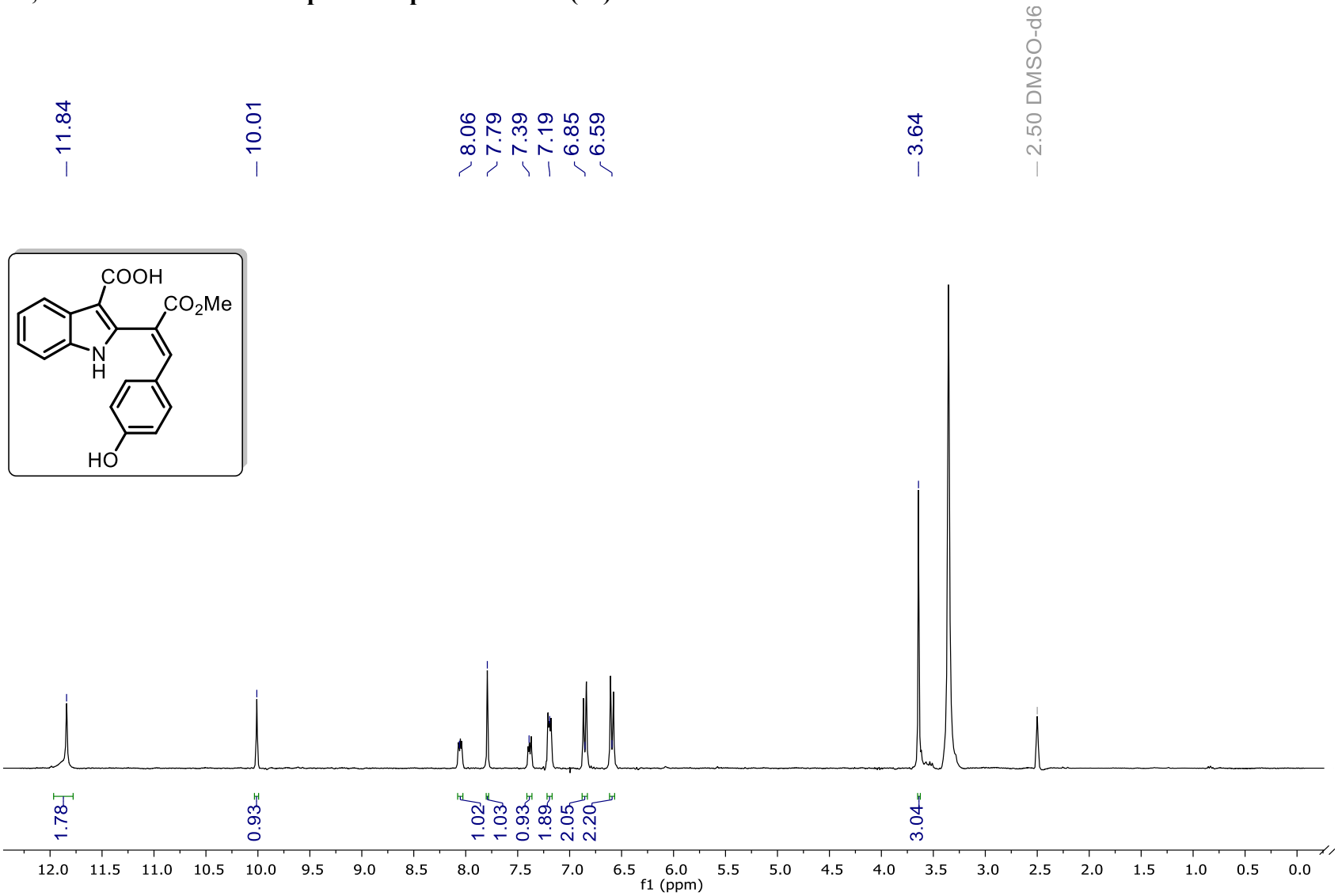

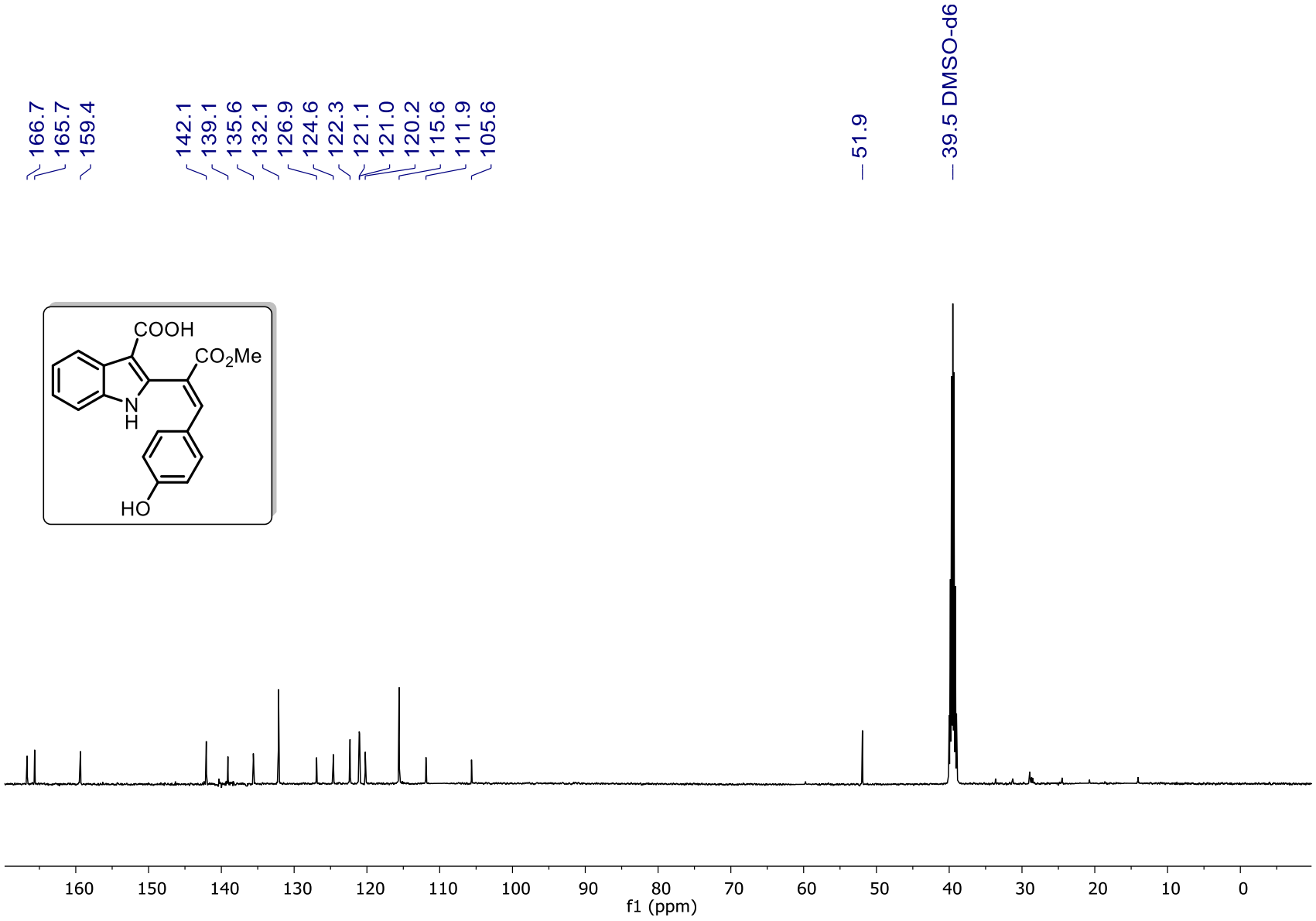
166.7
165.7
159.4
142.1
139.1
135.6
132.1
126.9
124.6
122.3
121.1
121.0
120.2
115.6
111.9
105.6
51.9
39.5 DMSO-d6
COOH
CO2Me
N
H
HO
160
150
140
130
120
110
100
90
80
70
60
50
40
30
20
10
0
f1 (ppm)

^{1}H, ^{13}C NMR and NOESY Spectra of prenostodione (3a)

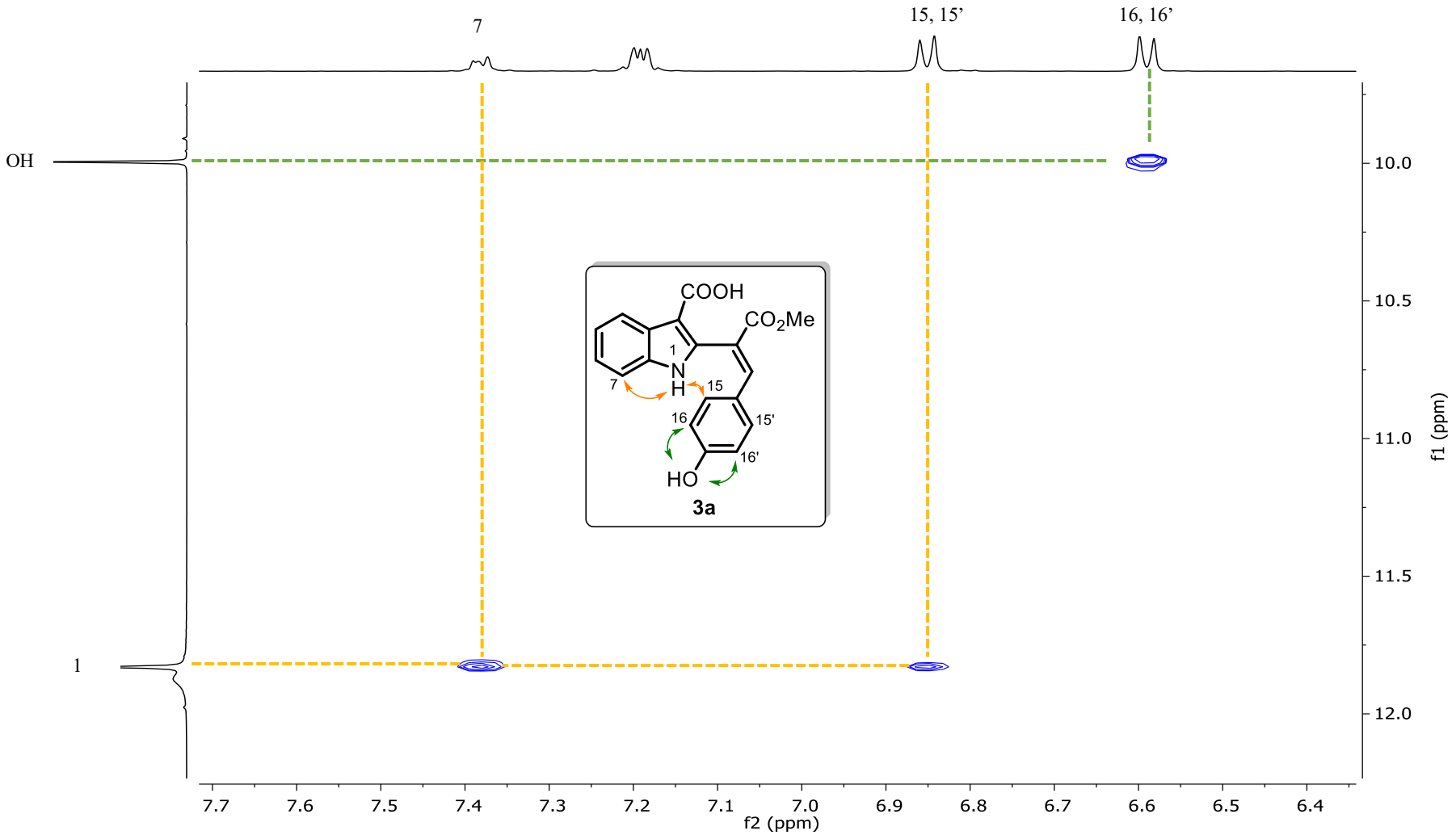

^{1}H and ^{13}C NMR Spectra of 3b

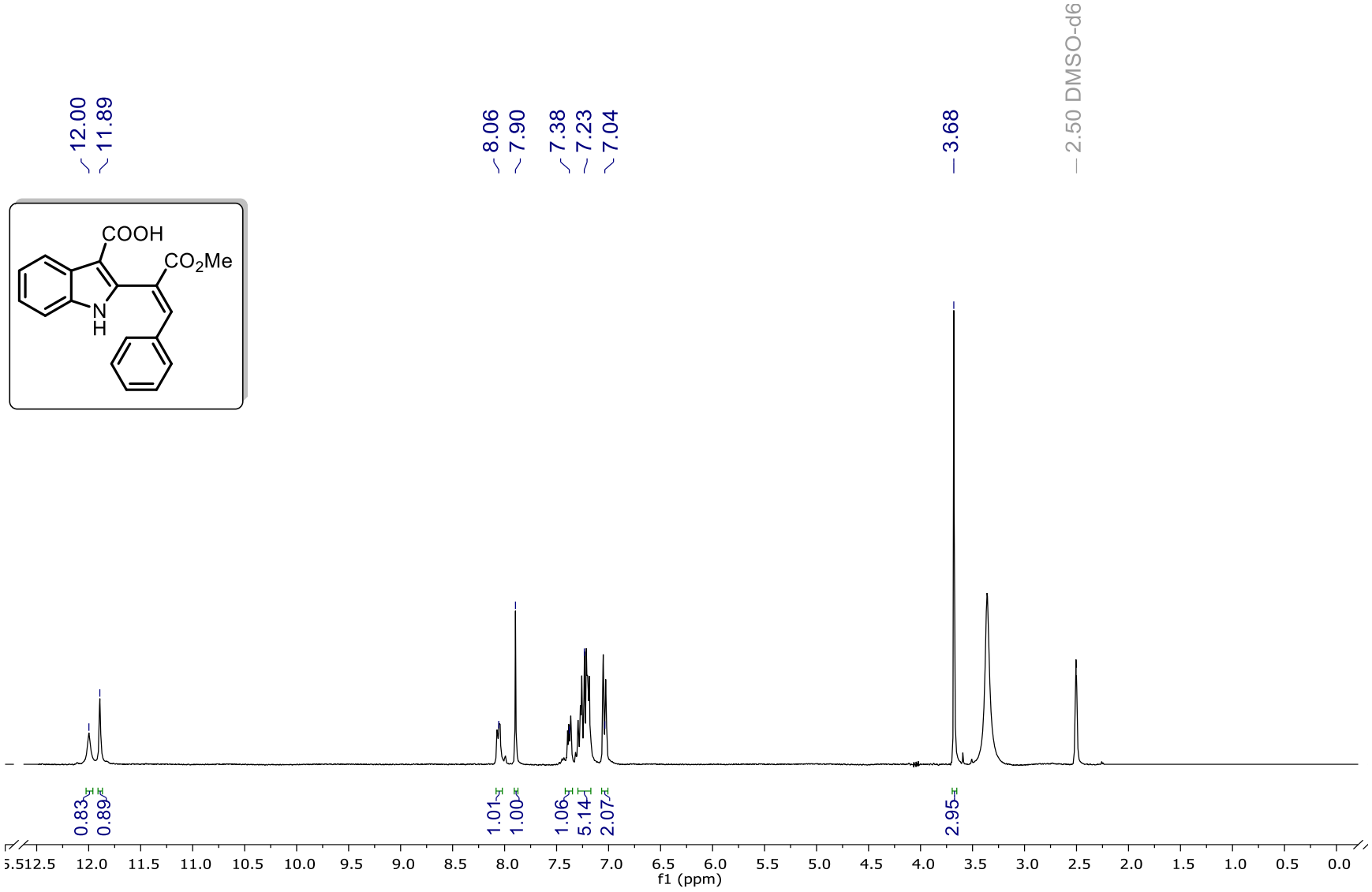

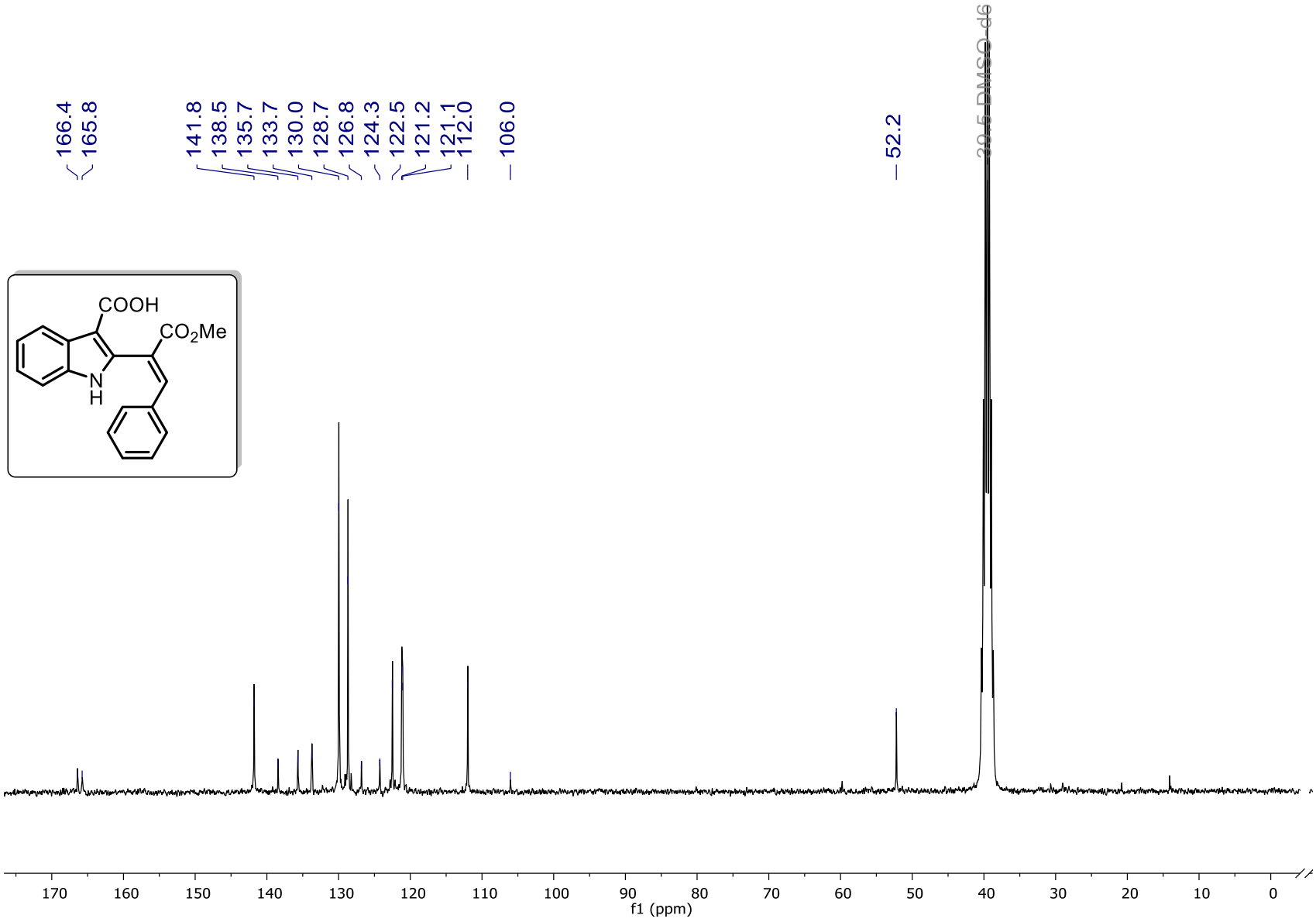
166.4
165.8
141.8
138.5
135.7
133.7
130.0
128.7
126.8
124.3
122.5
121.2
121.1
112.0
106.0
52.2
39.5 DMSO-d6
COOH
CO2Me
N
H
170
160
150
140
130
120
110
100
90
80
70
60
50
40
30
20
10
0
f1 (ppm)

^{1}H and ^{13}C NMR Spectra of 3c

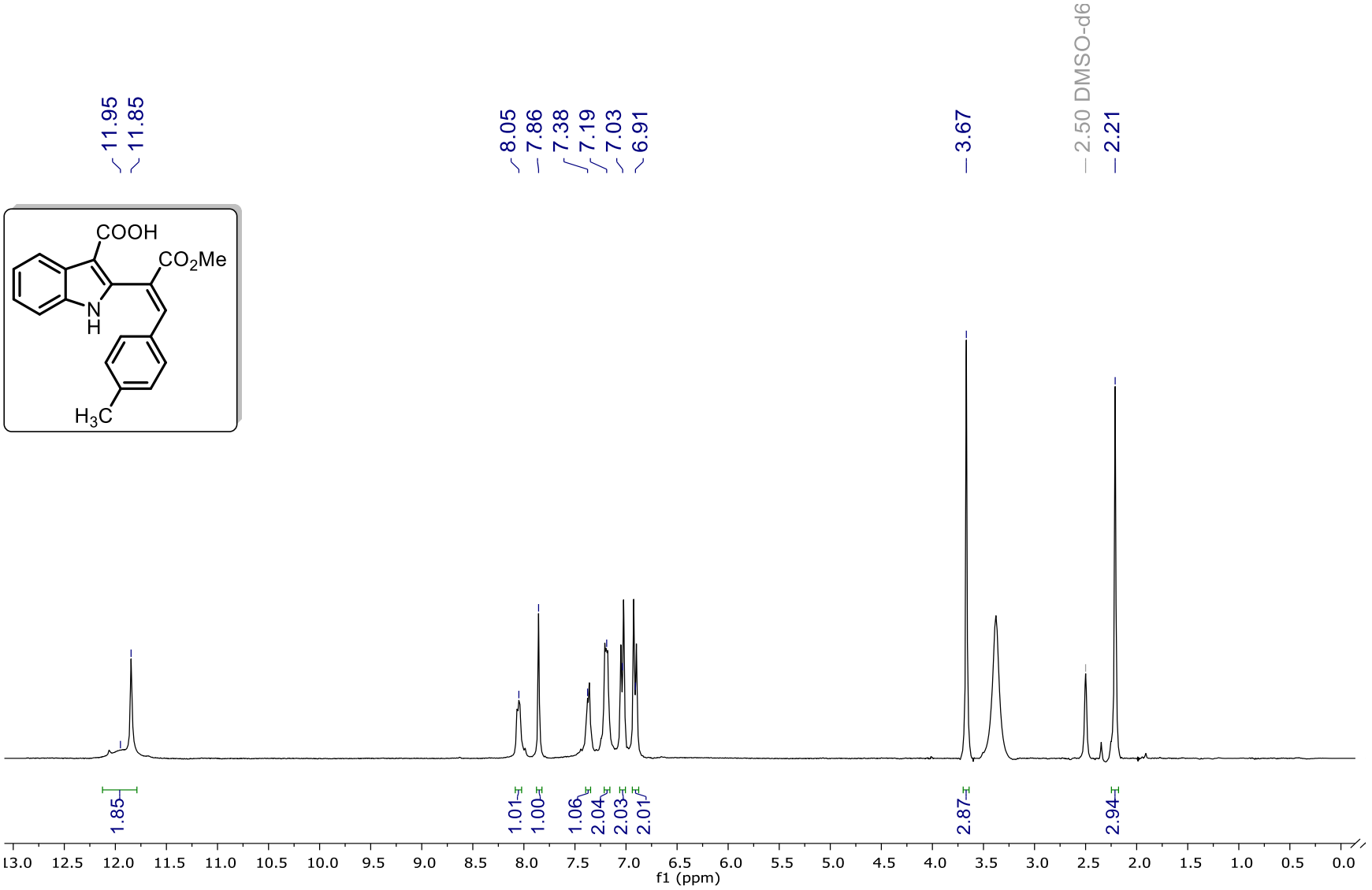

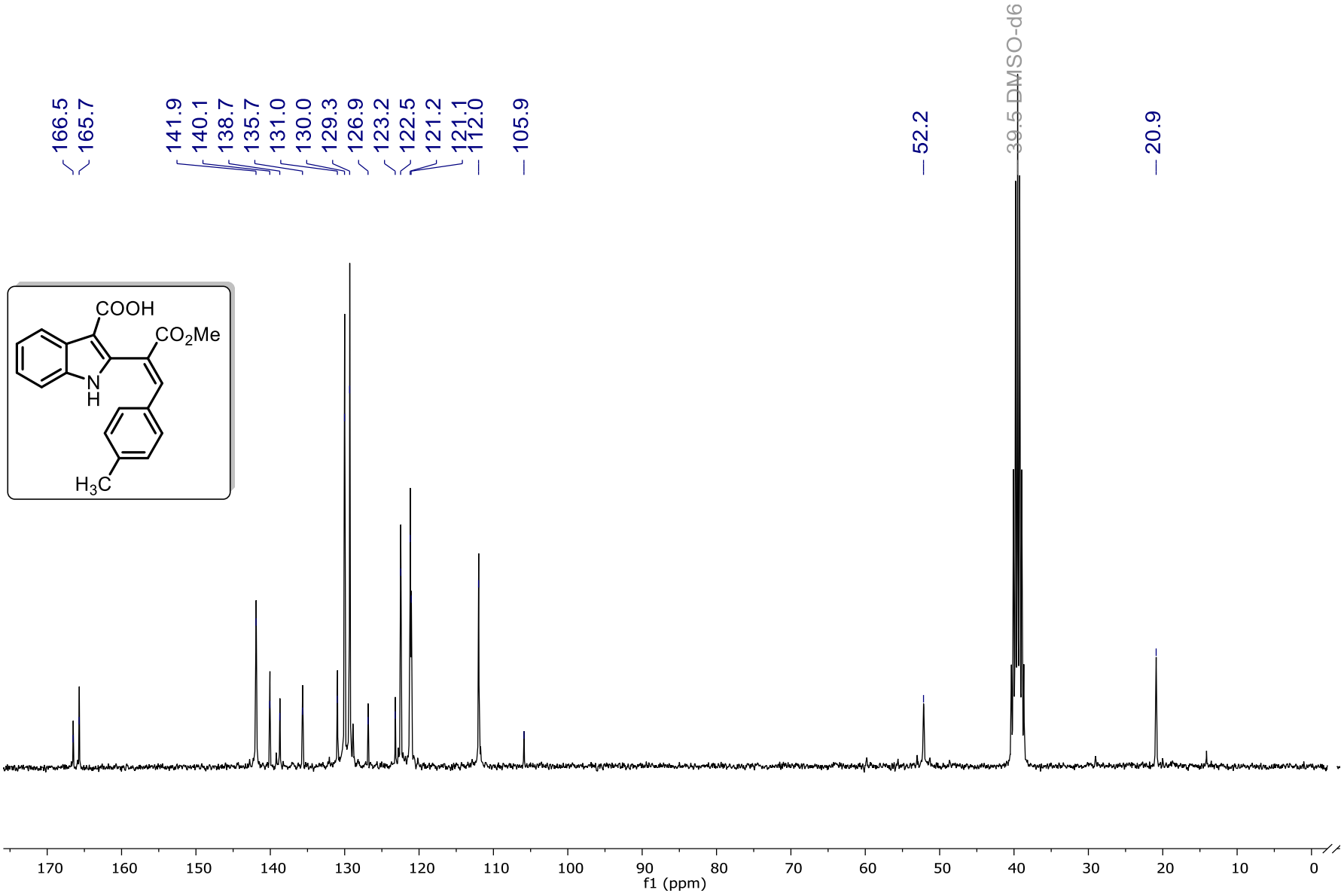
166.5
165.7
141.9
140.1
138.7
135.7
131.0
130.0
129.3
126.9
123.2
122.5
121.2
121.1
112.0
105.9
52.2
39.5 DMSO-d6
20.9
COOH
CO2Me
N
H
H3C
170
160
150
140
130
120
110
100
90
80
70
60
50
40
30
20
10
0
f1 (ppm)

^{1}H and ^{13}C NMR Spectra of 3d

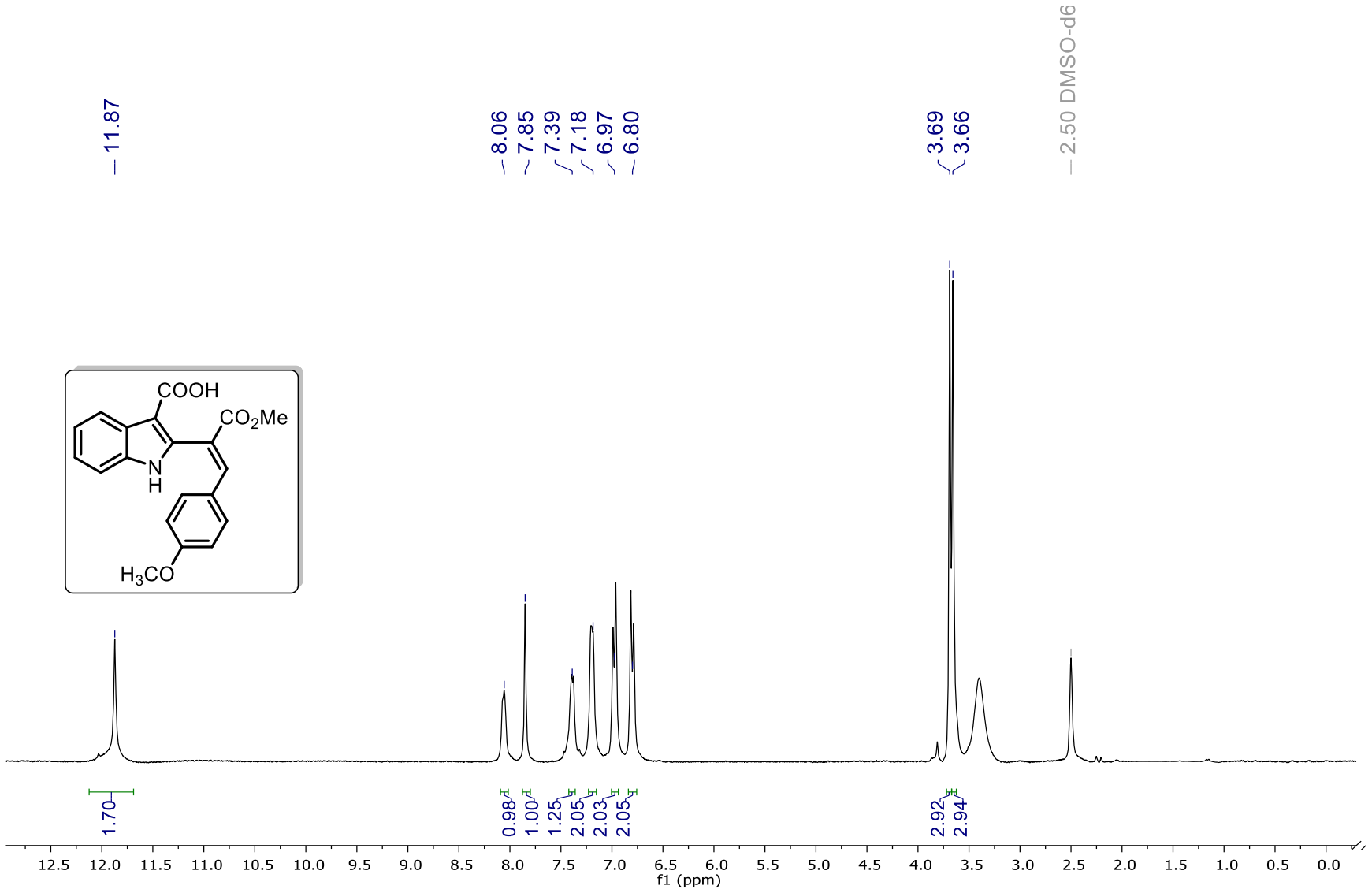

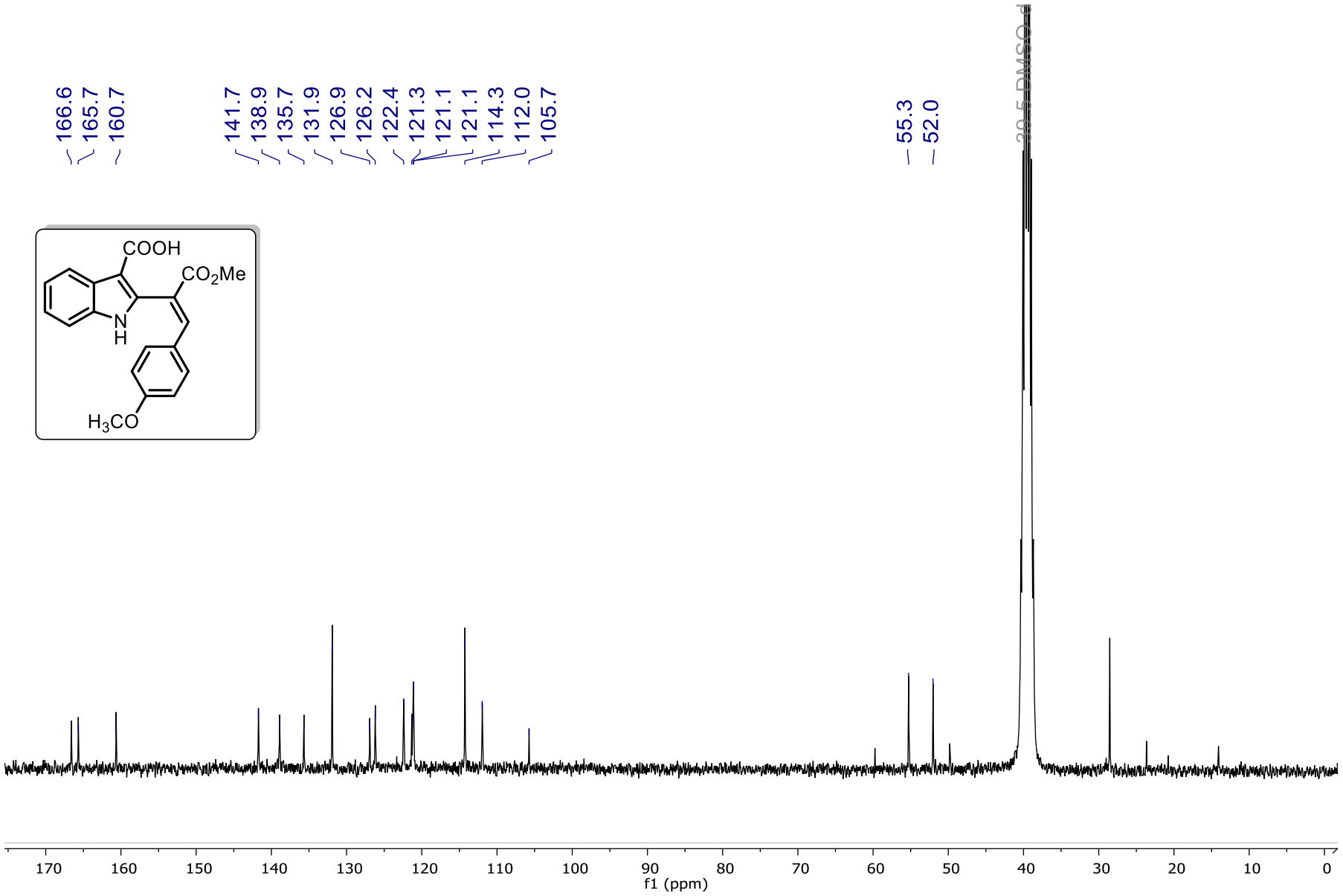
166.6
165.7
160.7
141.7
138.9
135.7
131.9
126.9
126.2
122.4
121.3
121.1
121.1
114.3
112.0
105.7
55.3
52.0
39.5 DMSO-d
COOH
CO2Me
N
H
H3CO
170
160
150
140
130
120
110
100
90
80
70
60
50
40
30
20
10
0
f1 (ppm)

^{1}H and ^{13}C NMR Spectra of 3e

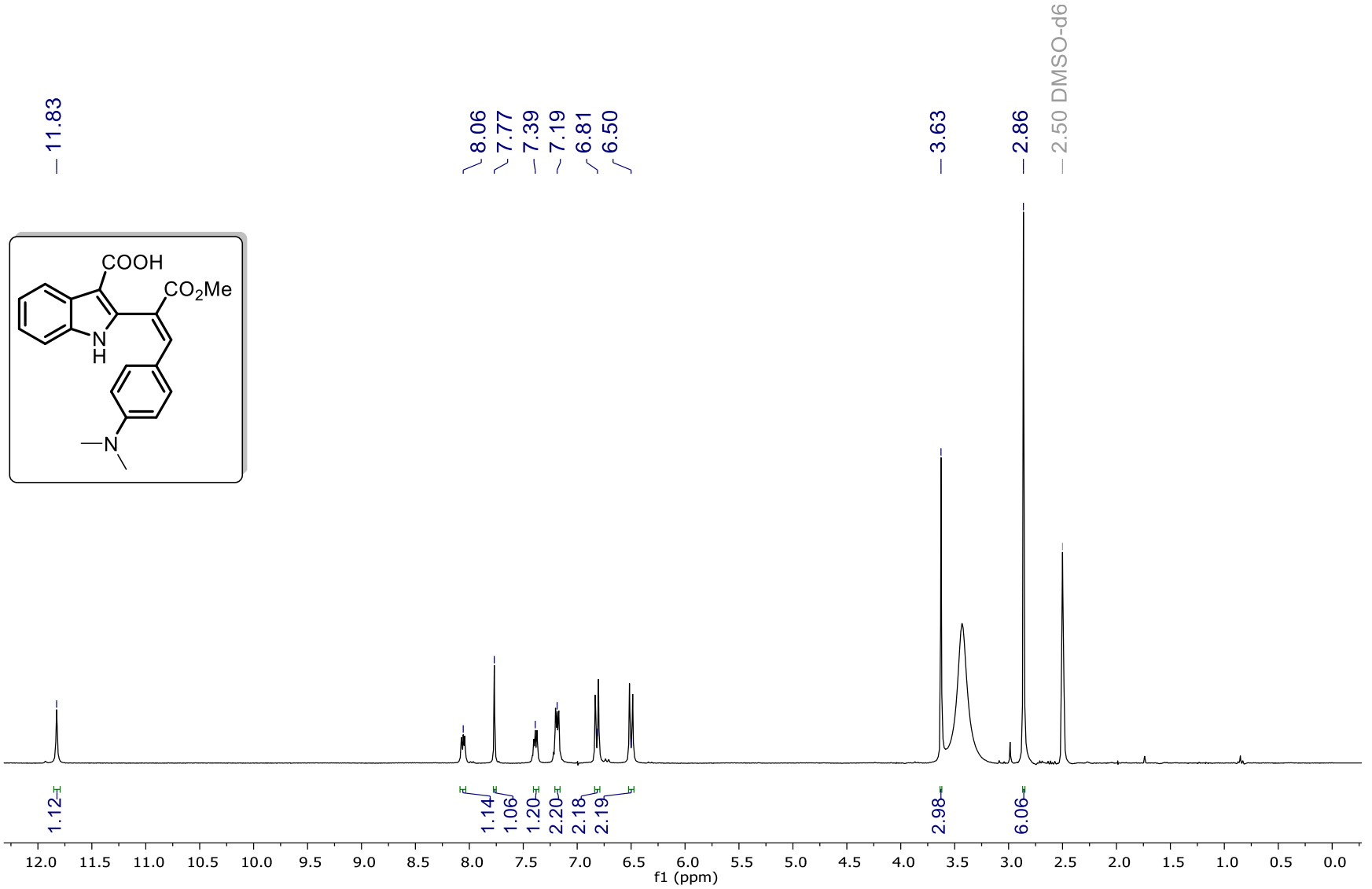

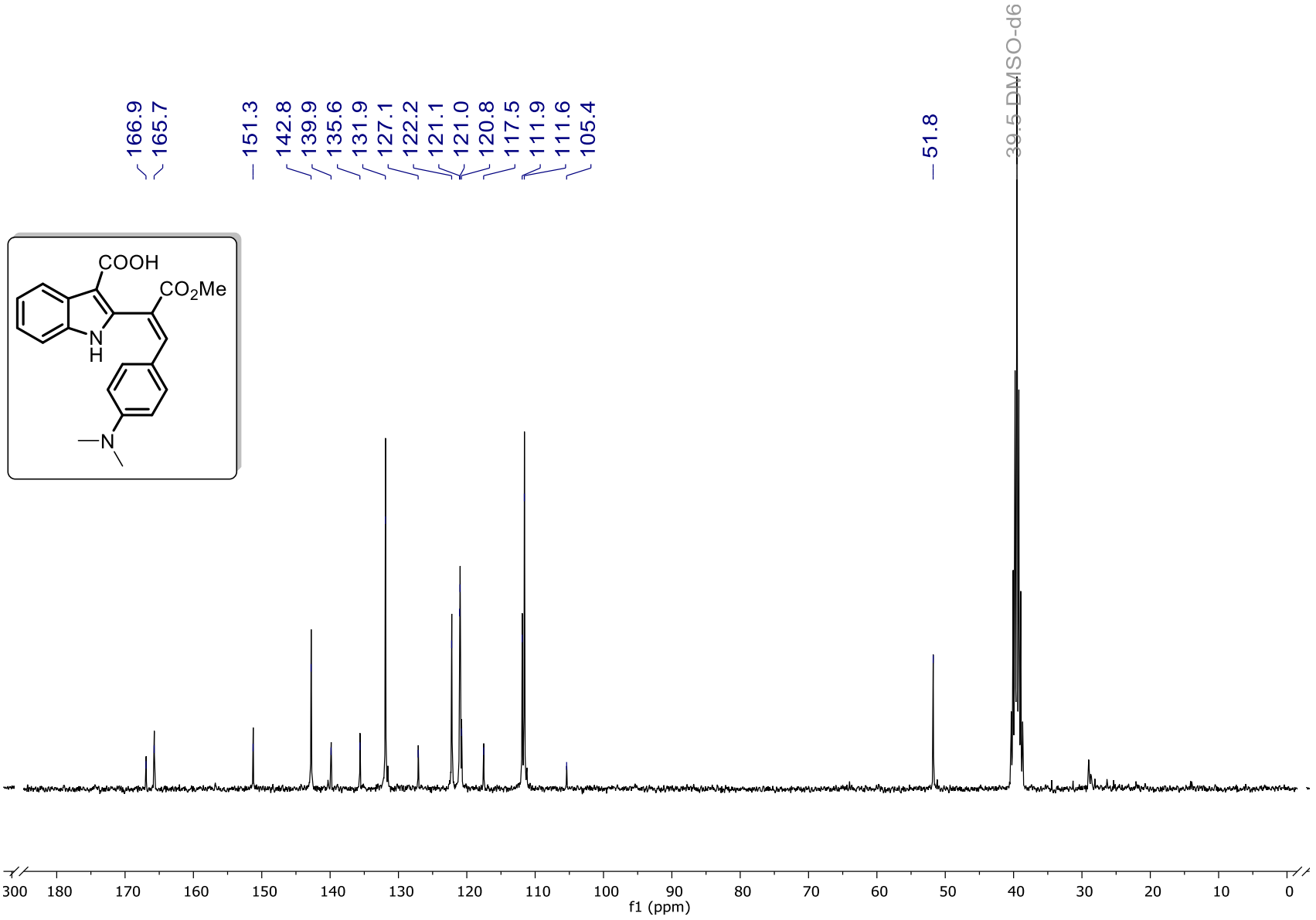
166.9
165.7
151.3
142.8
139.9
135.6
131.9
127.1
122.2
121.1
121.0
120.8
117.5
111.9
111.6
105.4
51.8
39.5 DMSO-d6
COOH
CO2Me
N
H
N
300 180 170 160 150 140 130 120 110 100 90 80 70 60 50 40 30 20 10 0
f1 (ppm)

^{1}H and ^{13}C NMR Spectra of 3f

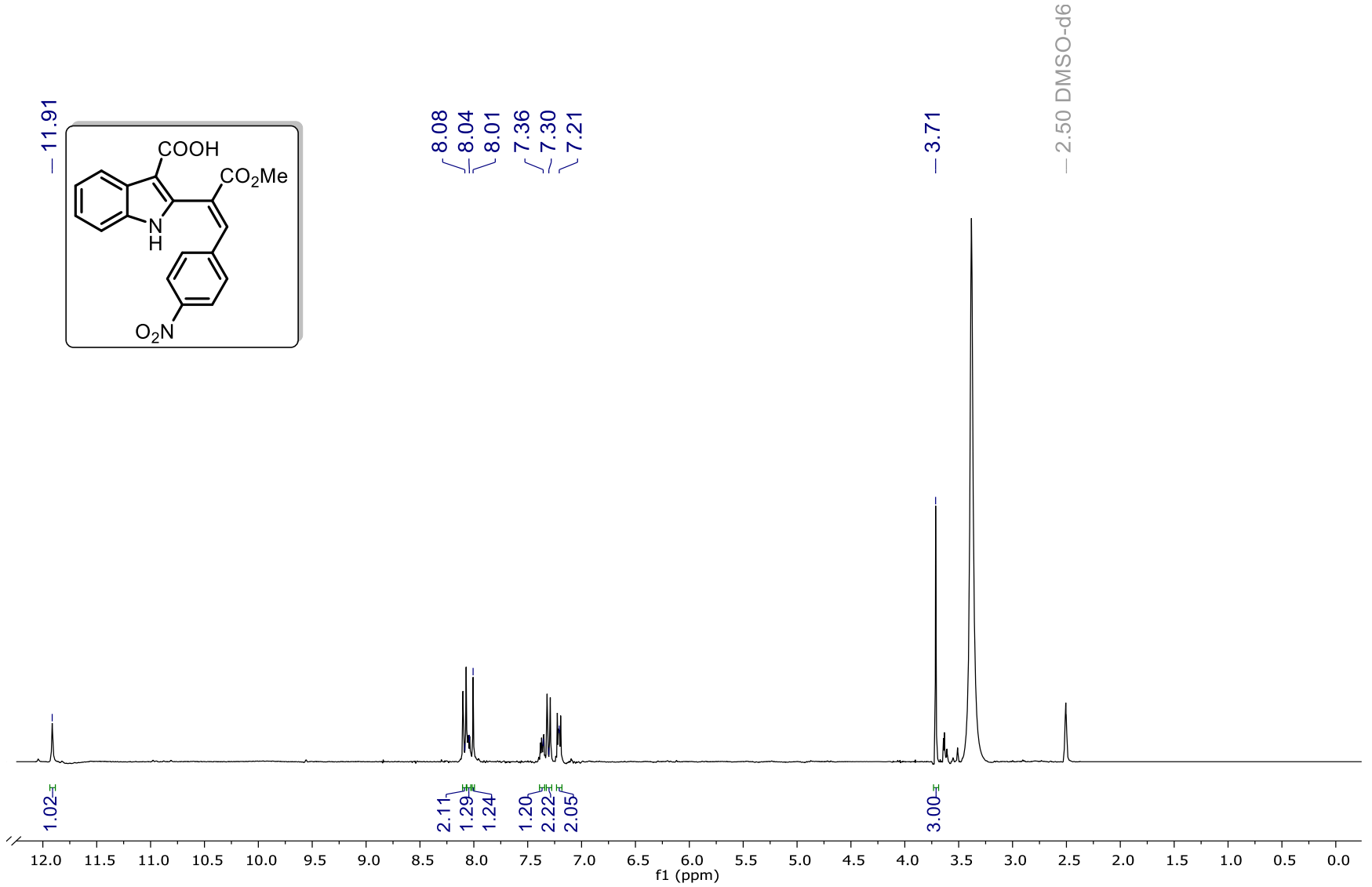

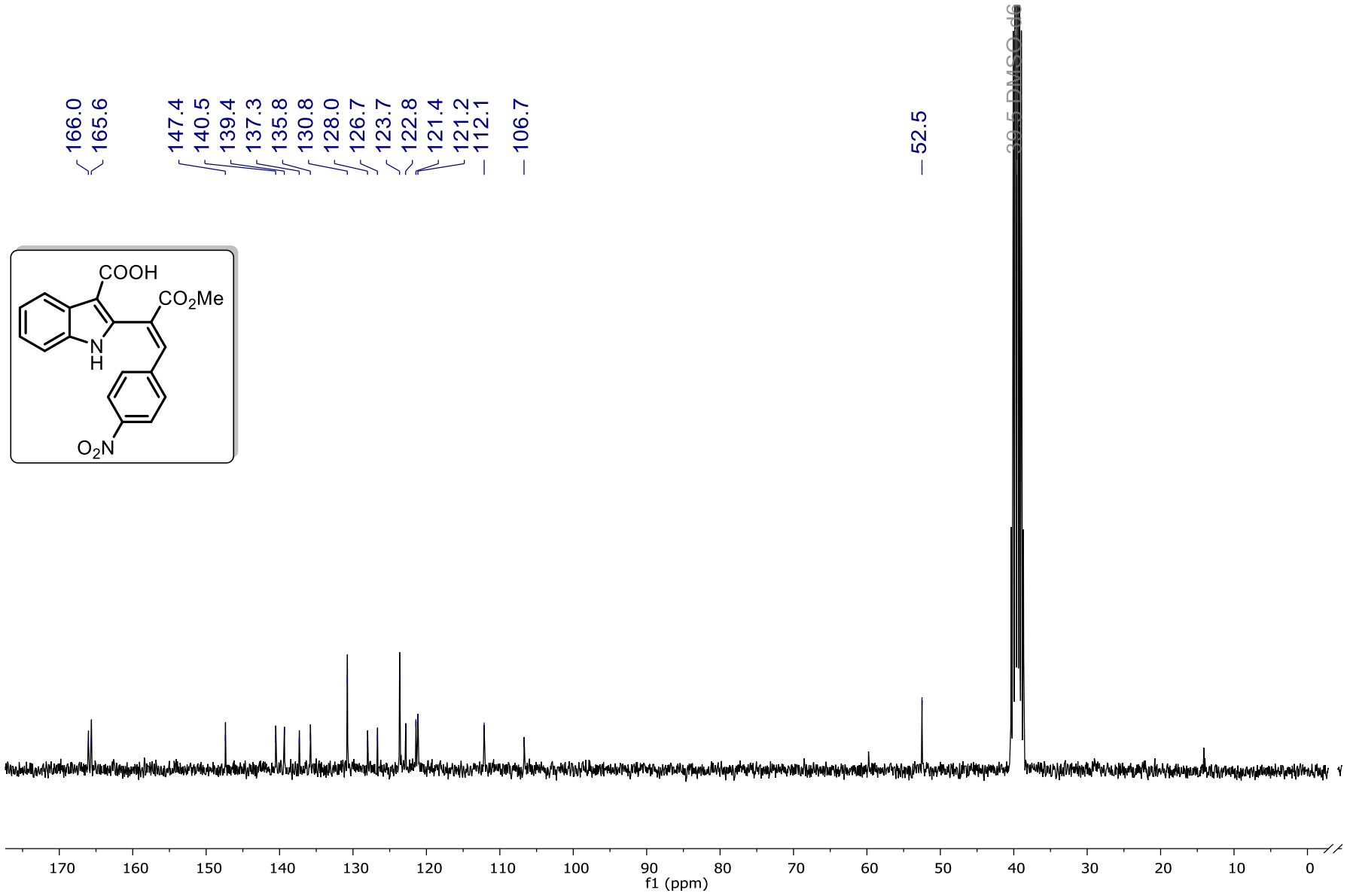
166.0
165.6
147.4
140.5
139.4
137.3
135.8
130.8
128.0
126.7
123.7
122.8
121.4
121.2
112.1
106.7
52.5
39.5 DMSO-d6
COOH
CO2Me
N
H
O2N
170
160
150
140
130
120
110
100
90
80
70
60
50
40
30
20
10
0
f1 (ppm)

^{1}H and ^{13}C NMR Spectra of 3g

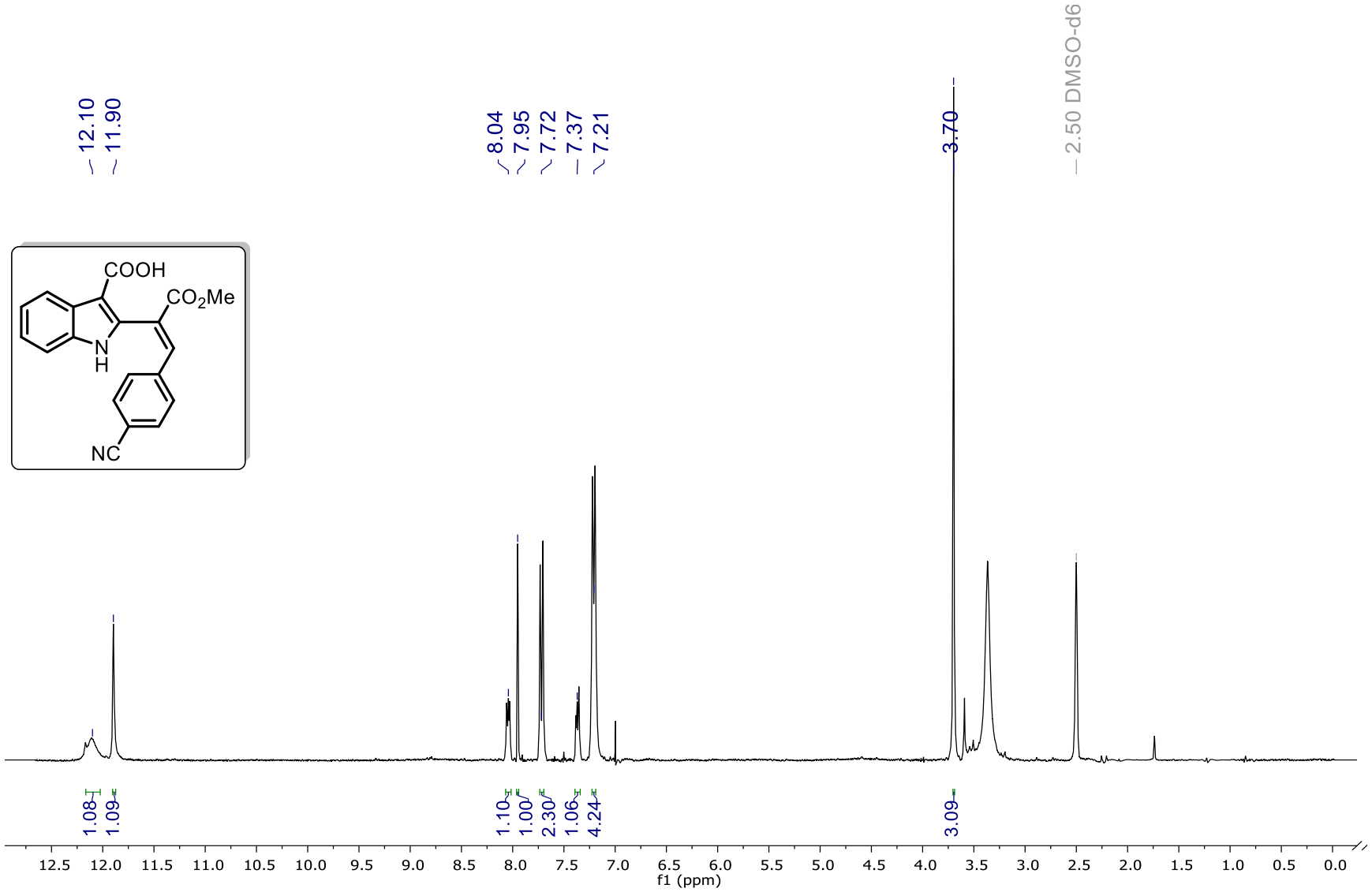

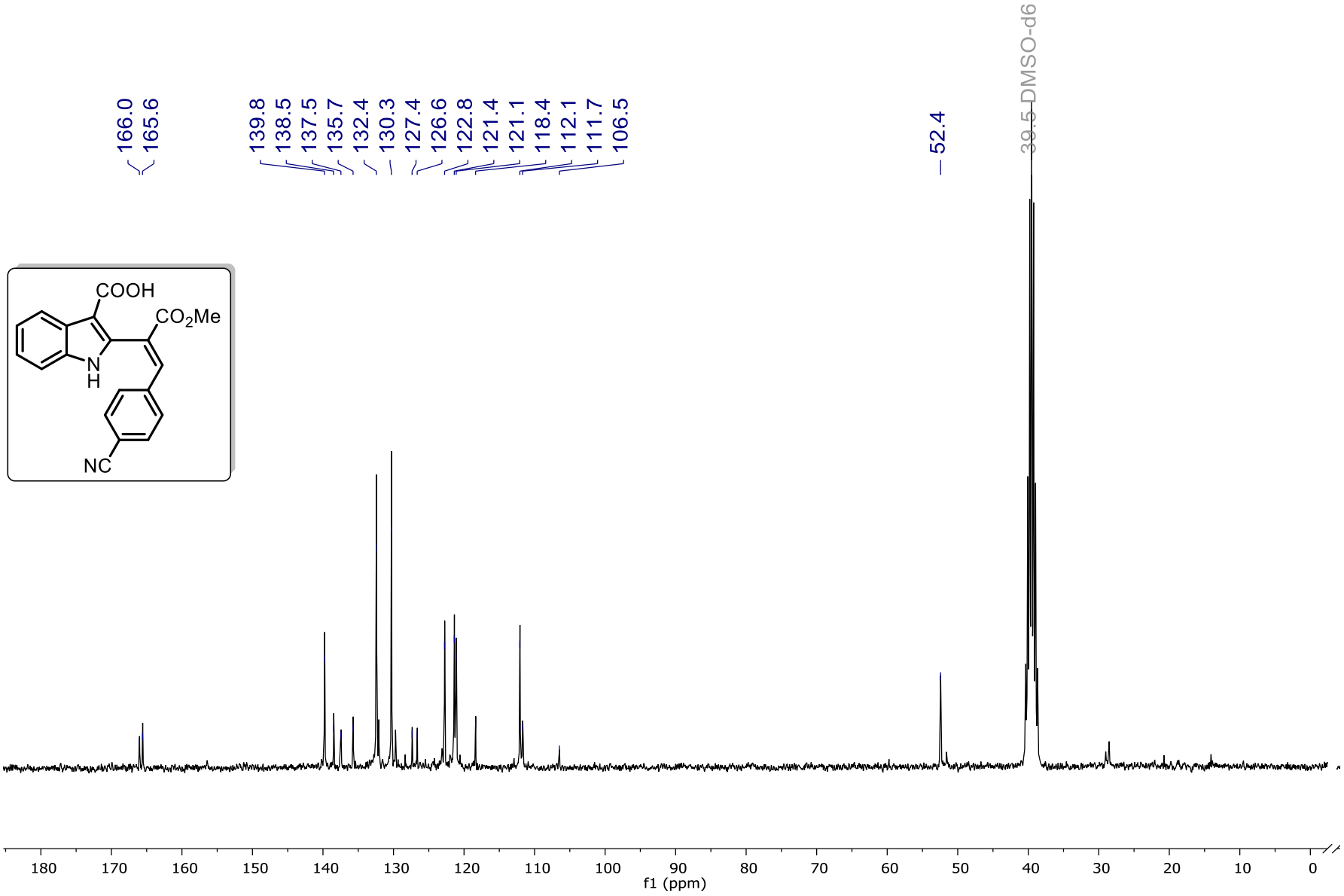
166.0
165.6
139.8
138.5
137.5
135.7
132.4
130.3
127.4
126.6
122.8
121.4
121.1
118.4
112.1
111.7
106.5
52.4
39.5 DMSO-d6
COOH
CO2Me
N
H
NC
180
170
160
150
140
130
120
110
100
90
80
70
60
50
40
30
20
10
0
f1 (ppm)

^{1}H and ^{13}C NMR Spectra of 3h

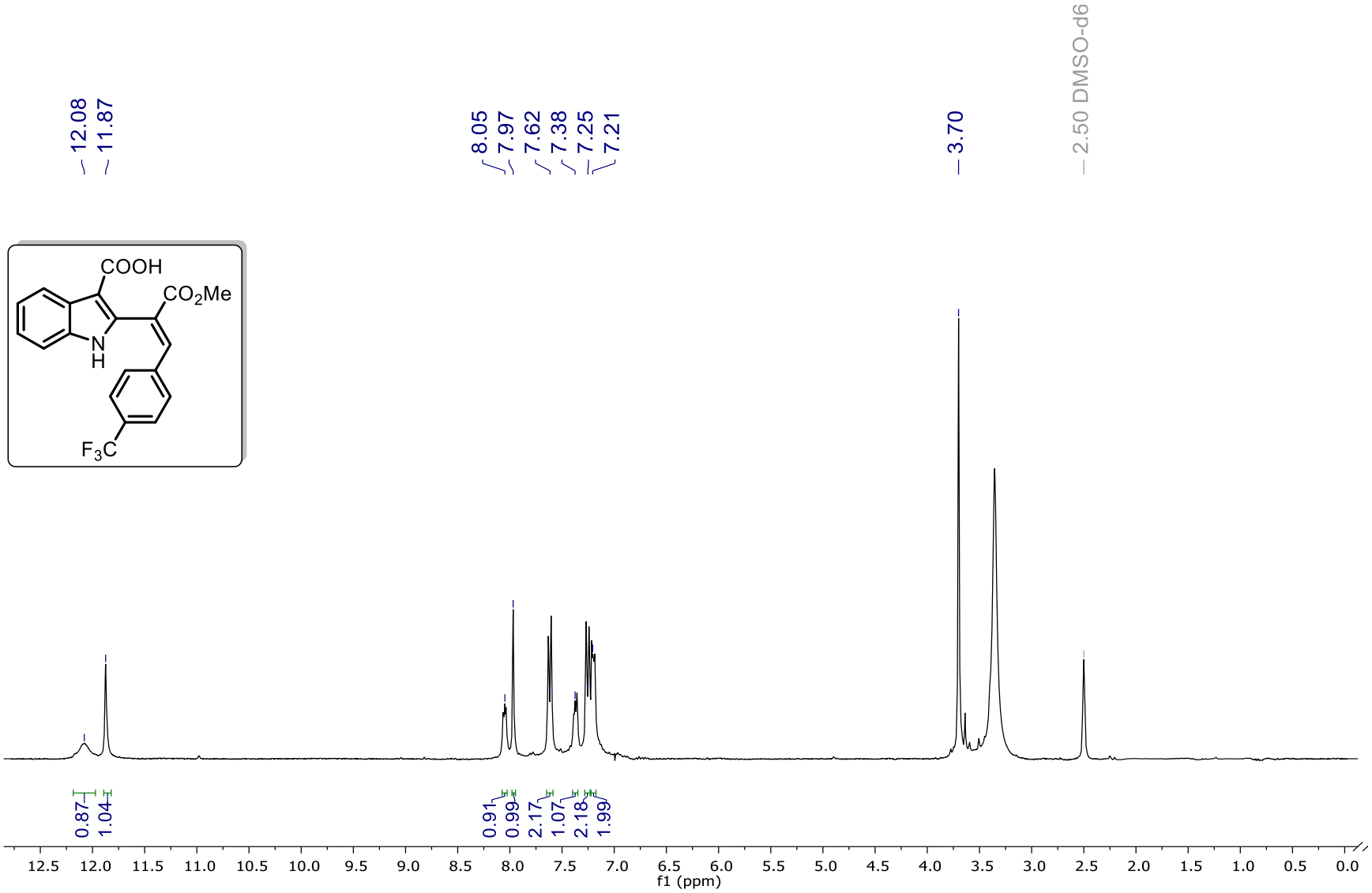

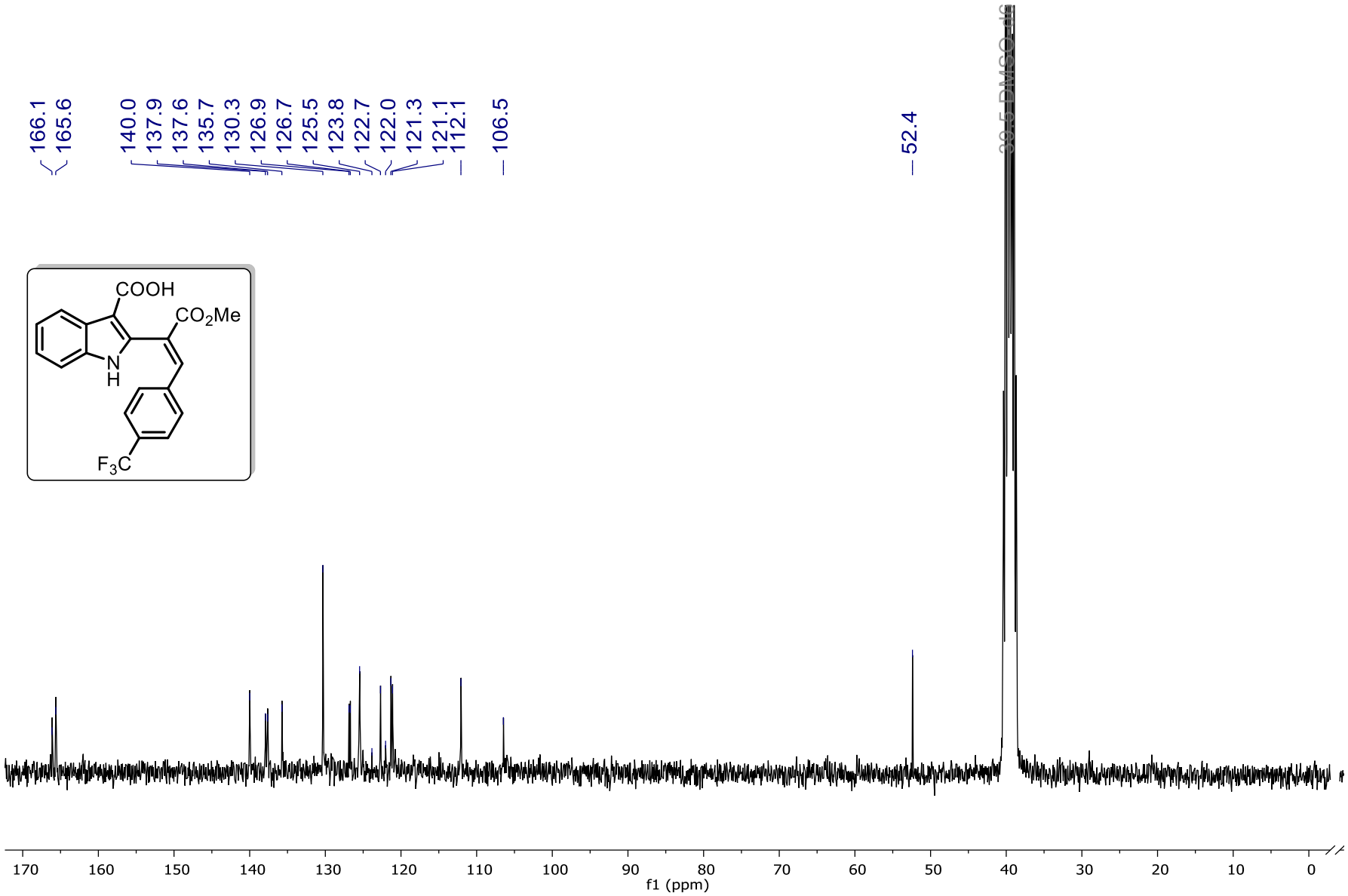
166.1
165.6
140.0
137.9
137.6
135.7
130.3
126.9
126.7
125.5
123.8
122.7
122.0
121.3
121.1
112.1
106.5
52.4
COOH
CO2Me
N
H
F3C
170
160
150
140
130
120
110
100
90
80
70
60
50
40
30
20
10
0
f1 (ppm)

^{1}H and ^{13}C NMR Spectra of 3i

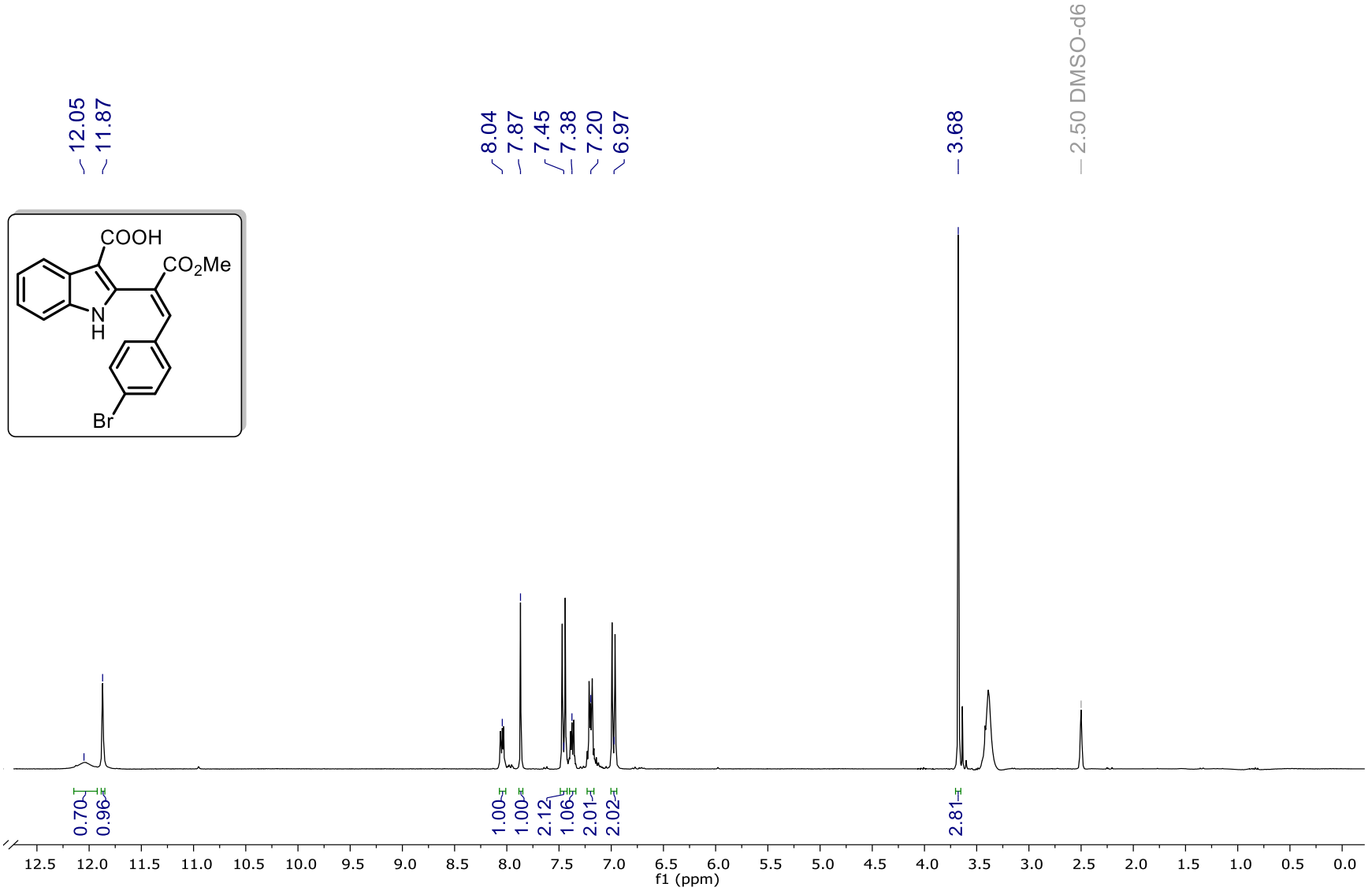

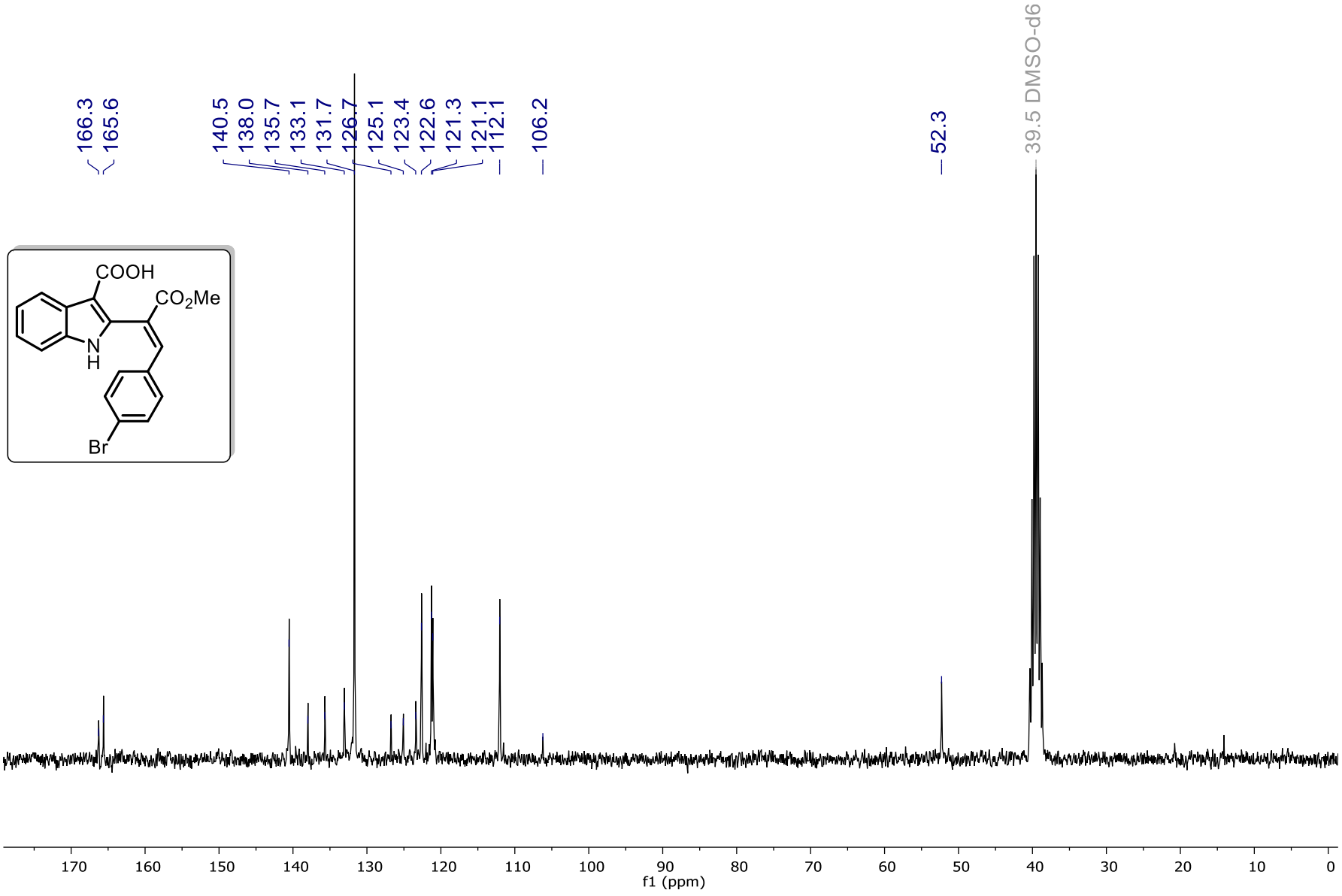
166.3
165.6
140.5
138.0
135.7
133.1
131.7
126.7
125.1
123.4
122.6
121.3
121.1
112.1
106.2
52.3
39.5 DMSO-d6
COOH
CO2Me
N
H
Br
170
160
150
140
130
120
110
100
90
80
70
60
50
40
30
20
10
0
f1 (ppm)

^{1}H and ^{13}C NMR Spectra of 3j

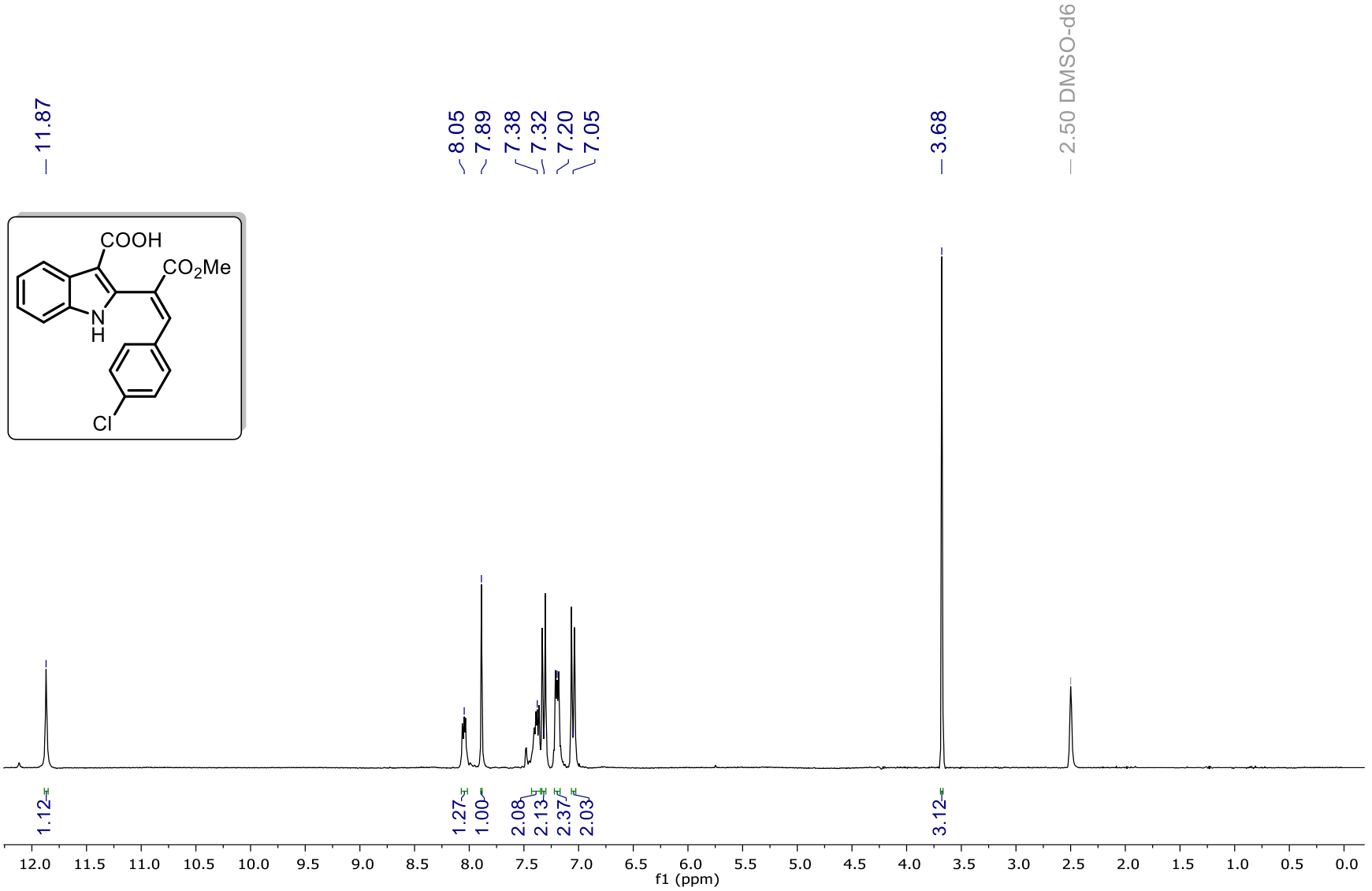

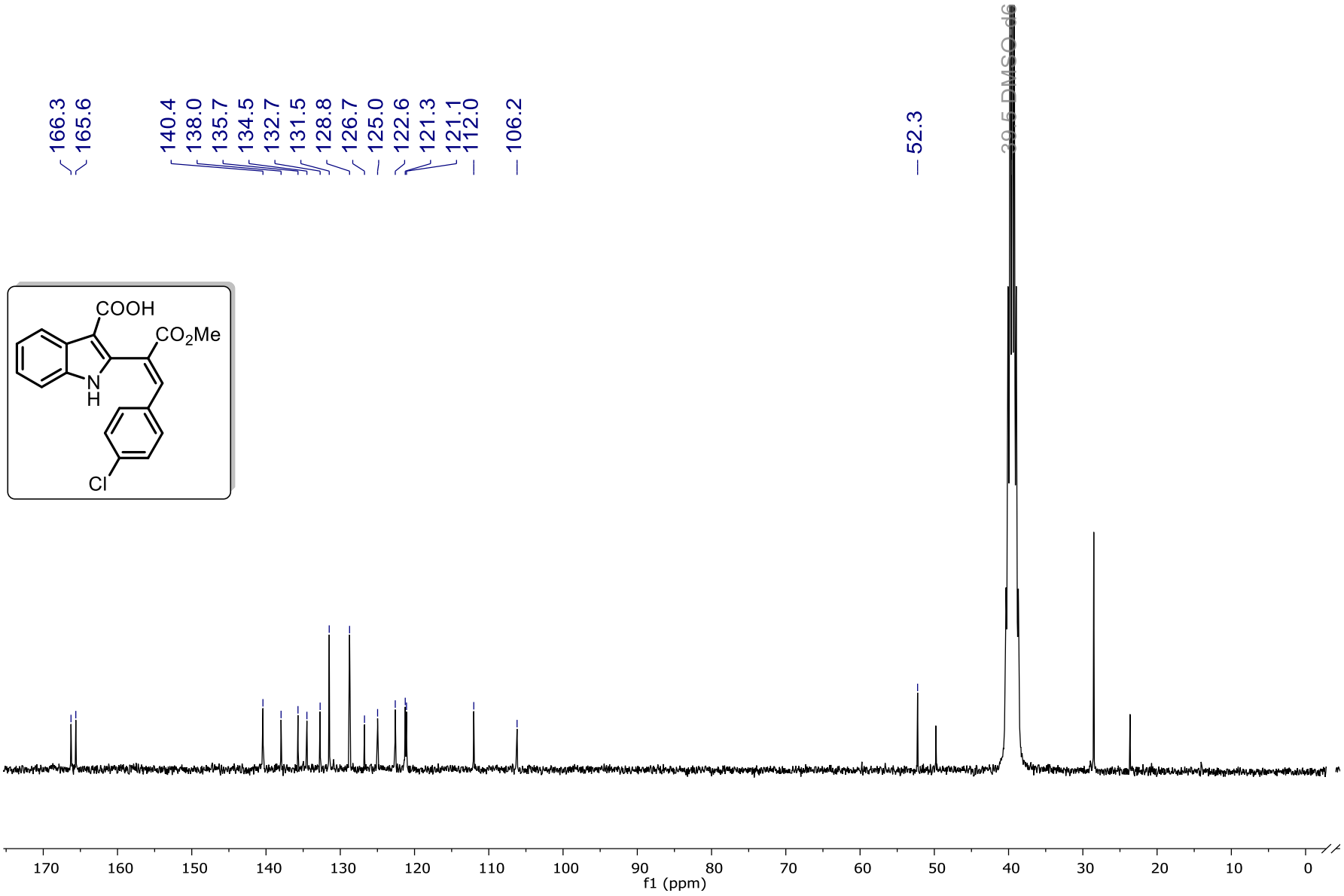
166.3
165.6
140.4
138.0
135.7
134.5
132.7
131.5
128.8
126.7
125.0
122.6
121.3
121.1
112.0
106.2
52.3
39.5 DMSO-d6
COOH
CO2Me
N
H
Cl
170
160
150
140
130
120
110
100
90
80
70
60
50
40
30
20
10
0
f1 (ppm)

^{1}H and ^{13}C NMR Spectra of 3k

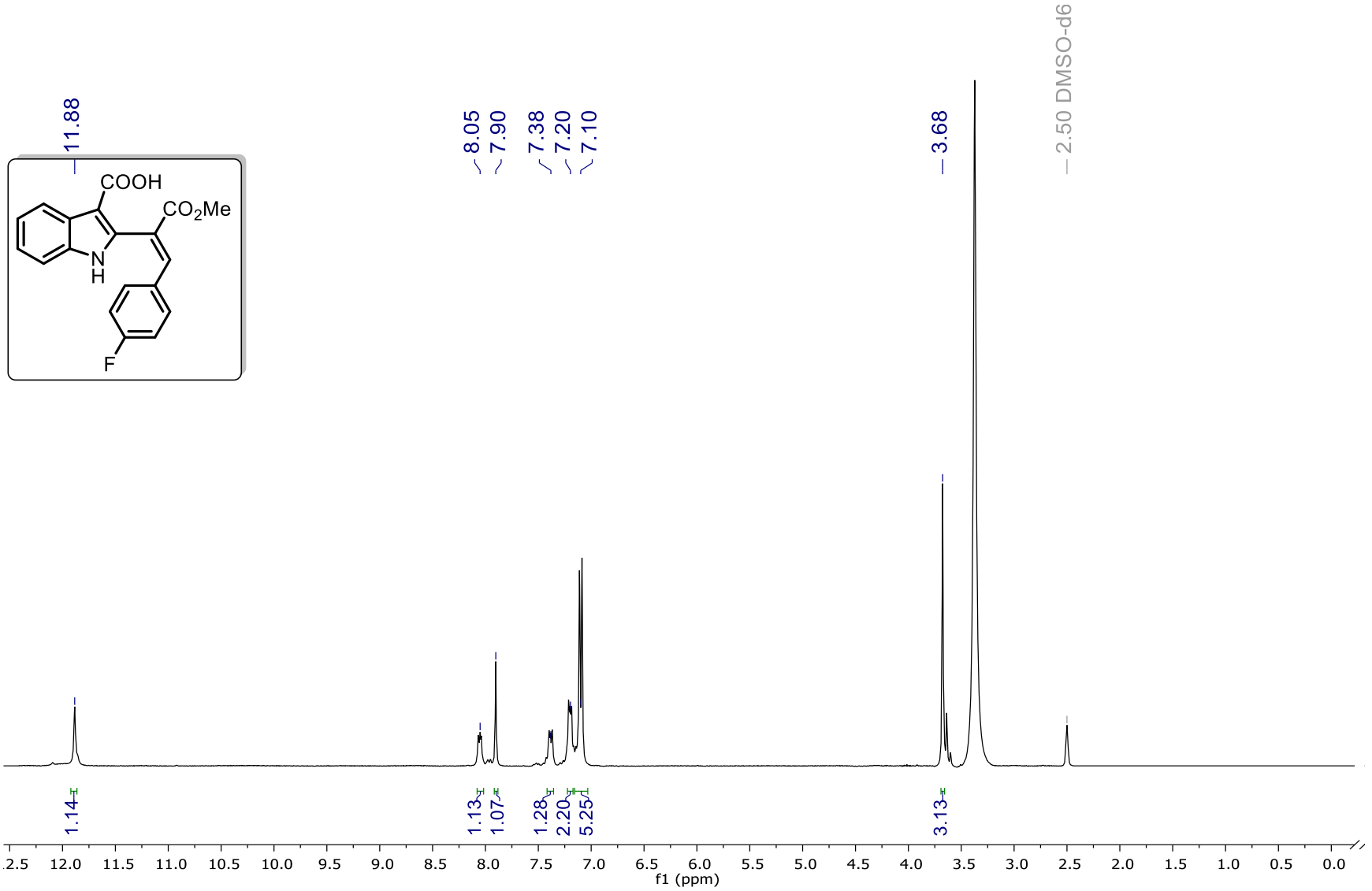

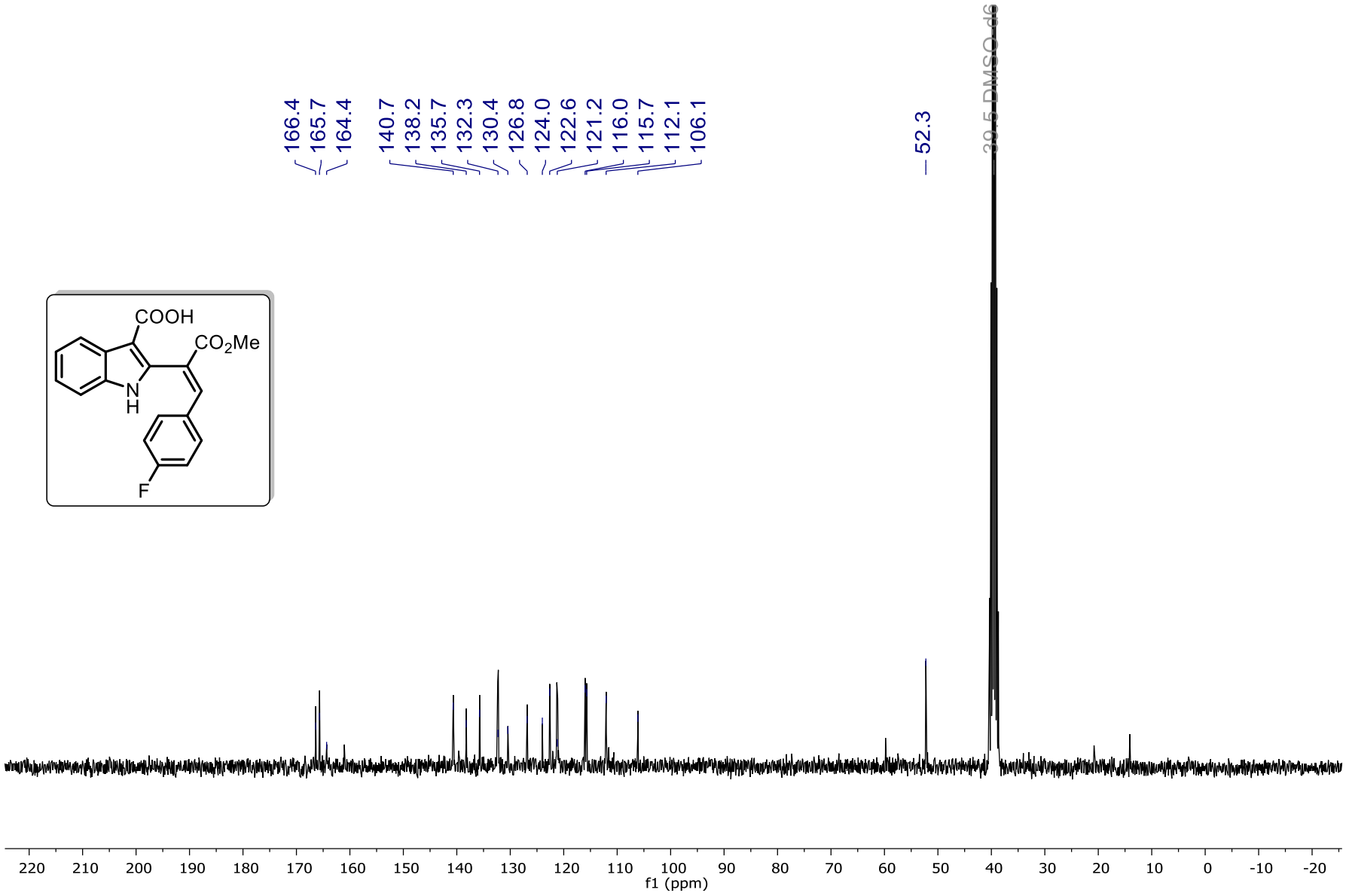
166.4
165.7
164.4
140.7
138.2
135.7
132.3
130.4
126.8
124.0
122.6
121.2
116.0
115.7
112.1
106.1
52.3
39.5 DMSO-d6
COOH
CO2Me
N
H
F
220 210 200 190 180 170 160 150 140 130 120 110 100 90 80 70 60 50 40 30 20 10 0 -10 -20
f1 (ppm)

9. High-resolution mass spectroscopy reports

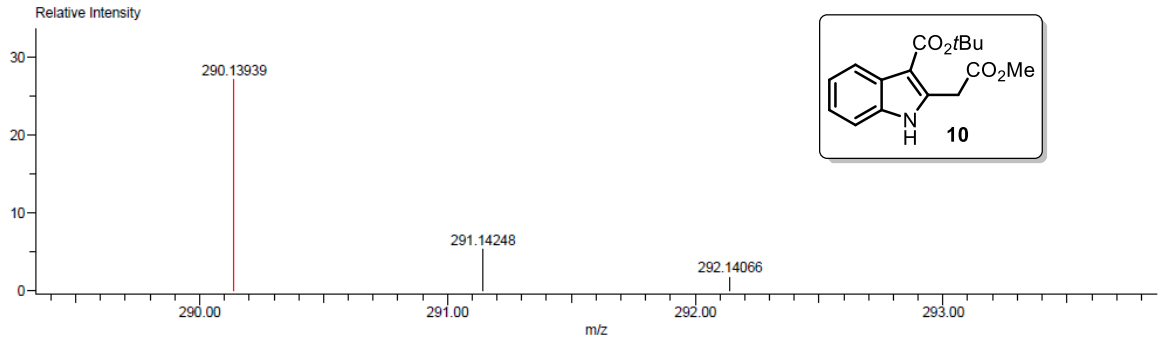

Mass	Intensity	Calc. Mass	Mass Difference (mmu)	Mass Difference (ppm)	Possible Formula	Unsaturation Number
290.13939	111249.63	290.13923	0.16	0.56	$^{12}C_{16}{}^{1}H_{20}{}^{14}N_{1}{}^{16}O_{4}$	7.5

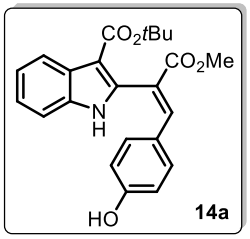

	Observed m/z	Int%					
	304.0623	81.81					
	Estimated m/z	Err[ppm / mmu]	U.S.	C	H	N	O
1	304.0610	+4.3 / +1.3	14.5	18	10	1	4

	Observed m/z	Int%					
	337.0951	100.00					
	Estimated m/z	Err[ppm / mmu]	U.S.	C	H	N	O
2	337.0950	+0.2 / +0.1	13.0	19	15	1	5

	Observed m/z	Int%					
	393.1561	19.79					
	Estimated m/z	Err[ppm / mmu]	U.S.	C	H	N	O
3	393.1576	-3.9 / -1.5	13.0	23	23	1	5

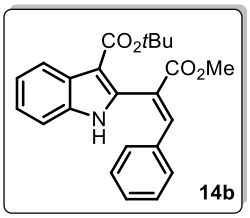

	Observed m/z	Int%					
	377.1640	99.01					
	Estimated m/z	Err[ppm / mmu]	U.S.	C	H	N	O
1	377.1627	+3.4 / +1.3	13.0	23	23	1	4

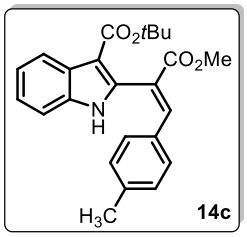

	Observed m/z	Int%					
	391.1794	37.27					
	Estimated m/z	Err[ppm / mmu]	U.S.	C	H	N	O
1	391.1784	+2.7 / +1.0	13.0	24	25	1	4

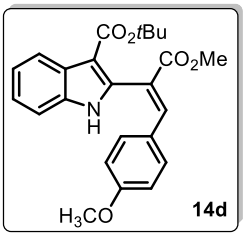

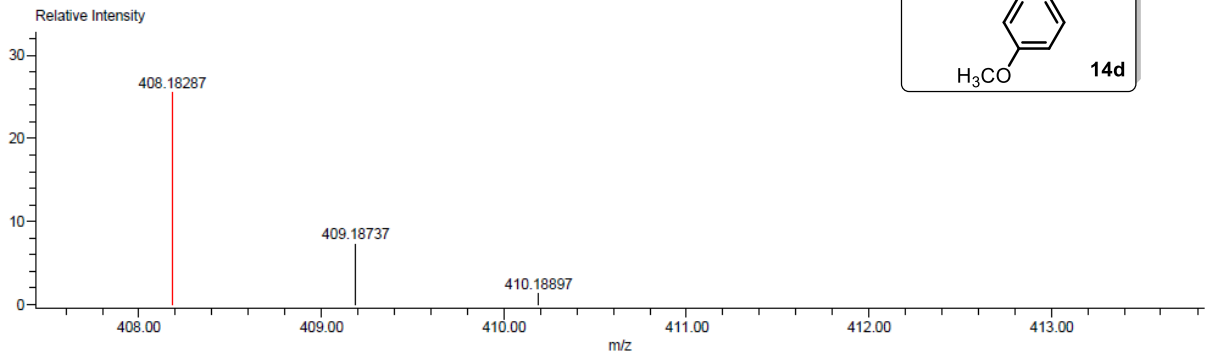

Mass	Intensity	Calc. Mass	Mass Difference (mmu)	Mass Difference (ppm)	Possible Formula	Unsaturation Number
408.18287	354744.33	408.18110	1.77	4.35	$^{12}C_{24}{}^{1}H_{26}{}^{14}N_{1}{}^{16}O_{5}$	12.5

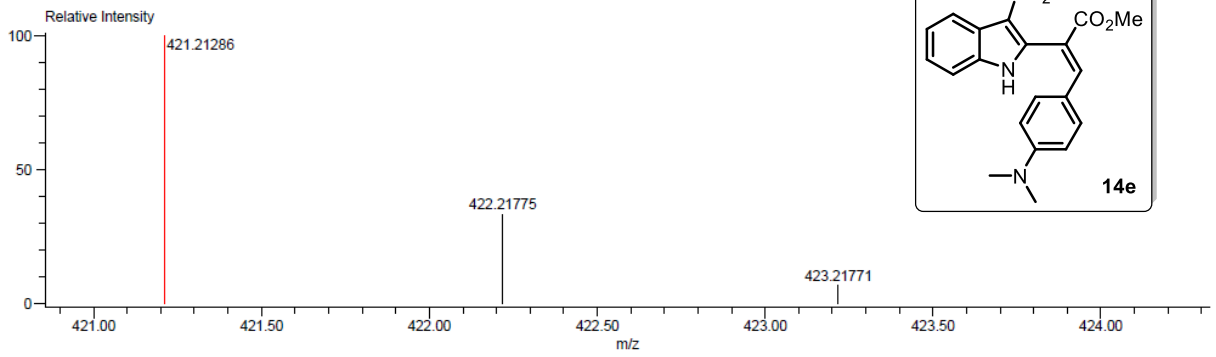

Mass	Intensity	Calc. Mass	Mass Difference (mmu)	Mass Difference (ppm)	Possible Formula	Unsaturation Number
421.21286	24114.33	421.21273	0.13	0.31	$^{12}C_{25}{}^{1}H_{29}{}^{14}N_{2}{}^{16}O_{4}$	12.5

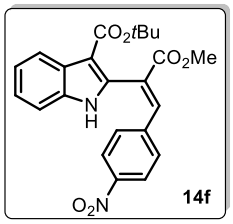

	Observed m/z	Int%					
	422.1457	71.19					
	Estimated m/z	Err[ppm / mmu]	U.S.	C	H	N	O
1	422.1478	-4.9 / -2.1	14.0	23	22	2	6

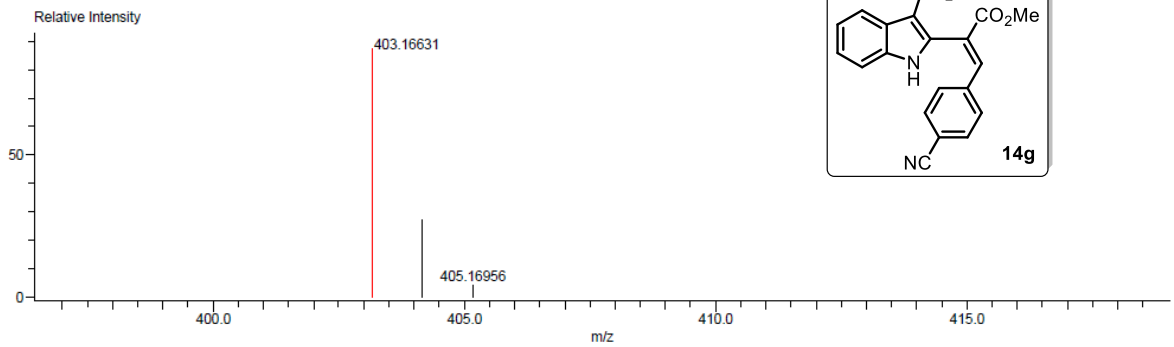

Mass	Intensity	Calc. Mass	Mass Difference (mmu)	Mass Difference (ppm)	Possible Formula	Unsaturation Number
403.16631	3228463.05	403.16578	0.53	1.32	$^{12}C_{24}{}^{1}H_{23}{}^{14}N_{2}{}^{16}O_{4}$	14.5

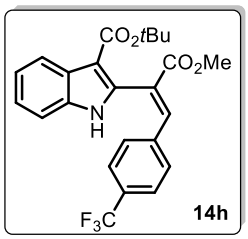

	Observed m/z	Int%							
	445.1515	12.78							
	Estimated m/z	Err[ppm / mmu]	U.S.	C	H	F	N	O	
1	445.1501	+3.2 / +1.4	13.0	24	22	3	1	4	

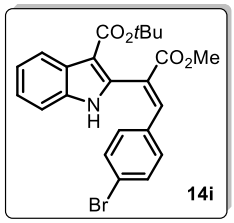

	Observed m/z	Int%							
	455.0725	97.12							
	Estimated m/z	Err[ppm / mmu]	U.S.	C	H	79Br	81Br	N	O
1	455.0732	-1.6 / -0.7	13.0	23	22	1	-	1	4

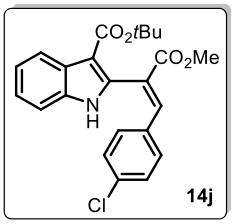

	Observed m/z	Int%							
	411.1244	40.54							
	Estimated m/z	Err[ppm / mmu]	U.S.	C	H	35Cl	37Cl	N	O
1	411.1237	+1.6 / +0.7	13.0	23	22	1	-	1	4

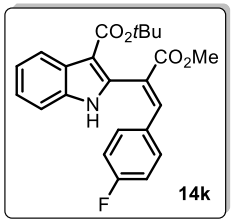

	Observed m/z	Int%						
	395.1538	24.47						
	Estimated m/z	Err[ppm / mmu]	U.S.	C	H	F	N	O
1	395.1533	+1.3 / +0.5	13.0	23	22	1	1	4

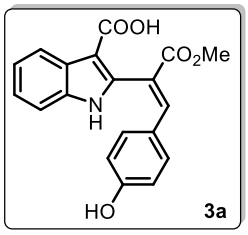

	Observed m/z	Int%					
	337.0937	56.18					
	Estimated m/z	Err[ppm / mmu]	U.S.	C	H	N	O
1	337.0950	-3.9 / -1.3	13.0	19	15	1	5

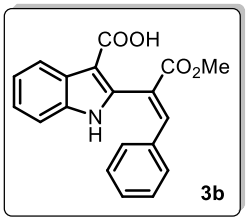

	Observed m/z	Int%					
	321.0989	20.32					
	Estimated m/z	Err[ppm / mmu]	U.S.	C	H	N	O
1	321.1001	-3.8 / -1.2	13.0	19	15	1	4

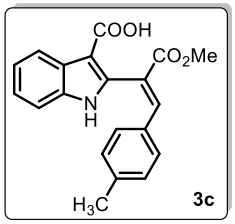

	Observed m/z	Int%					
	335.1151	100.00					
	Estimated m/z	Err[ppm / mmu]	U.S.	C	H	N	O
1	335.1158	-2.0 / -0.7	13.0	20	17	1	4

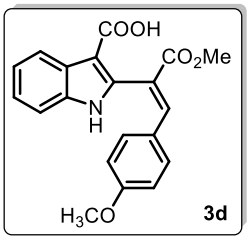

	Observed m/z	Int%					
	351.1117	28.54					
	Estimated m/z	Err[ppm / mmu]	U.S.	C	H	N	O
1	351.1107	+2.9 / +1.0	13.0	20	17	1	5

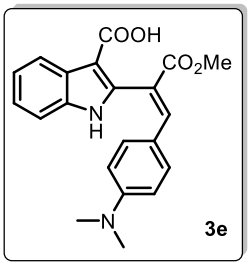

	Observed m/z	Int%					
	364.1435	89.95					
	Estimated m/z	Err[ppm / mmu]	U.S.	C	H	N	O
1	364.1423	+3.3 / +1.2	13.0	21	20	2	4

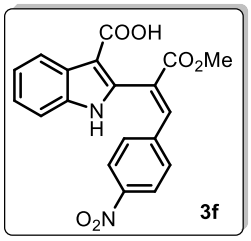

	Observed m/z	Int%
	366.0848	24.54

	Estimated m/z	Err[ppm / mmu]	U.S.	C	H	N	O
1	366.0852	-1.1 / -0.4	14.0	19	14	2	6

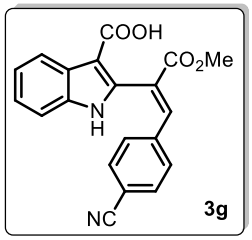

	Observed m/z	Int%
	346.0966	25.45

	Estimated m/z	Err[ppm / mmu]	U.S.	C	H	N	O
1	346.0954	+3.6 / +1.2	15.0	20	14	2	4

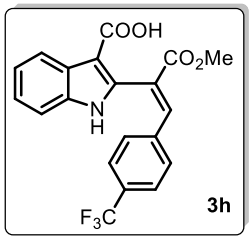

	Observed m/z	Int%
	389.0878	100.00

	Estimated m/z	Err[ppm / mmu]	U.S.	C	H	F	N	O
1	389.0875	+0.8 / +0.3	13.0	20	14	3	1	4

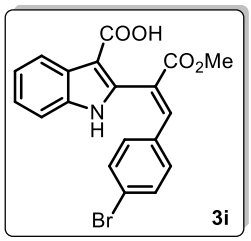

	Observed m/z	Int%								
	399.0103	24.58								
	Estimated m/z	Err[ppm / mmu]	U.S.	C	H	79Br	81Br	N	O	
1	399.0106	-0.8 / -0.3	13.0	19	14	1	-	1	4	

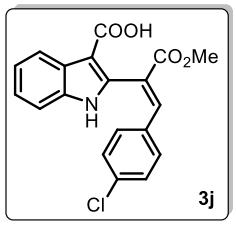

	Observed m/z	Int%								
	355.0603	35.06								
	Estimated m/z	Err[ppm / mmu]	U.S.	C	H	35Cl	37Cl	N	O	
1	355.0611	-2.4 / -0.8	13.0	19	14	1	-	1	4	

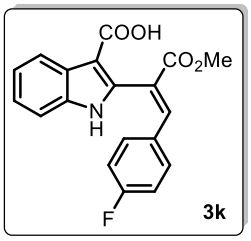

	Observed m/z	Int%							
	339.0895	100.00							
	Estimated m/z	Err[ppm / mmu]	U.S.	C	H	F	N	O	
1	339.0907	-3.5 / -1.2	13.0	19	14	1	1	4	

10. HPLC chromatograms

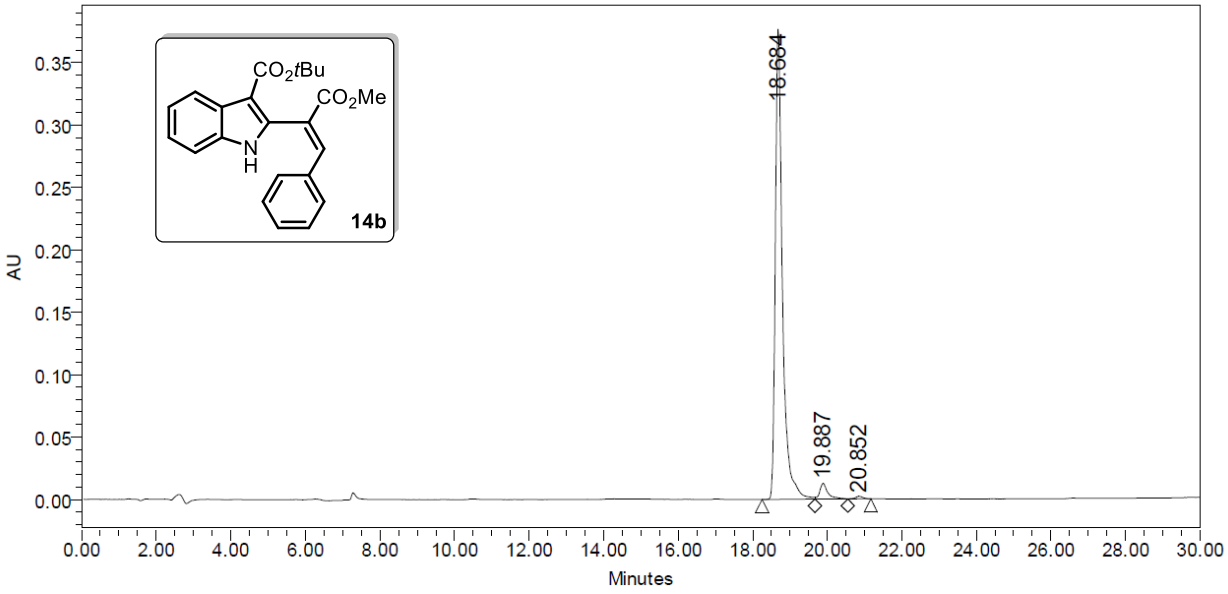

Peak Results

	Name	RT	Area	% Area	Int Type	Processed Channel Descr.	Width (sec)
1		18.684	5010237	95.80	BV	PDA 254.0 nm	85.000
2		19.887	190286	3.64	VV	PDA 254.0 nm	53.000
3		20.852	29373	0.56	VB	PDA 254.0 nm	37.000

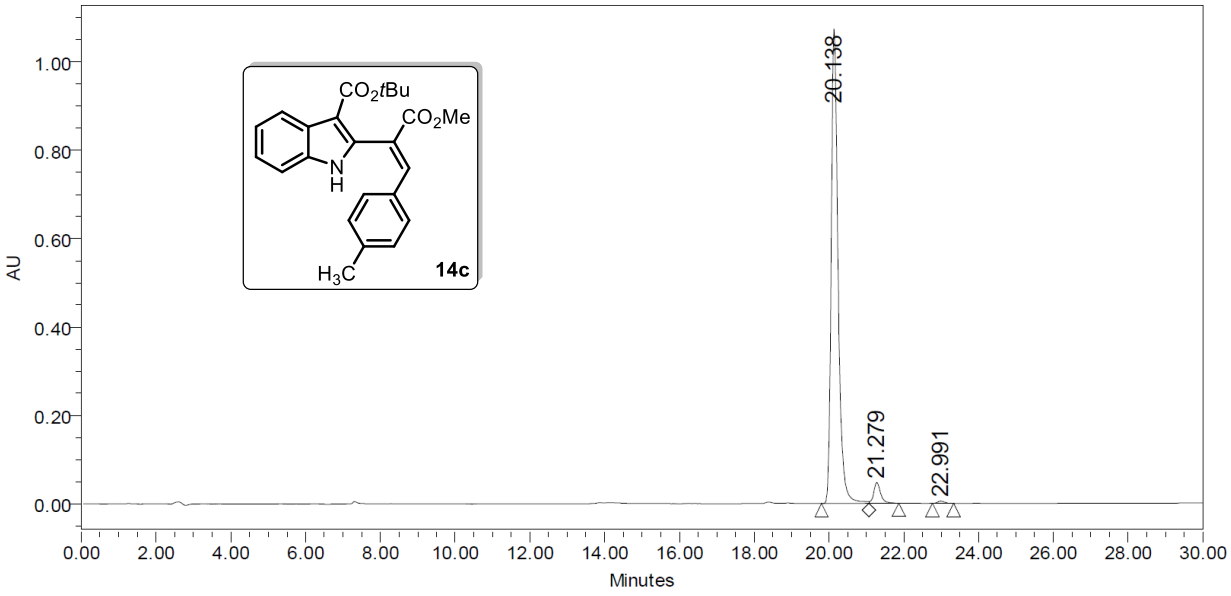

Peak Results

	Name	RT	Area	% Area	Int Type	Processed Channel Descr.	Width (sec)
1		20.138	13684971	95.38	BV	PDA 254.0 nm	76.000
2		21.279	598310	4.17	VB	PDA 254.0 nm	48.000
3		22.991	64955	0.45	BB	PDA 254.0 nm	34.000

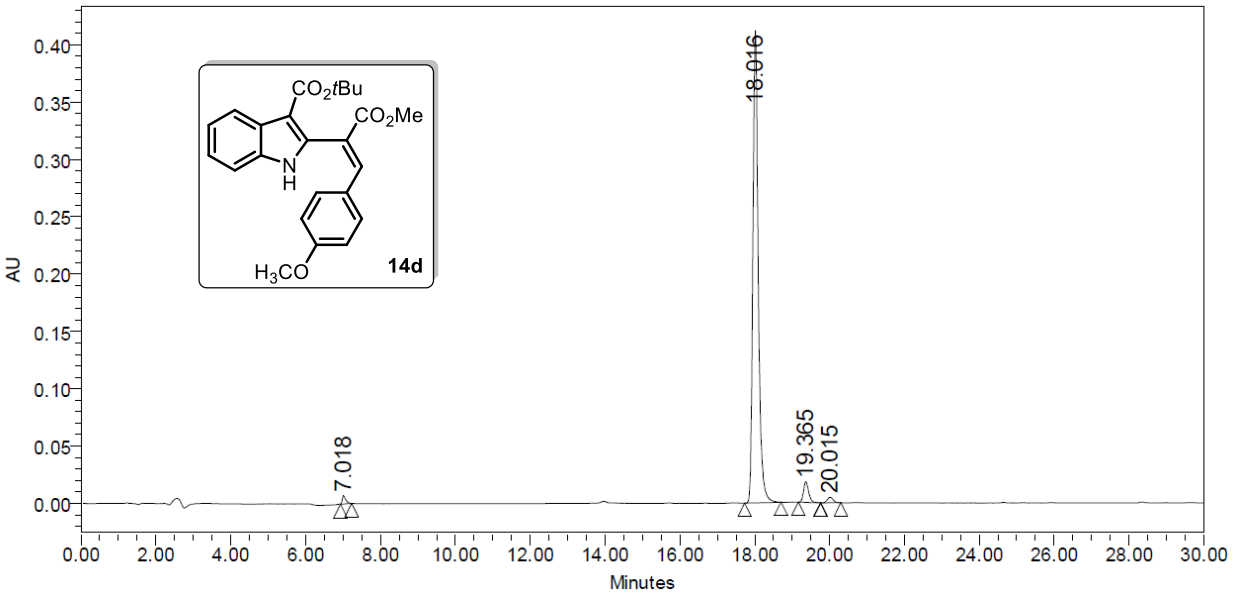

Peak Results

	Name	RT	Area	% Area	Int Type	Processed Channel Descr.	Width (sec)
1		7.018	48204	1.11	bb	PDA 254.0 nm	18.000
2		18.016	4090395	93.88	BB	PDA 254.0 nm	58.000
3		19.365	167928	3.85	BB	PDA 254.0 nm	35.000
4		20.015	50525	1.16	BB	PDA 254.0 nm	32.000

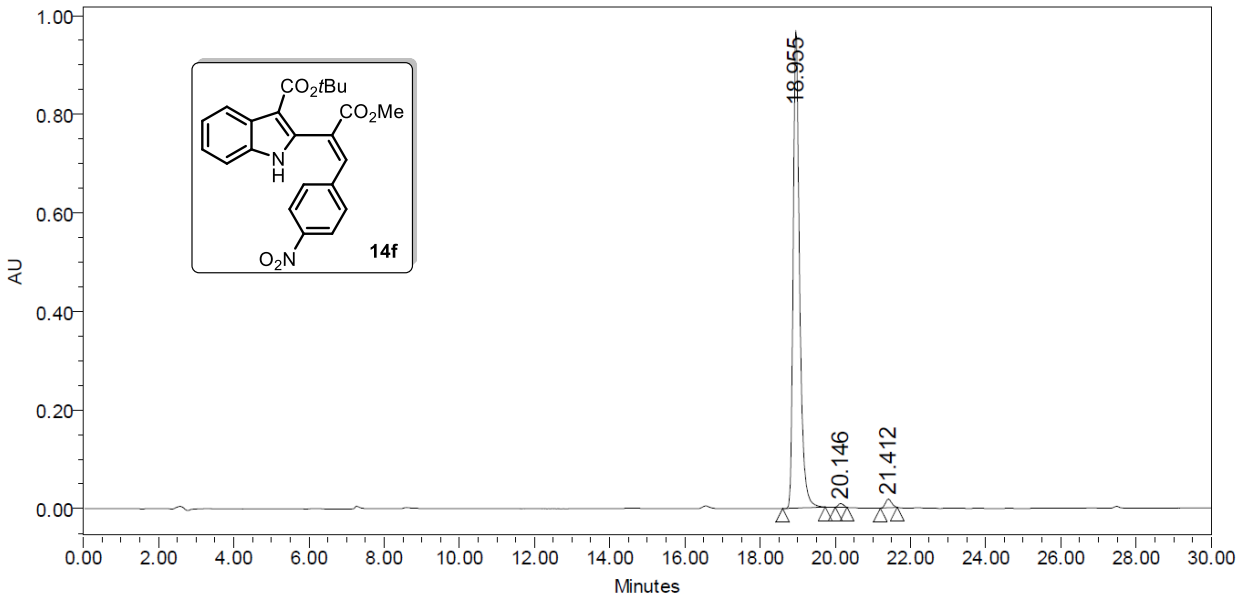

Peak Results

	Name	RT	Area	% Area	Int Type	Processed Channel Descr.	Width (sec)
1		18.955	11416738	97.67	Bb	PDA 254.0 nm	68.000
2		20.146	71027	0.61	bb	PDA 254.0 nm	19.000
3		21.412	201089	1.72	bb	PDA 254.0 nm	27.000

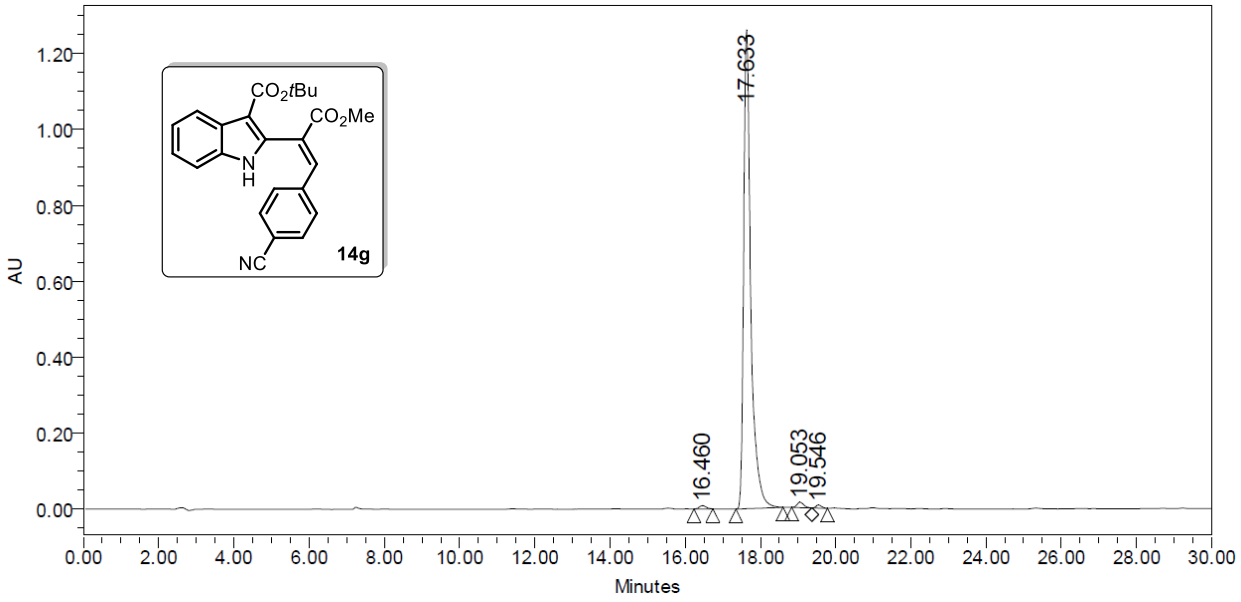

Peak Results

	Name	RT	Area	% Area	Int Type	Processed Channel Descr.	Width (sec)
1		16.460	111930	0.66	Bb	PDA 254.0 nm	30.000
2		17.633	16525331	97.84	BB	PDA 254.0 nm	75.000
3		19.053	170395	1.01	BV	PDA 254.0 nm	32.000
4		19.546	82574	0.49	VB	PDA 254.0 nm	25.000

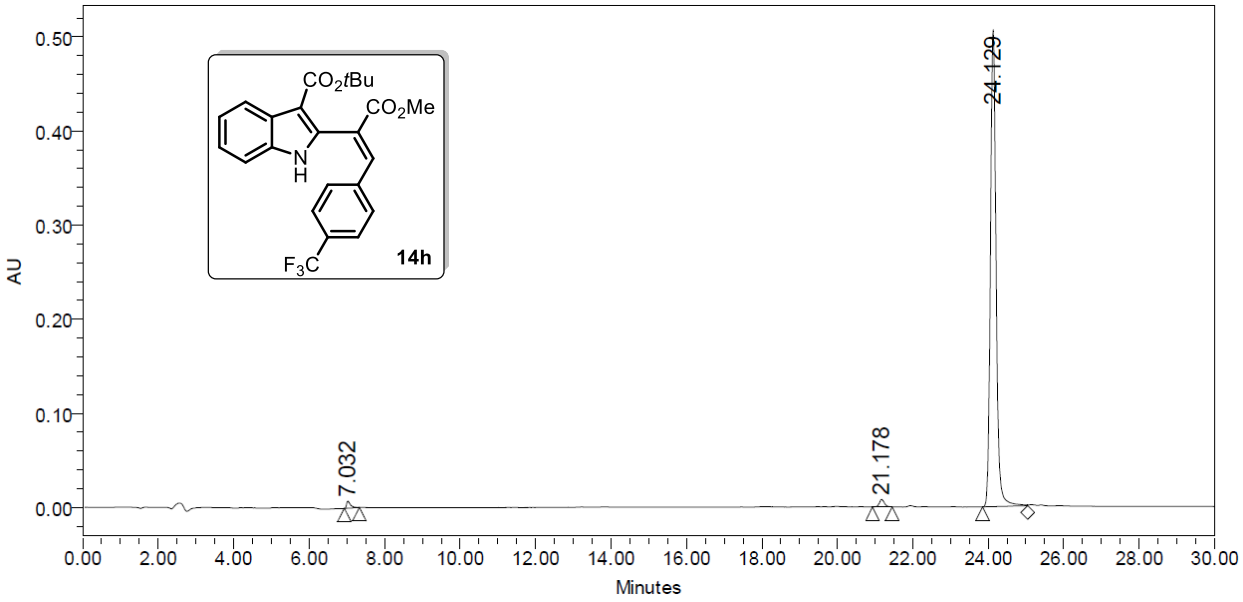

Peak Results

	Name	RT	Area	% Area	Int Type	Processed Channel Descr.	Width (sec)
1		7.032	53003	0.98	BB	PDA 254.0 nm	24.000
2		21.178	73285	1.36	BB	PDA 254.0 nm	31.000
3		24.129	5276910	97.66	BV	PDA 254.0 nm	72.000

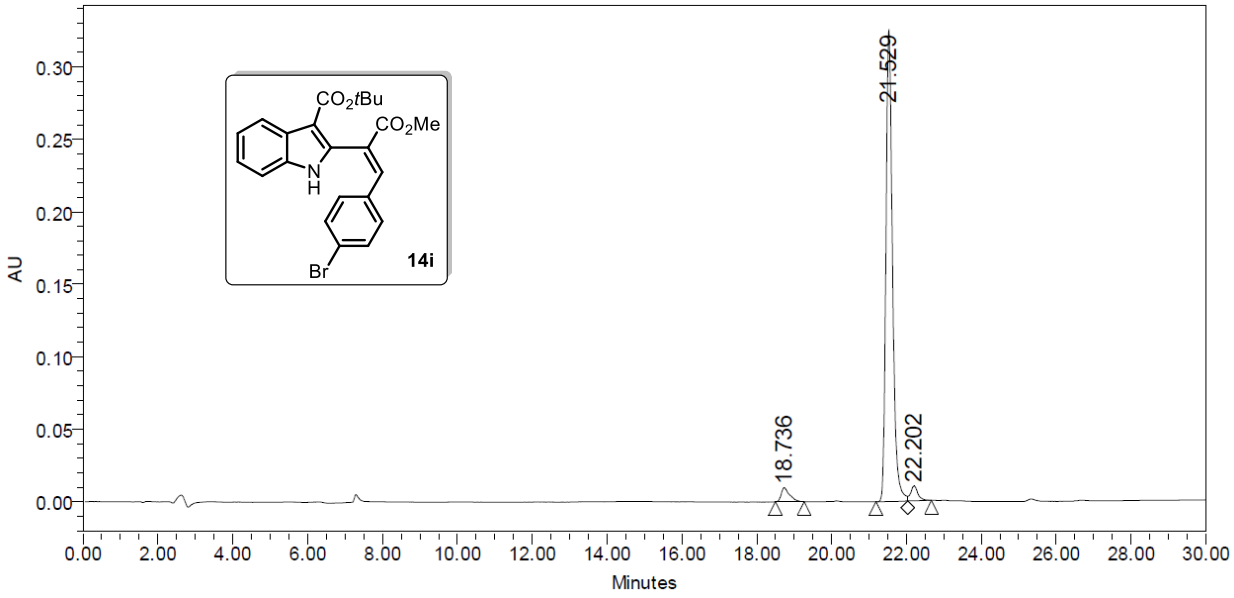

Peak Results

	Name	RT	Area	% Area	Int Type	Processed Channel Descr.	Width (sec)
1		18.736	149678	3.52	BB	PDA 254.0 nm	46.000
2		21.529	3958231	93.18	BV	PDA 254.0 nm	51.000
3		22.202	140225	3.30	VB	PDA 254.0 nm	38.000

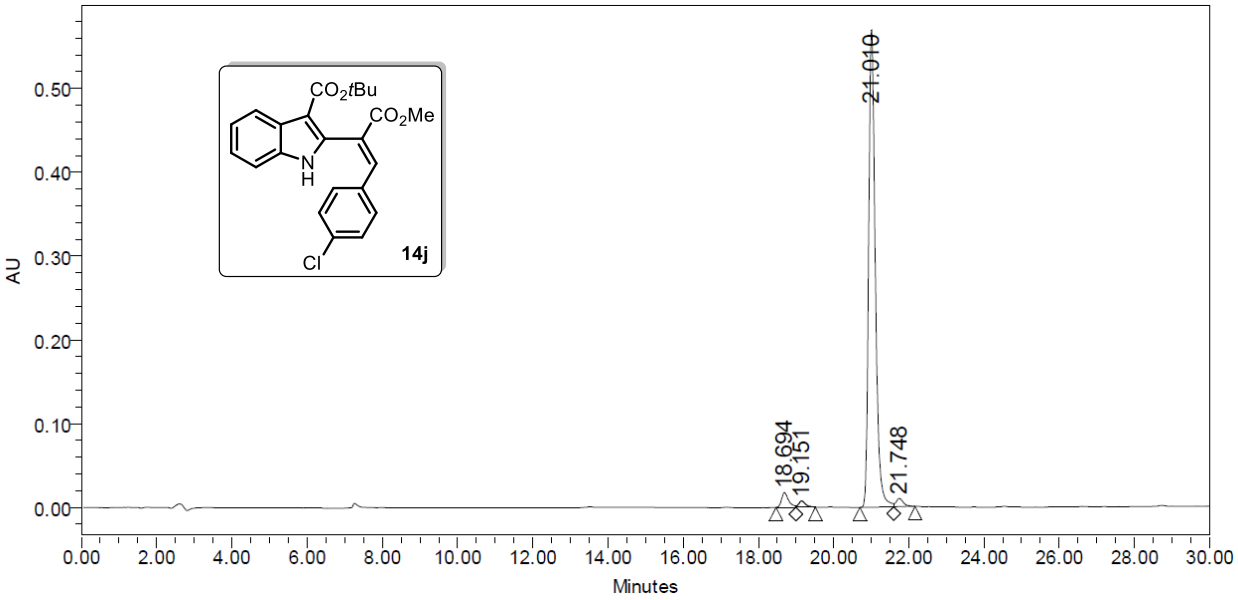

Peak Results

	Name	RT	Area	% Area	Int Type	Processed Channel Descr.	Width (sec)
1		18.694	228904	3.07	bV	PDA 254.0 nm	32.000
2		19.151	95221	1.28	Vb	PDA 254.0 nm	31.000
3		21.010	7001127	93.91	BV	PDA 254.0 nm	54.000
4		21.748	130256	1.75	VB	PDA 254.0 nm	34.000

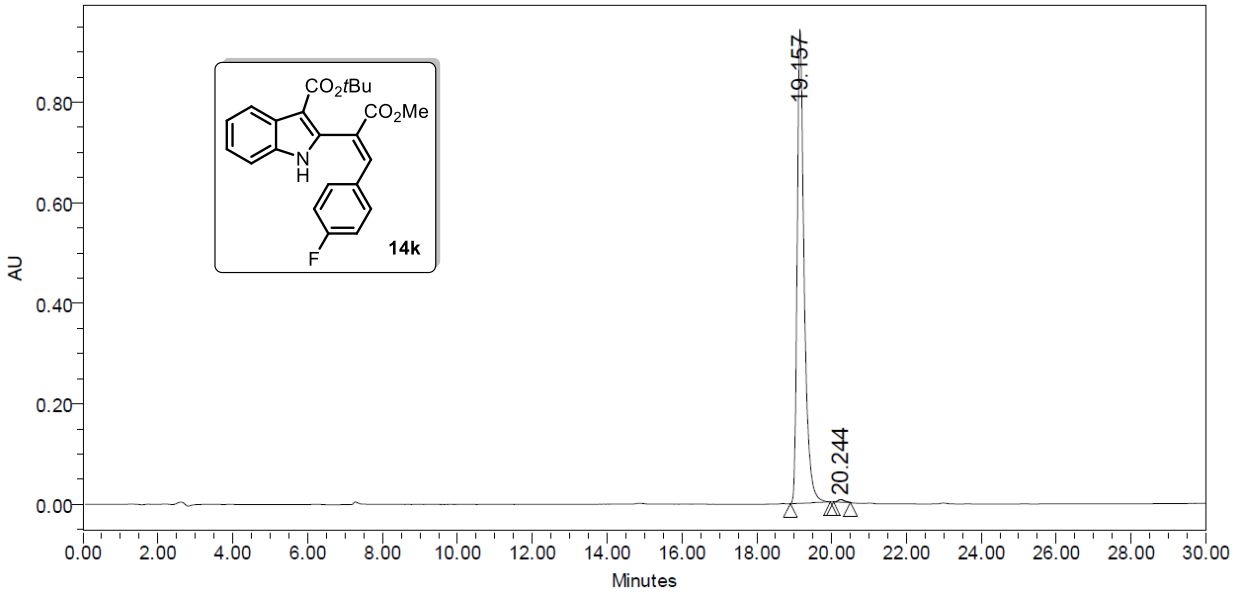

Peak Results

	Name	RT	Area	% Area	Int Type	Processed Channel Descr.	Width (sec)
1		19.157	12200907	99.47	bb	PDA 254.0 nm	64.000
2		20.244	64578	0.53	bb	PDA 254.0 nm	27.000

Laboratorio de Cromatografía
Condiciones Cromatográficas

Muestras:

ARV-10	210823-tor-01
ARV-03	210823-tor-02
ARV-06	210823-tor-03
ARV-12	210823-tor-04
ARV-05	210823-tor-05
ARV-08	210823-tor-06
ARV-07	210823-tor-07

Cromatógrafo de Líquidos	Agilent 1200		
Detector	UV-Vis Arreglo de diodos Waters 2996		
Columna	Luna 3 µm C18(2) 100 Å 100 x 2 mm		
Eluyente	Acetonitrilo	Agua 0.1% Ácido acético	
inicial	30	70	
30 min	100	0	
Flujo	0.2 mL/min		
Longitud de onda del cromatograma	254 nm		
Disolvente de la muestra	Diclorometano		
Fecha 25-08-2021	Analizó: M. en C. Lucero Rios		
	Revisó: M. en C. Carmen Márquez		